HIGH PRESSURE ADSORPTION OF PURE COALBED GASES ON DRY COALS

By

ARUNKUMAR ARUMUGAM

Bachelor of Technology

Sri Venkateswara College of Engineering

Chennai, India

1999

Submitted to the Faculty of the
Graduate College of the
Oklahoma State University
in partial fulfillment of
the requirements for
the Degree of
MASTER OF SCIENCE
December 2004

HIGH PRESSURE ADSORPTION OF PURE

COALBED GASES ON DRY COALS

Thesis Approved:

KHALED A. M. GASEM

_____

Thesis Adviser

ROBERT L. ROBINSON, Jr.

_____

GARY FOUTCH

_____

A. GORDON EMSLIE

_____

Dean of the Graduate College

ACKNOWLEDGMENTS

I would like to express my gratitude to my adviser, Professor Khaled A. M. Gasem, for giving me the opportunity to work on this project. My sincere appreciation goes to Dr. Gasem for his intelligent guidance, invaluable assistance and endless support throughout my graduate studies at Oklahoma State University.

My gratitude is also extended to Dr. Robert L. Robinson, Jr., for his expertise, valuable advice and encouragement during my Master's program.

I would also like to thank my graduate advisory committee member, Dr. Gary Foutch, for his valuable input.

I am grateful to my colleagues, Dr. James E. Fitzgerald and Dr. Mahmud Sudibandriyo, who have been great mentors to me. Their friendship and insight was most critical to the successful completion of this study.

Finally, I would like to extend my sincere thanks to my family and friends, for their patience, understanding, and support during the course of my graduate program.

TABLE OF CONTENTS

LIST OF TABLES

LIST OF FIGURES

Figure Page

Figure Page

NOMENCLATURE

1/B	Langmuir pressure (psia)
C	maximum adsorption capacity in OK model (mmol/g)
k	Boltzman constant (J m^{-2} K^{-4})
L	maximum adsorption capacity in the Langmuir model and LRC (mmol/g)
M	total number of lattice cells; molecular weight (g/mol)
m	number of layers in the lattice model
N_i	number of molecules of component i
n_{ads}^{Gibbs}	the amount of gas adsorbed (mmol/g)
n_{unads}^{Gibbs}	the amount of gas unadsorbed (mmol/g)
n_{inj}	amount of gas injected from the pump section into the cell section (mmol/g)
P	pressure (MPa)
R	universal gas constant (psi cm^3/mol R)
T	temperature (K)
V	volume (cm^3)
V_{ads}	adsorbed-phase volume (cm^3)
V_{void}	void volume (cm^3)
x_{ads}	fractional coverage of a pure component in the monolayer lattice model
x_i	mole fraction of component i in an adsorbed-phase
$x_{i,b}$	fraction that gas molecule i that occupies cells in a layer of the lattice model

$x_{i,t}$ fractional coverage of component i in t^{th} layer of the lattice model

x_t fractional coverage of pure component in t^{th} layer of the lattice model

Z compressibility factor

z_i feed gas mole fraction

z_0 lattice coordination number

z_1 parallel coordination number representing the number of primary nearest-neighbor cells in parallel direction

Greek Symbols

ε_{ff} fluid-fluid interaction energy parameter in the OK model (J m^{-2} K^{-3})

ε_{fs} fluid-solid interaction energy parameter in the OK model (J m^{-2} K^{-3})

η exponent in LRC model

ρ density (mol/cm^3)

ρ_{ads} adsorbed-phase density (mol/cm^3)

ρ_{mc} adsorbed-phase density corresponding to the maximum adsorption capacity (mol/cm^3)

σ diameter of a molecule (^oA); the expected experimental uncertainty

θ fractional coverage in the Langmuir adsorption isotherm model

ω amount of gas adsorbed per unit mass of adsorbent (mmol/g)

Subscripts

1,2 conditions pertaining to before and after injection in cell or pump section

ads the adsorbed amount within the equilibrium cell (mmol/g)

b bulk phase or the gas phase

He properties obtained with the use of helium gas

i, j component i, j

unads unadsorbed amount within the equilibrium cell

Superscripts

Abs absolute adsorption

a adsorbed phase

Gibbs Gibbs excess adsorption

Abbreviations

Ads. Adsorption

Err. Error

CHAPTER 1

INTRODUCTION

Natural gas, once considered a waste product of oil production, is currently experiencing a huge increase in demand around the world. Because of its cleaner burning capacity, it is an attractive alternative energy source to oil and coal. The increased use of natural gas offers reduced emissions and significant environmental benefits. According to the United States Department of Energy, in the year 2000, the United States consumed 22.5 Trillion cubic feet (Tcf) of natural gas, which was approximately 20% of all the fossil fuel used.

The United States has vast resources of conventional natural gas available for extraction. The estimate of technically recoverable natural gas resources is 1,190 Tcf according to the Energy Information Administration, 1,779 Tcf according to the National Petroleum Council, and 1,090 Tcf according to the Potential Gas Committee [NaturalGas.org]. However, the estimated recoverable natural gas can only last for few decades at current the consumption rate.

Coalbed methane (CBM), an unconventional natural gas resource, has received significant attention since the 1990's. Deep coalbeds retain large quantities methane through the phenomenon of adsorption. When a gas adheres to the surface of coal, the solid-gas interactions present can change the apparent gas density to that comparable to liquids. In coalbed reservoirs, methane resides inside the microporous coal structure at

higher densities than the free gas phase due to physical adsorption. Gas species other than methane also reside in the coal seam: roughly 90% is methane, 8% carbon dioxide, 2% nitrogen, with traces of other hydrocarbons [Mavor et al., 1999]. As reported by the United States Geological Survey, the in-place CBM resources of the United States are estimated to be more than 700 Tcf, of which about 100 Tcf may be economically recoverable. Currently, CBM constitutes about 7.5% of the natural gas production in the USA [USGS.gov].

Currently, enhanced coalbed methane recovery (ECBM) processes utilize CO_2, nitrogen or mixtures of both gases to improve production rates. Specifically, nitrogen injections into CBM production wells are used to help displace methane gas [Stevens et al., 1998]. By combining CO_2 with nitrogen, ECBM can displace more methane from coalbeds than with nitrogen alone [Arri et al., 1992]. CO_2 injection selectively frees adsorbed methane gas from the coal because CO_2 equilibrium adsorption is greater than that of methane [Hall et al., 1993; Stevens et al., 1998]. CO_2 injection into coalbed reservoirs also may serve a sequestration function, which is a potential environmental benefit.

The economic viability of ECBM technology, however, is dependent on a number of technical factors including coal seam thickness, adsorption isotherm (gas adsorption capacity), reservoir pressure, permeability, porosity, water saturation, diffusion, etc. Among these contributing factors, the adsorption isotherm is the most critical factor. Specifically, accurate adsorption isotherms for CO_2, methane, nitrogen and their mixtures are required to develop optimized processes for enhanced methane recovery.

Thermodynamic models for adsorption provide crucial information for designing processes to sequester CO_2 and recover natural gas from unminable coalbeds. These models can describe the quantity of gas initially residing in the coalbeds and how, through the process of ECBM recovery, reservoir changes in pressure, temperature, and gas composition affect the quantity and quality of the recovered natural gas. To evaluate the efficiency of the model and to improve their predicting capability, accurate experimental data are needed. The major objectives of the research group at Oklahoma State University (OSU) are to:

- Measure the adsorption behavior of pure CO_2, methane, nitrogen and their binary and their ternary mixtures on several selected coals, having different properties at various temperatures
- Test and/or develop theoretically based mathematical models to represent accurately the adsorption behavior of mixtures of the type for which measurements are made
- Generalize the adsorption model parameters in terms of appropriate properties of the adsorbates and the coals to facilitate adsorption behavior predictions for coals other than those studied

In previous studies at OSU, adsorption isotherms of pure CO_2, methane and nitrogen and their binary and ternary mixtures were conducted on activated carbon and a number of wet coals at different temperatures and pressures to 13.8 MPa (2000 psia). Thermodynamic models such as two-dimensional equation of state [Zhou et al., 1994; Pan, 2003], simplified local density model [Fitzgerald et al., 2003] and Ono-Kondo lattice

model [Sudibandriyao et al., 2003] were further modified to represent accurately the adsorption isotherms as well as to improve their predictive capability.

An experimental database of high pressure gas adsorption on coals has been developed [Gasem et al., 2003] to delineate the adsorption behavior of pure fluids and mixtures on different coals. In these previous endeavors, gas adsorption measurements have been performed exclusively on (a) water-moistened coal to represent *in-situ* coalbed conditions, and (b) dry activated carbon as a reference carbon matrix for high pressure adsorption. To assess the effect of water on gas adsorption, our goal is to measure the pure-gas adsorption on selected coals, namely Illinois #6, Wyodak, Pocahontas #3, Beulah Zap and Upper Freeport. These coals were selected to compliment an inter-laboratory study conducted by the Department of Energy (DOE) and the National Energy Technology Laboratory (NETL) [Goodman et al., 2004]. The present work addresses the adsorption measurements on dry coals. The specific objectives of this study are to:

- Measure the adsorption isotherm of pure methane, nitrogen, CO_2, and ethane adsorption on dry Illinois #6, Wyodak, Pocahontas #3, Beulah Zap and Upper Freeport coals at 131^{o}F (328.2 K) and pressures to 13.8 MPa (2000 psia).
- Model the adsorption isotherms for the five dry coals under study using Ono-Kondo lattice model and the Langmuir Loading-ratio correlation (LRC).

Chapter 2 describes the experimental setup used in this study. Chapter 3 presents mainly the pure-gases adsorption data on the five coals. Chapter 4 and 5 discuss the modeling capabilities of the Langmuir model, Loading-ratio correlation and the Ono-Kondo lattice model. Chapter 6 outlines the conclusions and recommendations of this study.

CHAPTER 2

EXPERIMENTAL APPARATUS AND PROCEDURE

In this chapter, a brief overview of the current methods for measuring high pressure gas adsorption, the experimental apparatus and the procedures used in this study are outlined.

2.1 Review of Experimental Techniques

Four widely used gas adsorption experimental techniques are reviewed briefly. They are the volumetric, gravimetric, gas flow, and chromatographic methods. The volumetric gas adsorption method calls for measuring the gas pressure in a calibrated constant volume cell, at a set temperature. The pressure and temperature of each dose of gas are measured, and the gas is metered into the equilibrium cell for adsorption. After adsorption equilibrium has been established, the amount adsorbed is calculated from the change in pressure. This technique can only be used to measure the gas adsorption point-by-point, which is referred to as a discontinuous procedure. Also, when building a complete isotherm, additional successive errors might result from the dosing device. Because of its simplicity, however, many researchers use this technique [Reich et al., 1980; Hall et al., 1993; Vermesse et al., 1996; Krooss et al., 2002; Fitzgerald et al., 2003; Sudibandriyo et al., 2003].

The gravimetric technique determines directly the amount adsorbed from the increase in mass measured by a balance. A simple gravimetric method uses a spring

balance to determine the amount of gas adsorbed. However, in recent years spring balances have been superseded largely by electronic microbalance [Salem et al., 1998;Vaart et al., 2000; Beutekamp et al., 2002; Frére et al., 2002; Humayun et al., 2000]. An extremely sensitive gravimetric technique is based on the effect of change of mass on the resonance frequency of vibrating quartz crystal. In this case, the adsorbent must be firmly attached to the crystal [Krim et al., 1991].

In gas flow techniques, a flowmeter is used to determine the amount of gas adsorbed. The flowmeter can be a differential type [Nelsen et al., 1958] or a thermal detector [Pieters et al., 1984]. The thermal detector provides a signal, which depends on the heat capacity, the thermal conductivity, and the mass flow rate of the gas. These gas flow techniques can be used for either a continuous or discontinuous procedure.

The chromatographic technique involves a column packed with the adsorbent to separate the flowing species [Haydel et al., 1967]. The chromatographic analysis method is simple and fast in producing data but suffers from inherently larger errors [de Boer, 1968].

Detailed descriptions of the above experimental methods are given elsewhere [Sudibandriyo, 2003].

2.2 Experimental Setup and Method

Our experiments are based on the volumetric method. A brief description of the apparatus and procedures follows, taken closely from our previous work by Gasem et al., (2003) and Sudibandriyo et al., (2003).

The experimental apparatus, shown schematically in Figure 1, has been used successfully in previous studies [e.g., Hall, 1993]. The pump and cell sections of the apparatus are maintained in a constant temperature air bath. The equilibrium cell has a volume of 110 cm^3 and is filled with the adsorbent to be studied. The cell is placed under

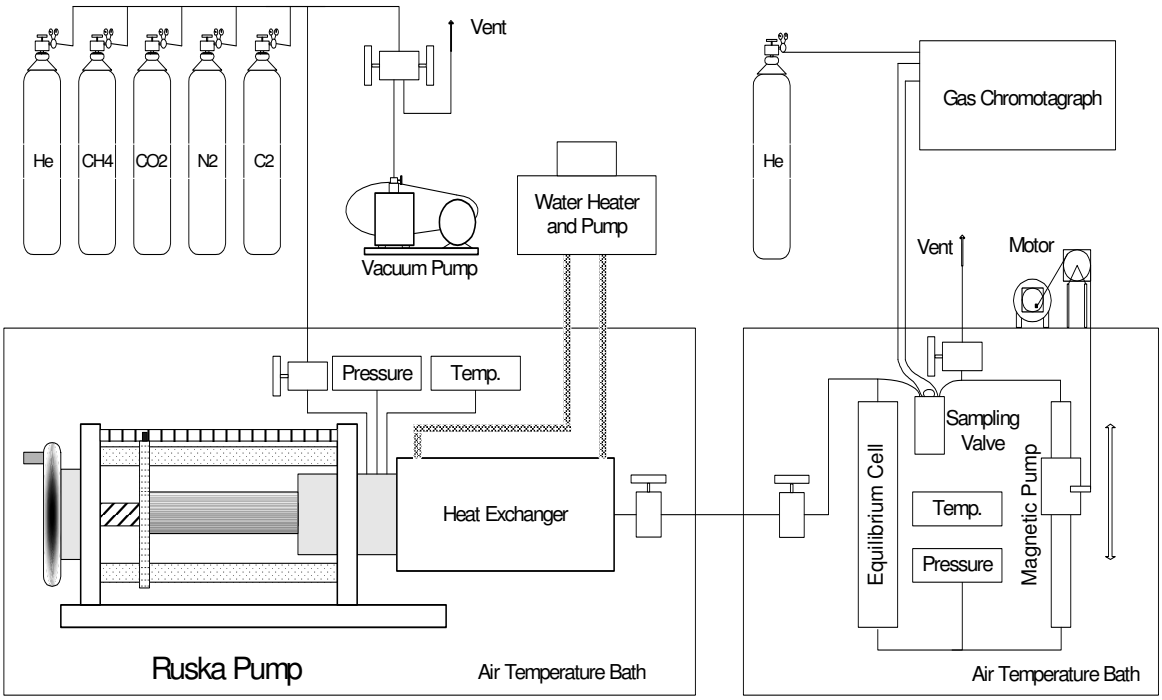

Figure 1. Schematic Diagram of the Experimental Apparatus

vacuum prior to gas injection. The void volume V_{void} in the equilibrium cell is then determined by injecting known quantities of helium from a calibrated injection pump (Ruska Pump). Since helium is not significantly adsorbed, the void volume can be determined from measured values of temperature, pressure and amount of helium injected into the cell. Several injections made into the cell at different pressures show consistency in the calculated void volume. Generally, the void volume calculated from sequential

injections varies less than 0.3 cm^3 from the average value based on at least five injections. The mass-balance equation, expressed in volumetric terms, is:

$$V_{void} = \frac{\left(\frac{P\Delta V}{ZT}\right)_{pump}}{\left(\frac{P_2}{Z_2 T} - \frac{P_1}{Z_1 T}\right)_{cell}} \tag{2-1}$$

where ΔV is the volume injected from the pump, Z is the compressibility factor of helium, T is the temperature, P is the pressure, subscripts "cell" and "pump" refer to conditions in the cell and pump sections of the apparatus, respectively, and "1" and "2" refer to conditions in the cell before and after injection of gas from the pump, respectively.

For void volume determination, the compressibility of helium is given by

$$Z_{He} = 1 + \left(1.47\text{x}10^{-3} - 4.779\text{x}10^{-6}\,T + 4.92\text{x}10^{-9}\,T^2\right)/P \tag{2-2}$$

where T is in Kelvin and P is in atmospheres. This expression was obtained from Hall (1994). This void volume is used in subsequent measurements of adsorption, as follows.

The Gibbs adsorption (also known as the excess adsorption) is calculated directly from experimental quantities. For pure-gas adsorption measurements, a known quantity, n_{inj}, of gas (e.g., methane) is injected from the pump section into the cell section. Some of the injected gas will be adsorbed, and the remainder, n_{unads}^{Gibbs}, will exist in the equilibrium bulk (gas) phase in the cell. A molar balance is used to calculate the amount adsorbed, n_{ads}^{Gibbs}, as:

$$n_{ads}^{Gibbs} = n_{inj} - n_{unads}^{Gibbs} \tag{2-3}$$

The amount injected can be determined from pressure, temperature and volume measurements of the pump section:

$$n_{inj} = \left(\frac{P\Delta V}{ZRT} \right)_{pump} \tag{2-4}$$

The amount of unadsorbed gas is calculated from conditions at equilibrium in the cell:

$$n_{unads}^{Gibbs} = \left(\frac{PV_{void}}{ZRT} \right)_{cell} \tag{2-5}$$

In Equations 2-4 and 2-5, *Z* is the compressibility of the pure gas at the corresponding conditions of temperature and pressure, evaluated from an equation of state [Angus et al., 1978; Angus et al., 1979; Friend et al., 1991; Span et al., 1996].

The above steps are repeated sequentially at higher pressures to yield a complete adsorption isotherm. The amount adsorbed is usually presented as an intensive quantity (mmol adsorbed/g adsorbent or mmol/g) obtained by dividing n_{ads}^{Gibbs} by the mass of adsorbent in the cell. Inspection of Equations 2-3 to 2-5 reveals that the amount adsorbed may be calculated in a straightforward manner from experimental measurements of pressures, temperatures and volumes, coupled with independent knowledge of the gas compressibility factors, Z.

After completing the last point in adsorption isotherm, the gas is desorbed. The gas from the equilibrium cell, which is at higher pressure, is allowed to flow into the pump until the desired desorption pressure is attained in the equilibrium cell. To re-establish the initial pump pressure, the piston of the pump is moved back to accommodate the material transferred for the cell. The above steps are repeated

sequentially at lower pressures to yield a complete isotherm. The amount desorbed is calculated in the same way as that for adsorption.

2.3 Relationship between Gibbs and Absolute Adsorption

Adsorption data may also be reported in terms of absolute adsorption. Calculations for the Gibbs and absolute adsorption differ in the manner by which n_{unads} is calculated. The Gibbs adsorption calculation, described above, neglects the volume occupied by the adsorbed phase in calculating the amount of unadsorbed gas (i.e., in Equation 2-5, the entire void volume, V_{void}, is viewed as being available to the unadsorbed gas). First, consider the various volumes that can be used to characterize the state existing in the equilibrium cell. Using a representation that envisions two distinct, homogenous fluid phases (bulk gas and adsorbed phase), the total system volume V_{total} is the sum of the gas volume V_{gas}, the solid adsorbent volume V_{solid}, and the adsorbed-phase volume V_{ads}, as follows:

$$V_{total} = V_{solid} + V_{gas} + V_{ads} \tag{2-6}$$

The void volume, having been determined by helium injection, is related to these quantities as follows:

$$V_{void} = V_{gas} + V_{ads} = V_{total} - V_{solid} \tag{2-7}$$

Now, consider the amount of material adsorbed at equilibrium, which may be written in molar terms as follows:

$$n_{ads} = n_{total} - n_{unads} \tag{2-8}$$

The difference in the definitions of the Gibbs and total adsorption resides in the manner in which n_{unads} is related to the volume terms. As stated previously, in the Gibbs calculation, the volume occupied by the condensed phase is neglected in calculating

n_{unads}, and the amount of unadsorbed gas is calculated using the entire void volume; thus, Equation 2-8 becomes, using Equation 2-7 for V_{void},

$$n_{ads}^{Gibbs} = n_{total} - V_{void}\,\rho_{gas} \tag{2-8a}$$

where ρ denotes density. In the calculation of the absolute adsorption, n_{unads} is determined using the volume actually available to the bulk gas phase (accounting for the reduction of volume accessible to the gas as a result of the volume occupied by the adsorbed phase):

$$n_{ads}^{Abs} = n_{total} - V_{gas}\;\rho_{gas} \tag{2-9}$$

By combining Equations 2-8a and 2-9 to eliminate n_{total}, the following relation between Gibbs and absolute adsorption is obtained:

$$n_{ads}^{Gibbs} = n_{ads}^{Abs} - V_{ads}\;\rho_{gas} \tag{2-8b}$$

The volume of the adsorbed phase may be expressed in terms of the amount adsorbed and the density of the adsorbed phase as

$$V_{ads} = n_{ads}^{Abs} / \rho_{ads} \tag{2-10}$$

Combining Equations 2-8b and 2-10 yields

$$n_{ads}^{Gibbs} = V_{ads}\left(\rho_{ads} - \rho_{gas}\right) \tag{2-8c}$$

Equation 2-8c clearly illustrates the physical interpretation of the Gibbs adsorption, namely, the amount adsorbed in excess of that which would be present if the adsorbed phase volume were filled with bulk gas. Combining Equations 2-10 and 2-8c leads to:

$$n_{ads}^{Abs} = n_{ads}^{Gibbs} \left(\frac{\rho_{ads}}{\rho_{ads} - \rho_{gas}} \right) \tag{2-11}$$

where ρ is the fluid density of that noted phase. The density of the adsorbed phase is considered to be the average over the volume V_{ads}. At low pressures, the correction from the Gibbs excess to the absolute amount is negligible ($\rho_{gas} << \rho_{ads}$), but at higher pressures it becomes significant.

A commonly used approximation for the density of an adsorbed phase is to use the liquid density at the atmospheric pressure boiling point, as done by Arri et al. (1992). More accurate estimates for the adsorbed-phase density are required when the adsorbed-phase density is similar to the bulk gas density.

Calibrations were performed routinely during the course of the experiments. The temperature measuring devices were calibrated against a Minco platinum resistance reference thermometer (Appendix A1), and the pressure transducers were calibrated (Appendix A2) against a Ruska deadweight tester with calibration traceable to the National Institute of Science and Technology. An error analysis (Appendix B) was performed to measure the uncertainty associated with each experimental data point by propagating the errors from the primary pressure, temperature and volume measurements.

The coals used in the present work namely, Illinois #6, Wyodak, Pocahontas, Beulah Zap and Upper Freeport, were dried under vacuum in an equilibrium cell at 353 K for 36 hours before being used in the adsorption measurements [Goodman et al., 2004]. The mass of the coal sample was weighed before and after drying under vacuum.

CHAPTER 3

HIGH PRESSURE ADSORPTION MEASUREMENTS FOR PURE COALBED GASES ON DRY COALS

High pressure adsorption of pure methane, nitrogen, CO_2 and ethane at 328.2 K (131°F) and pressures to 13.8 MPa (2000 psia) were measured on five coal samples from the Argonne National Laboratory. The amount of adsorption varies for different coals, because each coal has a unique composition. The coals considered in this study were:

- Beulah-Zap - lignite
- Wyodak - sub-bituminous
- Illinois #6 – high volatile bituminous
- Upper Freeport – medium volatile bituminous
- Pocahontas #3 – low volatile bituminous

These coals were selected to complement an inter-laboratory experimental study conducted by the Department of Energy (DOE) and the National Energy Technology Laboratory [Goodman et al., 2004].

Table 1 presents the compositional analysis for the coals considered. The ultimate and proximate analyses of the coals were conducted by Argonne National Laboratory and are presented in Table 1. The fixed carbon of these coals varies from 30.7% for the lignite Beulah Zap to 76.1% for the low volatile bituminous Pocahontas #3, and the volatile matter ranged from 18.5% to 30.5% for the five coals, respectively. The particulate size of the coals used in this study was less than 150 μm (no.100 mesh sieve).

Table 1: Compositional Analysis of Coals from Argonne National Laboratory

Analysis	**Beulah Zap**	**Wyodak**	**Illinois #6**	**Upper Freeport**	**Pocahontas #3**
Ultimate					
Carbon %	72.9	75.0	77.7	85.5	91.1
Hydrogen %	4.83	5.35	5.00	4.70	4.44
Oxygen %	20.3	18.0	13.5	7.5	2.5
Sulfur %	0.80	0.63	4.83	2.32	0.66
Ash %	9.7	8.8	15.5	13.2	4.8
Proximate					
Moisture %	32.2	28.1	8.0	1.1	0.7
Vol. Matter %	30.5	32.2	36.9	27. 1	18.5
Fixed Carbon %	30.7	33.0	40.9	58.7	76.1
Ash %	6.6	6.3	14.3	13.0	4.7

The original moisture content of the coal samples ranged from 0.7 % to 32.2%; however, prior to the adsorption measurements, the coal samples were dried under vacuum, as prescribed by the National Energy Technology Laboratory (NETL) drying protocol [Goodman et al., 2004].

Adsorption of pure methane, nitrogen, CO_2 and ethane at 328.2 K (131 °F) and pressures to 13.8 MPa (2000 psia) were measured on the above-mentioned dry coals. The data are presented in terms of both Gibbs and absolute adsorption since absolute adsorption is the quantity most familiar to practitioners in coalbed methane (CBM) operations. Also for convenience, the data are reported in both SI and English engineering units. In this study, unless otherwise noted, we use the adsorbed-phase density approximation suggested by Arri et al., (1992) and Fitzgerald et al., (2003). For nitrogen, methane, ethane, and CO_2, densities of 0.808, 0.421, 0.444 and 1.027 g/cm^3, respectively, were used to convert the Gibbs excess adsorption to absolute adsorption.

For each gas, two replicate adsorption runs as well as desorption measurements from the first run are shown. These redundant measurements were made to (a) establish the precision of the experimental reproducibility, and (b) examine the predisposition of each coal to hysteresis effects upon adsorption/desorption.

The data tables include the expected experimental uncertainties associated with the adsorption measurements. Error analysis indicates that average uncertainties for the methane, nitrogen, ethane, and CO_2 adsorption measurements are approximately 2.4% (0.02-0.03 mmol/g), 2.7% (0.03-0.04 mmol/g), 10.1% (0.09-0.13 mmol/g) and 5.4% (0.06-0.12 mmol/g), respectively. These estimates, which are depicted as error bars in the following figures, were generated by propagation of uncertainties in all measured quantities. In general, the replicate runs confirm the favorable precision of the present measurements; in fact, the replicate data indicate a conservative estimate for the expected uncertainties. Reproducibility of the replicate runs is further supported by the constancy of the void volume measurements before and after the adsorption; i.e., the void volumes before the first run and after the second run for the gases under study varied by less than 0.5% from their initial values.

Following is a discussion of the adsorption isotherm for each coal (in the order in which the experiments were done).

3.1 Adsorption on Dry Illinois #6 Coal

Adsorption of pure methane, nitrogen, CO_2 and ethane were measured at the above-mentioned experimental conditions. Tables 2 through 7 present the gas adsorption measurements on dry Illinois #6 coal. Figures 2 through 6 depict the effect of pressure on

Gibbs excess adsorption of pure methane, nitrogen, CO_2 and ethane on dry Illinois #6 coal.

Figures 2 and 3 present the adsorption isotherms for pure nitrogen and methane, respectively. As indicated by the figures, all the sorption measurements (adsorption and desorption) agree within the experimental uncertainty of about 4%. Agreement among the adsorption and desorption data for both nitrogen and methane indicate no discernable structural change in the coal after adsorption.

Table 2: Adsorption of Pure Nitrogen on Dry Illinois #6 Coal at 328.2 K (Run 1)

SI Units

Void Volume (m^3)	0.00009483
Pump Press. (MPa)	6.94
Pump T (K)	328.2
Cell T (K)	328.2
Adsorbent mass (g)	45.5
Moist.content (%)	0.0
Ads.Phase Density (g/cm^3)	0.808

Pressure (MPa)	Gibbs Ads. (mmol/g)	Abs. Ads. (mmol/g)	Err.Gibbs (mmol/g)	Err.Abs. (mmol/g)
0.69	0.084	0.085	0.024	0.024
1.39	0.135	0.138	0.024	0.024
2.78	0.211	0.218	0.023	0.024
4.19	0.267	0.282	0.023	0.024
5.52	0.310	0.333	0.023	0.025
6.95	0.344	0.377	0.024	0.026
8.32	0.373	0.416	0.024	0.027
9.70	0.397	0.452	0.025	0.029
11.08	0.416	0.482	0.026	0.030
12.46	0.431	0.510	0.027	0.032
13.87	0.446	0.537	0.029	0.034
Desorption				
10.94	0.424	0.490	-	-
8.27	0.386	0.430	-	-
5.50	0.320	0.344	-	-
2.76	0.231	0.239	-	-

British Units

Void Volume (ft^3)	0.003349
Pump Press. (psia)	1006.0
Pump T (°F)	131.0
Cell T (°F)	131.0
Adsorbent mass (lb)	0.1003
Moist.content (%)	0.0
Ads.Phase Density (lb/ft^3)	50.44

Pressure (psia)	Gibbs Ads. (SCF/ton)	Abs. Ads. (SCF/ton)	Err.Gibbs (SCF/ton)	Err.Abs. (SCF/ton)
99.7	63.9	64.5	18.2	18.4
201.9	102.8	104.7	18.0	18.3
403.4	159.8	165.6	17.7	18.3
607.7	202.9	214.3	17.6	18.6
800.4	234.9	252.5	17.7	19.0
1007.7	261.2	286.3	18.0	19.7
1206.2	282.9	315.8	18.5	20.6
1407.1	301.2	342.7	19.1	21.7
1607.2	315.7	366.0	19.8	23.0
1807.5	327.3	386.8	20.7	24.5
2012.0	338.5	407.9	21.7	26.1
Desorption				
1587.4	321.5	371.9	-	-
1198.9	292.9	326.6	-	-
797.5	243.0	261.0	-	-
399.9	175.2	181.5	-	-

Table 3: Adsorption of Pure Nitrogen on Dry Illinois #6 Coal at 328.2 K (Run 2)

SI Units

Void Volume (m^3)	0.00009477
Pump Press. (MPa)	6.92
Pump T (K)	328.2
Cell T (K)	328.2
Adsorbent mass (g)	45.5
Moist.content (%)	0.0
Ads.Phase Density (g/cm^3)	0.808

Pressure (MPa)	Gibbs Ads. (mmol/g)	Abs. Ads. (mmol/g)	Err.Gibbs (mmol/g)	Err.Abs. (mmol/g)
0.69	0.078	0.078	0.024	0.024
1.61	0.141	0.144	0.024	0.024
5.55	0.298	0.321	0.023	0.025
9.69	0.383	0.435	0.025	0.029
13.76	0.427	0.513	0.028	0.034

British Units

Void Volume (ft^3)	0.003347
Pump Press. (psia)	1003.2
Pump T (°F)	131.0
Cell T (°F)	131.0
Adsorbent mass (lb)	0.1003
Moist.content (%)	0.0
Ads.Phase Density (lb/ft^3)	50.44

Pressure (psia)	Gibbs Ads. (SCF/ton)	Abs. Ads. (SCF/ton)	Err.Gibbs (SCF/ton)	Err.Abs. (SCF/ton)
100.3	59.0	59.5	18.2	18.4
233.6	107.3	109.5	17.9	18.3
804.9	226.3	243.4	17.7	19.0
1405.3	290.6	330.5	19.1	21.7
1995.5	323.7	389.4	21.6	26.0

Table 4: Adsorption of Pure Methane on Dry Illinois #6 Coal at 328.2 K (Run 1)

SI Units

Void Volume (m^3)	0.00009477
Pump Press. (MPa)	6.91
Pump T (K)	328.2
Cell T (K)	328.2
Adsorbent mass (g)	45.5
Moist.content (%)	0.0
Ads.Phase Density (g/cm^3)	0.421

Pressure (MPa)	Gibbs Ads. (mmol/g)	Abs. Ads. (mmol/g)	Err.Gibbs (mmol/g)	Err.Abs. (mmol/g)
0.67	0.264	0.267	0.028	0.028
2.45	0.459	0.476	0.027	0.028
3.93	0.565	0.600	0.027	0.028
5.54	0.649	0.707	0.027	0.029
6.94	0.689	0.769	0.027	0.030
8.30	0.736	0.842	0.028	0.032
9.69	0.769	0.904	0.029	0.034
11.03	0.788	0.951	0.030	0.036
12.44	0.802	0.996	0.032	0.039
13.80	0.818	1.045	0.039	0.050
Desorption				
10.67	0.785	0.941	-	-
8.29	0.735	0.841	-	-
5.53	0.644	0.702	-	-
2.46	0.457	0.474	-	-

British Units

Void Volume (ft^3)	0.003347
Pump Press. (psia)	1002.9
Pump T (°F)	131.0
Cell T (°F)	131.0
Adsorbent mass (lb)	0.1003
Moist.content (%)	0.0
Ads.Phase Density (lb/ft^3)	26.28

Pressure (psia)	Gibbs Ads. (SCF/ton)	Abs. Ads. (SCF/ton)	Err.Gibbs (SCF/ton)	Err.Abs. (SCF/ton)
96.8	200.7	202.6	21.0	21.2
355.8	348.4	361.1	20.4	21.2
569.5	429.1	455.1	20.2	21.4
803.2	492.6	536.7	20.2	22.1
1006.7	522.6	583.6	20.6	23.0
1204.4	558.4	639.3	21.1	24.1
1406.1	583.5	686.0	21.9	25.7
1600.1	598.0	721.8	22.8	27.5
1803.8	608.7	755.8	24.0	29.8
2001.2	621.0	793.3	29.7	38.0
Desorption				
1547.4	595.9	714.1	-	-
1202.7	557.7	638.3	-	-
802.2	489.0	532.7	-	-
356.5	346.8	359.5	-	-

Table 5: Adsorption of Pure Methane on Dry Illinois #6 Coal at 328.2 K (Run 2)

SI Units

Void Volume (m^3)	0.00009477
Pump Press. (MPa)	6.92
Pump T (K)	328.2
Cell T (K)	328.2
Adsorbent mass (g)	45.5
Moist.content (%)	0.0
Ads.Phase Density (g/cm^3)	0.421

Pressure (MPa)	Gibbs Ads. (mmol/g)	Abs. Ads. (mmol/g)	Err.Gibbs (mmol/g)	Err.Abs. (mmol/g)
0.73	0.255	0.258	0.028	0.028
1.41	0.370	0.377	0.028	0.028
5.66	0.679	0.742	0.027	0.029
9.68	0.781	0.918	0.029	0.034
13.77	0.828	1.057	0.041	0.052

British Units

Void Volume (ft^3)	0.003347
Pump Press. (psia)	1003.6
Pump T (°F)	131.0
Cell T (°F)	131.0
Adsorbent mass (lb)	0.1003
Moist.content (%)	0.0
Ads.Phase Density (lb/ft^3)	26.28

Pressure (psia)	Gibbs Ads. (SCF/ton)	Abs. Ads. (SCF/ton)	Err.Gibbs (SCF/ton)	Err.Abs. (SCF/ton)
106.0	193.4	195.4	21.3	21.5
204.4	280.5	286.2	21.0	21.4
820.3	515.7	563.0	20.5	22.3
1404.4	592.9	696.9	22.0	25.9
1997.8	628.1	802.0	31.0	39.5

Table 6: Adsorption of Pure CO_2 on Dry Illinois #6 Coal at 328.2 K

SI Units

Void Volume (m^3)	0.00009471
Pump Press. (MPa)	6.43
Pump T (K)	328.2
Cell T (K)	327.8
Adsorbent mass (g)	45.5
Moist.content (%)	0.0
Ads.Phase Density (g/cm^3)	1.027

Pressure (MPa)	Gibbs Ads. (mmol/g)	Abs. Ads. (mmol/g)	Err.Gibbs (mmol/g)	Err.Abs. (mmol/g)
0.70	0.591	0.598	0.059	0.060
1.41	0.822	0.842	0.057	0.059
2.78	1.096	1.153	0.056	0.059
4.16	1.282	1.392	0.055	0.059
5.57	1.403	1.583	0.054	0.061
6.94	1.485	1.761	0.054	0.064
8.25	1.502	1.904	0.055	0.070
9.64	1.432	2.025	0.068	0.096
10.98	1.232	2.081	0.100	0.169
12.29	1.033	2.144	0.105	0.218
13.81	0.912	2.274	0.119	0.296
Desorption				
11.24	1.224	2.156	-	-
8.40	1.514	1.936	-	-
5.48	1.412	1.590	-	-
2.79	1.103	1.160	-	-

British Units

Void Volume (ft^3)	0.003345
Pump Press. (psia)	932.7
Pump T (°F)	131.0
Cell T (°F)	130.3
Adsorbent mass (lb)	0.1003
Moist.content (%)	0.0
Ads.Phase Density (lb/ft^3)	64.11

Pressure (psia)	Gibbs Ads. (SCF/ton)	Abs. Ads. (SCF/ton)	Err.Gibbs (SCF/ton)	Err.Abs. (SCF/ton)
101.4	448.9	454.1	45.0	45.5
203.9	624.2	639.1	43.6	44.6
403.2	832.2	875.0	42.4	44.6
603.4	973.3	1056.2	41.4	44.9
807.6	1064.6	1201.9	40.7	45.9
1006.2	1126.9	1336.9	40.7	48.2
1197.2	1140.3	1445.4	42.0	53.3
1398.7	1087.0	1536.7	51.8	73.2
1592.9	935.4	1579.4	76.0	128.2
1782.8	783.9	1627.3	79.6	165.2
2002.5	692.6	1725.7	90.2	224.7
Desorption				
1630.7	929.1	1636.6	-	-
1218.0	1148.8	1469.1	-	-
795.4	1072.0	1207.0	-	-
405.0	836.9	880.3	-	-

Table 7: Adsorption of Pure Ethane on Dry Illinois #6 Coal at 328.2 K

SI Units

Void Volume (m^3)	0.00009471
Pump Press. (MPa)	8.99
Pump T (K)	328.2
Cell T (K)	328.2
Adsorbent mass (g)	45.5
Moist.content (%)	0.0
Ads.Phase Density (g/cm^3)	0.444

Pressure (MPa)	Gibbs Ads. (mmol/g)	Abs. Ads. (mmol/g)	Err.Gibbs (mmol/g)	Err.Abs. (mmol/g)
0.69	0.591	0.601	0.085	0.089
1.46	0.737	0.767	0.095	0.099
2.81	0.951	1.038	0.094	0.103
4.20	1.046	1.222	0.093	0.109
5.57	1.067	1.393	0.093	0.122
6.92	0.921	1.545	0.100	0.168
8.23	0.688	1.632	0.096	0.227
9.67	0.623	1.857	0.094	0.280
11.05	0.573	1.992	0.113	0.393
12.47	0.560	2.218	0.113	0.450
13.95	0.539	2.406	0.128	0.572
		Desorption		
11.30	0.563	2.009	-	-
8.30	0.696	1.674	-	-
6.32	0.995	1.449	-	-
3.45	0.979	1.100	-	-

British Units

Void Volume (ft^3)	0.003345
Pump Press. (psia)	1303.7
Pump T (°F)	131.0
Cell T (°F)	131.0
Adsorbent mass (lb)	0.1003
Moist.content (%)	0.0
Ads.Phase Density (lb/ft^3)	27.72

Pressure (psia)	Gibbs Ads. (SCF/ton)	Abs. Ads. (SCF/ton)	Err.Gibbs (SCF/ton)	Err.Abs. (SCF/ton)
99.7	448.3	456.2	64.5	67.6
211.3	559.1	582.0	72.0	75.0
406.8	721.9	788.2	71.3	77.9
608.5	793.6	927.6	70.7	82.6
807.3	809.5	1057.4	70.8	92.5
1003.2	699.3	1172.9	76.1	127.6
1194.1	522.1	1238.4	72.6	172.1
1403.0	472.8	1409.6	71.2	212.3
1602.1	434.9	1512.3	85.9	298.6
1809.1	424.7	1683.5	86.1	341.2
2023.4	409.3	1826.3	97.3	434.4
		Desorption		
1638.8	427.6	1524.5	-	-
1204.0	528.5	1270.8	-	-
916.1	755.0	1099.9	-	-
500.8	742.9	834.5	-	-

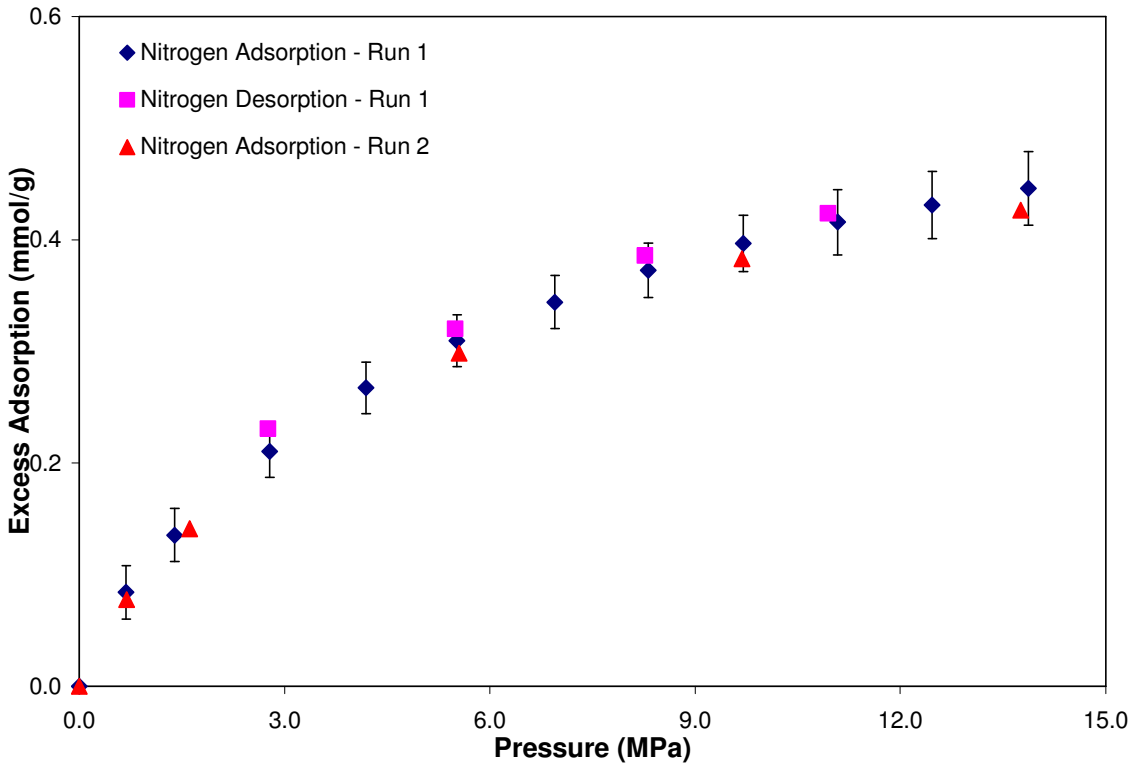

Figure 2: Excess Adsorption of Pure Nitrogen on Dry Illinois #6 Coal at 328.2 K

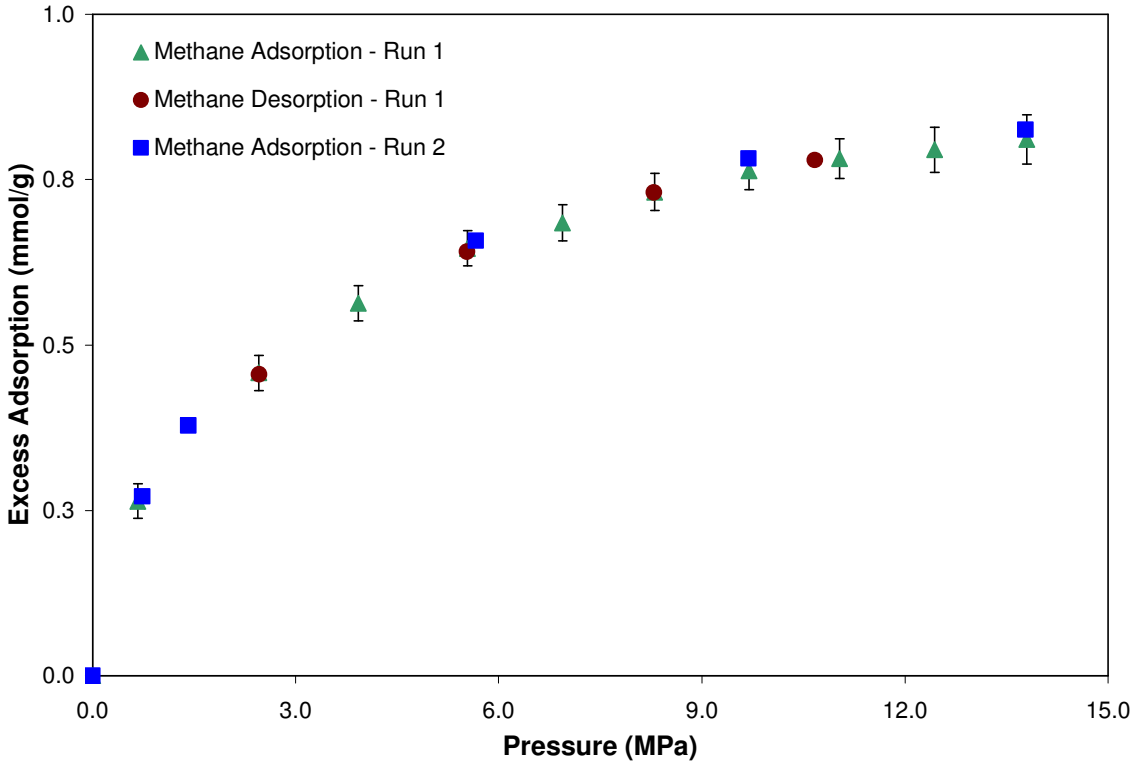

Figure 3: Excess Adsorption of Pure Methane on Dry Illinois #6 Coal at 328.2 K

The adsorption isotherm of CO_2 at 328.2 K is shown in Figure 4. As expected for a near-critical isotherm, CO_2 adsorption exhibits a maximum in the amount adsorbed at 8.3 MPa (1200 psia). The expected experimental uncertainty of the pure CO_2 adsorption data on Illinois #6, signified here by the error bars, is about 5.9%. The increased uncertainty of the CO_2 bulk density at higher pressure-temperature conditions amplifies the expected uncertainty in the amount adsorbed.

Further, comparison of the current adsorption measurements with comparable ones by Sudibandriyo (2003) shows agreement within 3% for most of the data. This level of agreement is well within the combined experimental uncertainty of the two data sets.

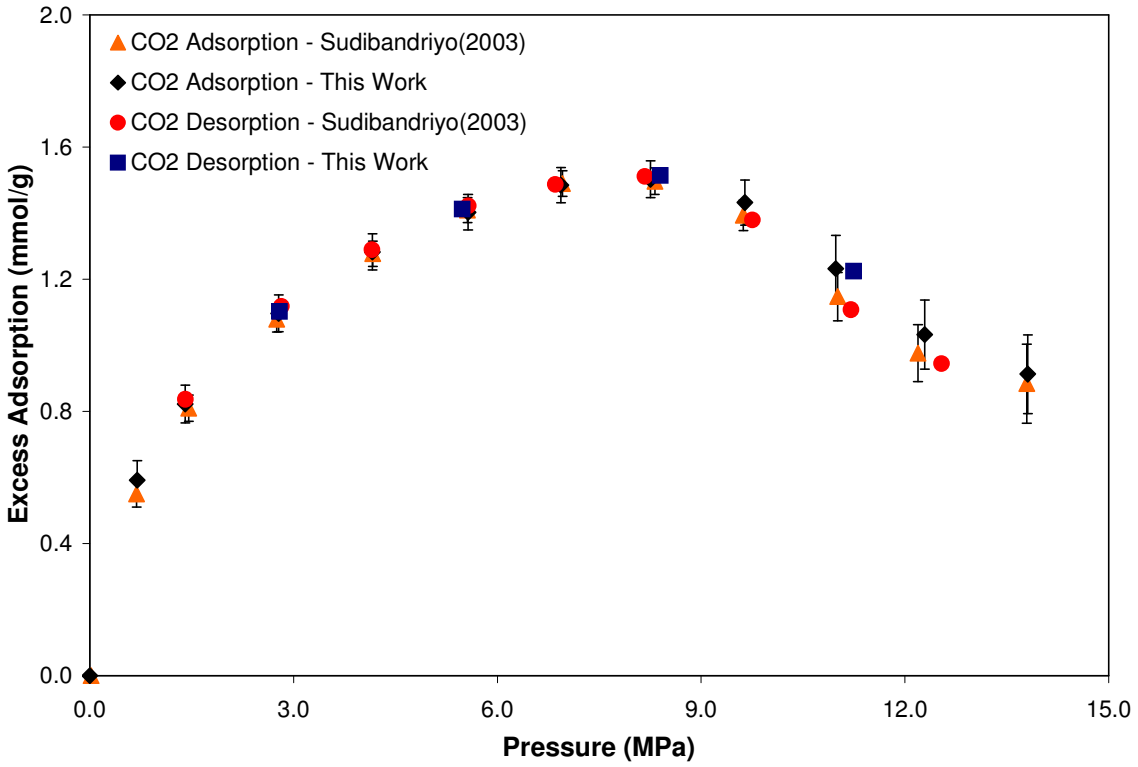

Figure 4: Excess Adsorption of Pure CO_2 on Dry Illinois #6 Coal at 328.2 K

Figure 5 depicts the adsorption isotherm for pure ethane at 328.2 K (131 °F) and pressures to 13.8 MPa (2000 psia). Similar to the CO_2 adsorption isotherm, ethane also exhibits a maximum in the adsorption amount at 5.6 MPa (800 psia).

The expected experimental uncertainty of the pure ethane adsorption data on Illinois #6 is about 9.9%. The larger uncertainty in ethane adsorption measurements is attributed to the sensitivity of ethane density calculations to small errors in pressure and temperature. Nevertheless, the adsorption and desorption data are within the experimental uncertainties.

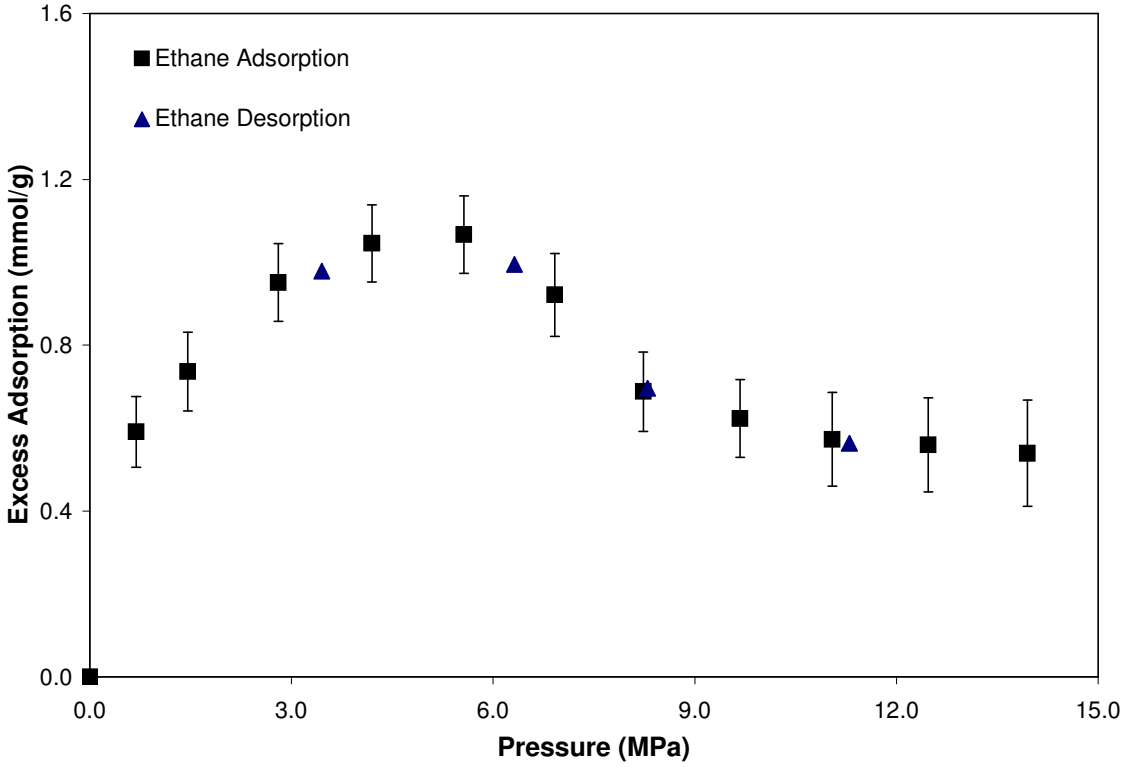

Figure 5: Excess Adsorption of Pure Ethane on Dry Illinois #6 Coal at 328.2 K

Figure 6 presents the Gibbs excess adsorption of pure methane, nitrogen, CO_2 and ethane at 328.2 K (131 °F) and pressures to 13.8 MPa (2000 psia) on dry Illinois #6 Coal. At low to moderate pressures, an increasing order in the amount of gas adsorbed on this coal is observed for nitrogen, methane, ethane and CO_2, respectively. Specifically, the

amount of adsorption at 5.6 MPa (808.6 psia) ranges form 0.3 mmol/g for the low adsorbed nitrogen to 1.4 mmol/g for CO_2.

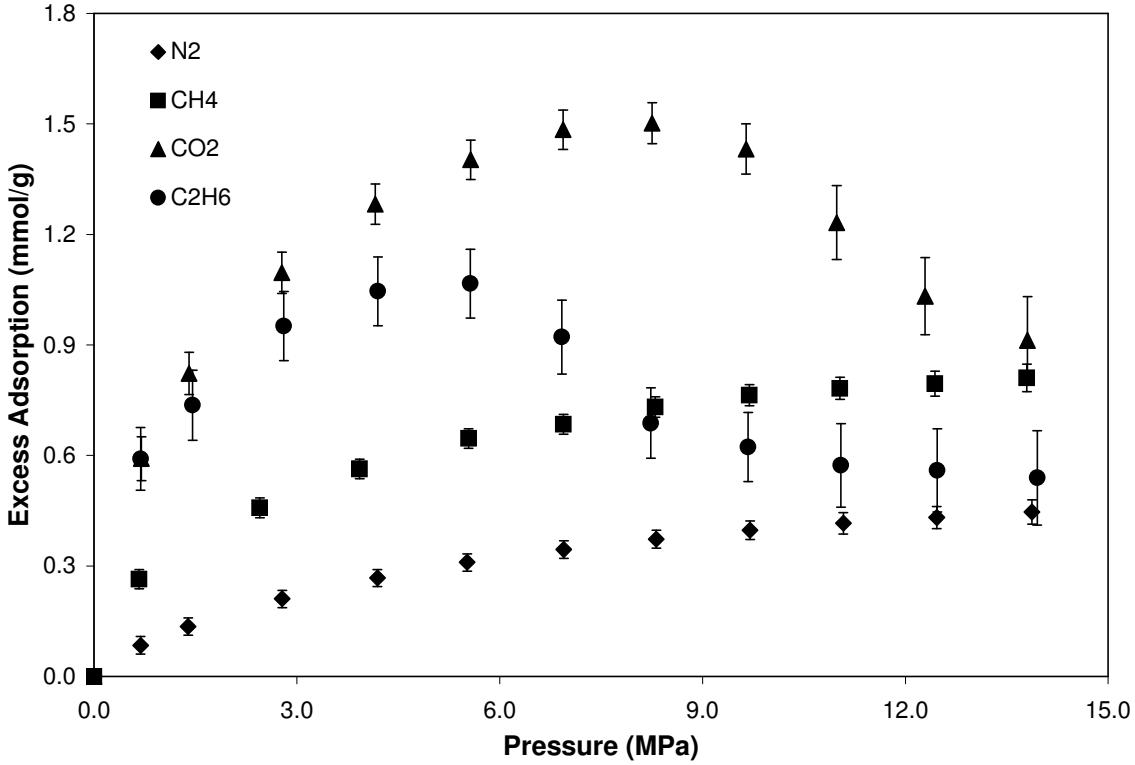

Figure 6: Excess Adsorption of Pure Coalbed Gases on Dry Illinois #6 Coal at 328.2 K

3.2 Adsorption on Dry Wyodak Coal

Adsorption of pure methane, nitrogen, CO_2 and ethane at 328.2 K (131 °F) and pressures to 13.8 MPa (2000 psia) were measured on dry Wyodak coal. Tables 8 through 14 present the gas adsorption measurements on this coal.

Figures 7 and 8 present the adsorption isotherms for pure nitrogen and methane, respectively. There is no significant difference observable in the amount adsorbed or the shapes of the adsorption isotherm, as both the coals almost have the same amount of carbon content as indicated by the ultimate analysis.

Table 8: Adsorption of Pure Nitrogen on Dry Wyodak Coal at 328.2 K (Run 1)

SI Units

Void Volume (m^3)	0.00009229
Pump Press. (MPa)	6.90
Pump T (K)	328.2
Cell T (K)	328.2
Adsorbent mass (g)	47.4
Moisture Content (%)	0.0
Ads.Phase Density (g/cm^3)	0.808

Pressure (MPa)	Gibbs Ads. (mmol/g)	Abs. Ads. (mmol/g)	Err.Gibbs (mmol/g)	Err.Abs. (mmol/g)
0.73	0.091	0.092	0.024	0.024
1.45	0.147	0.150	0.023	0.024
2.83	0.221	0.229	0.023	0.024
4.21	0.272	0.288	0.023	0.024
5.58	0.313	0.337	0.023	0.025
6.97	0.344	0.377	0.023	0.025
8.33	0.373	0.417	0.024	0.027
9.70	0.394	0.448	0.025	0.028
11.09	0.416	0.483	0.025	0.030
12.47	0.431	0.509	0.027	0.031
13.72	0.445	0.535	0.028	0.033
		Desorption		
10.98	0.417	0.483	-	-
8.27	0.374	0.417	-	-
5.53	0.316	0.340	-	-
2.80	0.219	0.227	-	-

British Units

Void Volume (ft^3)	0.003259
Pump Press. (psia)	1000.2
Pump T (°F)	131.0
Cell T (°F)	131.0
Adsorbent mass (lb)	0.1045
Moisture Content (%)	0.0
Ads.Phase Density (lb/ft^3)	50.44

Pressure (psia)	Gibbs Ads. (SCF/ton)	Abs. Ads. (SCF/ton)	Err.Gibbs (SCF/ton)	Err.Abs. (SCF/ton)
106.0	69.0	69.7	17.9	18.0
209.9	111.5	113.6	17.6	18.0
410.2	167.9	174.1	17.3	18.0
611.0	206.8	218.4	17.2	18.2
808.6	237.8	255.8	17.3	18.6
1010.2	261.3	286.4	17.6	19.3
1208.8	283.3	316.3	18.0	20.1
1406.9	298.7	339.9	18.6	21.2
1608.2	315.9	366.3	19.3	22.4
1808.6	326.8	386.3	20.1	23.8
1989.7	338.0	406.4	20.9	25.2
		Desorption		
1592.0	316.6	366.6	-	-
1200.1	284.0	316.9	-	-
802.4	239.7	257.7	-	-
405.4	166.5	172.7	-	-

Table 9: Adsorption of Pure Nitrogen on Dry Wyodak Coal at 328.2 K (Run 2)

SI Units

Void Volume (m^3)	0.00009229
Pump Press. (MPa)	6.91
Pump T (K)	328.2
Cell T (K)	328.2
Adsorbent mass (g)	47.4
Moist.content (%)	0.0
Ads.Phase Density (g/cm^3)	0.808

Pressure (MPa)	Gibbs Ads. (mmol/g)	Abs. Ads. (mmol/g)	Err.Gibbs (mmol/g)	Err.Abs. (mmol/g)
1.72	0.152	0.155	0.021	0.021
4.17	0.265	0.280	0.020	0.022
6.97	0.336	0.369	0.021	0.023

British Units

Void Volume (ft^3)	0.003259
Pump Press. (psia)	1002.0
Pump T (°F)	131.0
Cell T (°F)	131.0
Adsorbent mass (lb)	0.1045
Moist.content (%)	0.0
Ads.Phase Density (lb/ft^3)	50.44

Pressure (psia)	Gibbs Ads. (SCF/ton)	Abs. Ads. (SCF/ton)	Err.Gibbs (SCF/ton)	Err.Abs. (SCF/ton)
250.2	115.2	117.7	15.7	16.0
604.3	201.4	212.6	15.5	16.4
1010.5	255.2	279.7	16.1	17.6

Table 10: Adsorption of Pure Methane on Dry Wyodak Coal at 328.2 K (Run 1)

SI Units

Void Volume (m^3)	0.00009232
Pump Press. (MPa)	6.90
Pump T (K)	328.2
Cell T (K)	328.2
Adsorbent mass (g)	47.4
Moist.content (%)	0.0
Ads.Phase Density (g/cm^3)	0.421

Pressure (MPa)	Gibbs Ads. (mmol/g)	Abs. Ads. (mmol/g)	Err.Gibbs (mmol/g)	Err.Abs. (mmol/g)
0.69	0.242	0.245	0.027	0.027
1.42	0.355	0.362	0.027	0.027
2.80	0.481	0.501	0.026	0.027
4.19	0.565	0.601	0.026	0.028
5.57	0.624	0.681	0.026	0.028
6.95	0.671	0.749	0.026	0.030
8.34	0.701	0.803	0.027	0.031
9.70	0.721	0.848	0.028	0.033
11.10	0.740	0.895	0.029	0.035
12.46	0.770	0.956	0.040	0.049
13.71	0.782	0.997	0.047	0.060
		Desorption		
11.06	0.755	0.911	-	-
8.28	0.708	0.811	-	-
5.53	0.617	0.672	-	-
2.78	0.477	0.497	-	-

British Units

Void Volume (ft^3)	0.003260
Pump Press. (psia)	1000.4
Pump T (°F)	131.0
Cell T (°F)	131.0
Adsorbent mass (lb)	0.1045
Moist.content (%)	0.0
Ads.Phase Density (lb/ft^3)	26.28

Pressure (psia)	Gibbs Ads. (SCF/ton)	Abs. Ads. (SCF/ton)	Err.Gibbs (SCF/ton)	Err.Abs. (SCF/ton)
99.8	184.0	185.8	20.6	20.8
206.5	269.4	275.0	20.3	20.7
405.6	365.1	380.5	19.9	20.8
607.5	428.5	456.4	19.8	21.1
808.4	473.8	516.6	19.8	21.6
1008.3	509.1	568.6	20.1	22.5
1209.8	531.8	609.3	20.6	23.6
1406.7	547.3	643.5	21.3	25.1
1610.3	561.8	679.0	22.2	26.9
1806.7	584.2	725.8	30.0	37.3
1988.6	593.3	756.5	35.9	45.7
		Desorption		
1603.5	572.7	691.6	-	-
1201.4	537.6	615.2	-	-
801.8	468.0	509.8	-	-
403.4	362.0	377.1	-	-

Table 11: Adsorption of Pure Methane on Dry Wyodak Coal at 328.2 K (Run 2)

SI Units

Void Volume (m^3)	0.00009232
Pump Press. (MPa)	6.91
Pump T (K)	328.2
Cell T (K)	328.2
Adsorbent mass (g)	47.4
Moist.content (%)	0.0
Ads.Phase Density (g/cm^3)	0.421

Pressure (MPa)	Gibbs Ads. (mmol/g)	Abs. Ads. (mmol/g)	Err.Gibbs (mmol/g)	Err.Abs. (mmol/g)
1.47	0.361	0.369	0.023	0.023
4.22	0.573	0.611	0.024	0.026
6.99	0.671	0.750	0.025	0.027

British Units

Void Volume (ft^3)	0.003260
Pump Press. (psia)	1002.1
Pump T (°F)	131.0
Cell T (°F)	131.0
Adsorbent mass (lb)	0.1045
Moist.content (%)	0.0
Ads.Phase Density (lb/ft^3)	26.28

Pressure (psia)	Gibbs Ads. (SCF/ton)	Abs. Ads. (SCF/ton)	Err.Gibbs (SCF/ton)	Err.Abs. (SCF/ton)
213.1	274.3	280.1	17.1	17.5
612.1	435.2	463.9	18.2	19.4
1013.3	509.4	569.3	18.7	20.9

Table 12: Adsorption of Pure CO_2 on Dry Wyodak Coal at 328.2 K

SI Units

Void Volume (m^3)	0.00009217
Pump Press. (MPa)	6.76
Pump T (K)	328.2
Cell T (K)	328.2
Adsorbent mass (g)	47.4
Moist.content (%)	0.0
Ads.Phase Density (g/cm^3)	1.027

Pressure (MPa)	Gibbs Ads. (mmol/g)	Abs. Ads. (mmol/g)	Err.Gibbs (mmol/g)	Err.Abs. (mmol/g)
0.66	0.796	0.805	0.034	0.035
1.42	1.045	1.070	0.034	0.035
2.78	1.326	1.395	0.033	0.035
4.21	1.524	1.655	0.033	0.036
5.57	1.693	1.911	0.034	0.039
7.00	1.742	2.071	0.037	0.044
8.37	1.760	2.242	0.037	0.047
9.74	1.739	2.473	0.051	0.073
11.03	1.679	2.829	0.063	0.105
12.40	1.497	3.120	0.077	0.161
13.69	1.389	3.383	0.088	0.213
Desorption				
11.12	1.625	2.777	-	-
8.18	1.949	2.455	-	-
5.35	1.936	2.171	-	-
2.78	1.716	1.804	-	-

British Units

Void Volume (ft^3)	0.003255
Pump Press. (psia)	980.4
Pump T (°F)	131.0
Cell T (°F)	131.0
Adsorbent mass (lb)	0.1045
Moist.content (%)	0.0
Ads.Phase Density (lb/ft^3)	64.11

Pressure (psia)	Gibbs Ads. (SCF/ton)	Abs. Ads. (SCF/ton)	Err.Gibbs (SCF/ton)	Err.Abs. (SCF/ton)
96.3	604.2	610.7	26.1	26.4
206.3	793.2	812.4	25.8	26.4
402.8	1006.8	1058.5	25.4	26.7
609.9	1156.4	1256.1	25.4	27.6
808.2	1284.8	1450.1	26.2	29.5
1015.4	1322.5	1572.1	28.4	33.7
1213.6	1335.5	1701.8	28.0	35.7
1413.0	1319.7	1877.3	38.8	55.2
1599.5	1274.3	2147.1	47.5	80.0
1799.1	1136.0	2368.1	58.5	121.9
1985.2	1054.5	2567.4	66.4	161.7
Desorption				
1612.7	1233.0	2107.5	-	-
1186.6	1478.9	1863.7	-	-
776.5	1469.5	1647.5	-	-
402.6	1302.3	1369.1	-	-

Table 13: Adsorption of Pure Ethane on Dry Wyodak Coal at 328.2 K (Run 1)

SI Units

Void Volume (m^3)	0.00009237
Pump Press. (MPa)	9.00
Pump T (K)	328.2
Cell T (K)	328.2
Adsorbent mass (g)	47.4
Moist.content (%)	0.0
Ads.Phase Density (g/cm^3)	0.444

Pressure (MPa)	Gibbs Ads. (mmol/g)	Abs. Ads. (mmol/g)	Err.Gibbs (mmol/g)	Err.Abs. (mmol/g)
0.55	0.483	0.490	0.092	0.093
1.67	0.682	0.715	0.091	0.095
2.82	0.800	0.874	0.090	0.098
4.20	0.888	1.038	0.089	0.104
5.55	0.955	1.245	0.089	0.116
6.93	0.843	1.420	0.095	0.161
8.23	0.687	1.629	0.092	0.217
9.64	0.649	1.927	0.090	0.267
11.06	0.631	2.199	0.090	0.314
12.26	0.697	2.715	0.090	0.352
13.66	0.718	3.134	0.091	0.396
		Desorption		
10.98	0.628	2.171	-	-
8.35	0.665	1.615	-	-
6.11	0.954	1.341	-	-
3.10	0.806	0.891	-	-

British Units

Void Volume (ft^3)	0.003262
Pump Press. (psia)	1305.8
Pump T (°F)	131.0
Cell T (°F)	131.0
Adsorbent mass (lb)	0.1045
Moist.content (%)	0.0
Ads.Phase Density (lb/ft^3)	27.72

Pressure (psia)	Gibbs Ads. (SCF/ton)	Abs. Ads. (SCF/ton)	Err.Gibbs (SCF/ton)	Err.Abs. (SCF/ton)
79.9	366.9	372.2	69.5	70.5
242.6	517.8	542.7	68.9	72.3
408.8	607.5	663.7	68.4	74.7
608.6	674.0	787.8	67.8	79.3
805.0	725.0	945.3	67.8	88.4
1005.3	640.2	1078.1	72.4	121.9
1194.4	521.2	1236.8	69.5	164.9
1397.6	492.9	1462.6	68.4	203.0
1604.5	479.2	1669.3	68.5	238.5
1778.5	529.3	2060.4	68.7	267.3
1981.4	545.1	2378.8	68.9	300.8
		Desorption		
1592.3	477.0	1647.7	-	-
1211.2	504.7	1225.6	-	-
886.4	724.3	1017.9	-	-
450.3	611.8	676.4	-	-

Table 14: Adsorption of Pure Ethane on Dry Wyodak Coal at 328.2 K (Run 2)

SI Units

Void Volume (m^3)	0.00009225
Pump Press. (MPa)	8.99
Pump T (K)	328.2
Cell T (K)	328.2
Adsorbent mass (g)	47.4
Moist.content (%)	0.0
Ads.Phase Density (g/cm^3)	0.444

Pressure (MPa)	Gibbs Ads. (mmol/g)	Abs. Ads. (mmol/g)	Err.Gibbs (mmol/g)	Err.Abs. (mmol/g)
0.62	0.505	0.513	0.089	0.091
1.49	0.684	0.712	0.089	0.092
2.83	0.823	0.899	0.088	0.096
4.23	0.902	1.056	0.087	0.102
5.60	0.924	1.210	0.087	0.114
6.95	0.774	1.312	0.094	0.159
8.29	0.652	1.565	0.090	0.215
9.71	0.642	1.923	0.088	0.264
11.03	0.668	2.317	0.106	0.368
12.46	0.699	2.769	0.106	0.422
13.49	0.740	3.188	0.120	0.518

British Units

Void Volume (ft^3)	0.003258
Pump Press. (psia)	1303.4
Pump T (°F)	131.0
Cell T (°F)	131.0
Adsorbent mass (lb)	0.1045
Moist.content (%)	0.0
Ads.Phase Density (lb/ft^3)	27.72

Pressure (psia)	Gibbs Ads. (SCF/ton)	Abs. Ads. (SCF/ton)	Err.Gibbs (SCF/ton)	Err.Abs. (SCF/ton)
89.2	383.0	389.2	67.7	68.8
215.6	519.0	540.8	67.3	70.1
410.7	624.5	682.6	66.6	72.8
612.8	684.8	801.9	66.1	77.4
811.5	701.0	918.6	66.3	86.8
1008.3	587.7	995.5	71.4	121.0
1202.4	495.1	1188.2	68.0	163.1
1408.6	487.2	1459.7	66.9	200.5
1599.1	506.7	1758.3	80.6	279.6
1807.8	530.7	2101.9	80.8	320.0
1957.2	561.8	2420.1	91.2	392.8

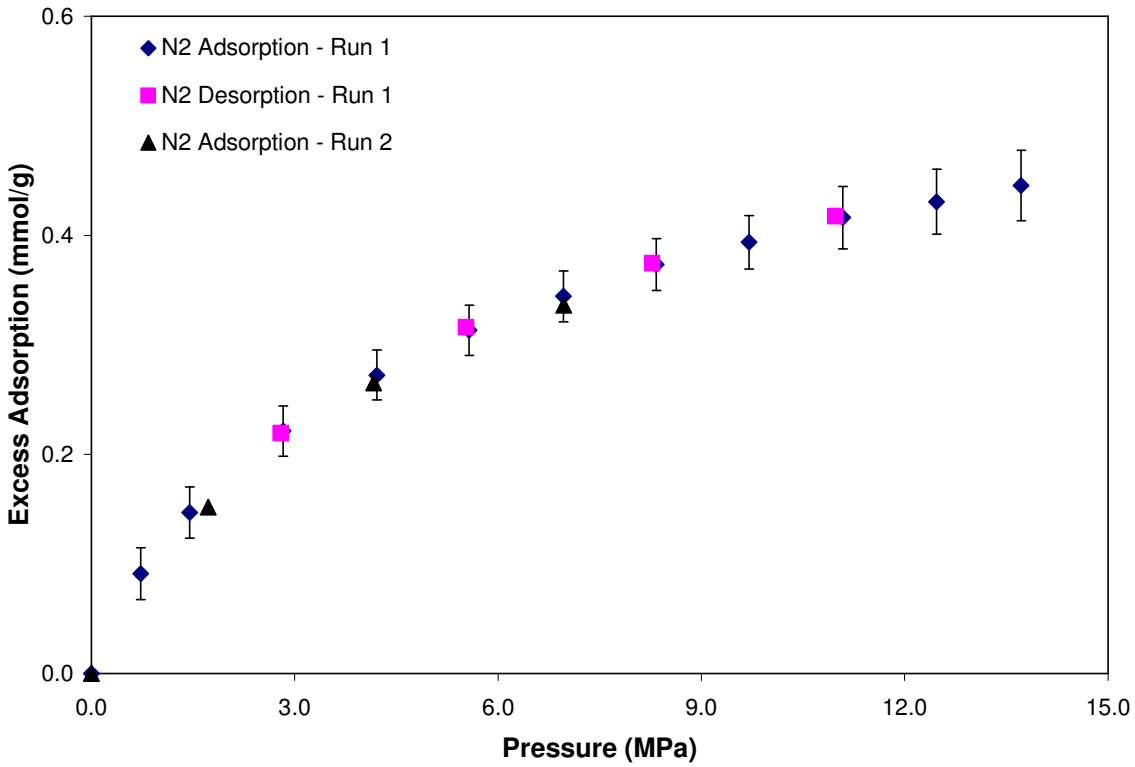

Figure 7: Excess Adsorption of Pure Nitrogen on Dry Wyodak Coal at 328.2 K

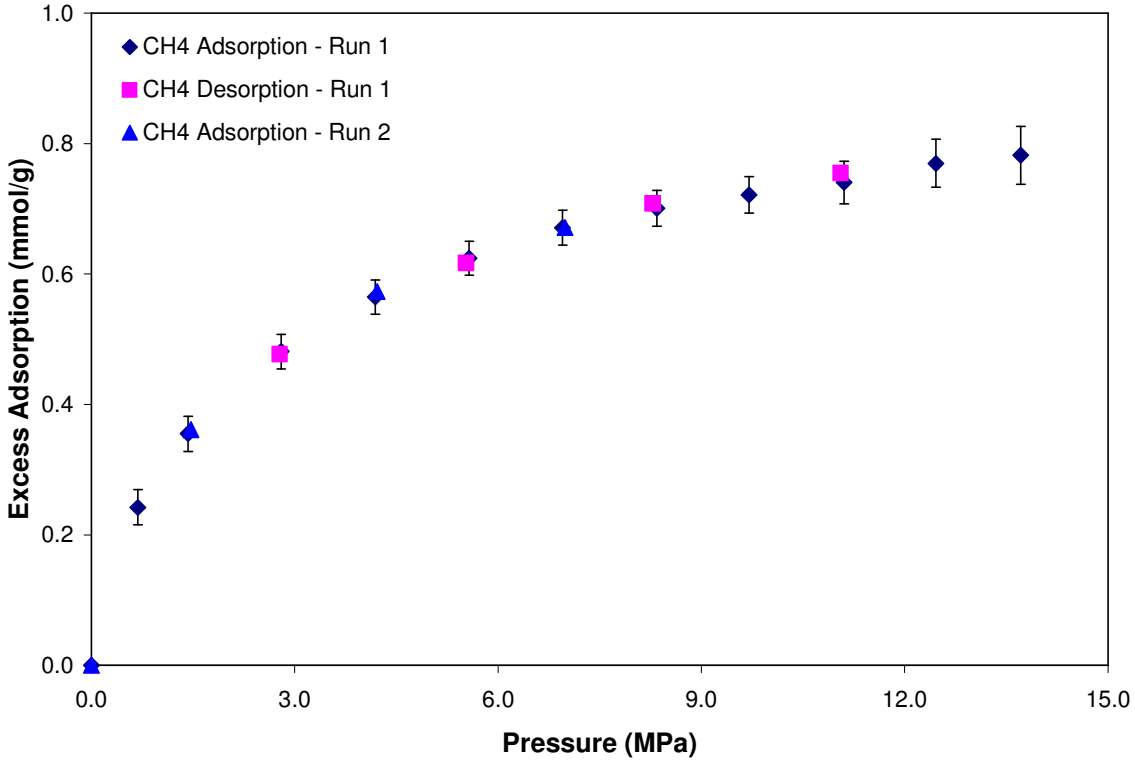

Figure 8: Excess Adsorption of Pure Methane on Dry Wyodak Coal at 328.2 K

The adsorption isotherm of pure CO_2 is presented in Figure 9. The CO_2 adsorption isotherm exhibits a maximum in the amount adsorbed at 8.3 MPa (1200 psia). The expected experimental uncertainty of the pure CO_2 adsorption data on Wyodak is about 7.1%.

Figure 9 indicates the presence of some hysteresis in the acquired data. Specifically, the desorption measurements for the Wyodak coal below 9 MPa show progressively larger amounts of adsorbed gas with decreasing pressure. This disparity among adsorption and desorption amounts (about 0.4 mmol/g at 3 MPa) was not observed for the Illinois #6 coal. The observed phenomenon, while related to the structure of the coal, is not well understood. Explanations offered in the literature for the sorption hysteresis include the possibility of irreversible matrix swelling, which occurs especially on lower rank coals characterized by larger pore shape and size distributions [Goodman et al., 2004]. Further investigation, however, is needed to explain the specific behavior of this coal.

Comparison of the current adsorption measurements with comparable ones by Sudibandriyo (2003) shows agreement within 8% for most of the data. This agreement is within the combined experimental uncertainty for the two data sets.

Figure 10 depicts the adsorption isotherm for pure ethane at 328.2 K (131 °F) and pressures to 13.8 MPa (2000 psia). Ethane also exhibits a maximum in the adsorption amount at 5.6 MPa (800 psia) similar to CO_2. However, a minimum is observed in the amount of adsorbed at about 10 MPa. Replicate runs yielded identical results within the experimental uncertainty. As such, further investigation is needed to explain this behavior.

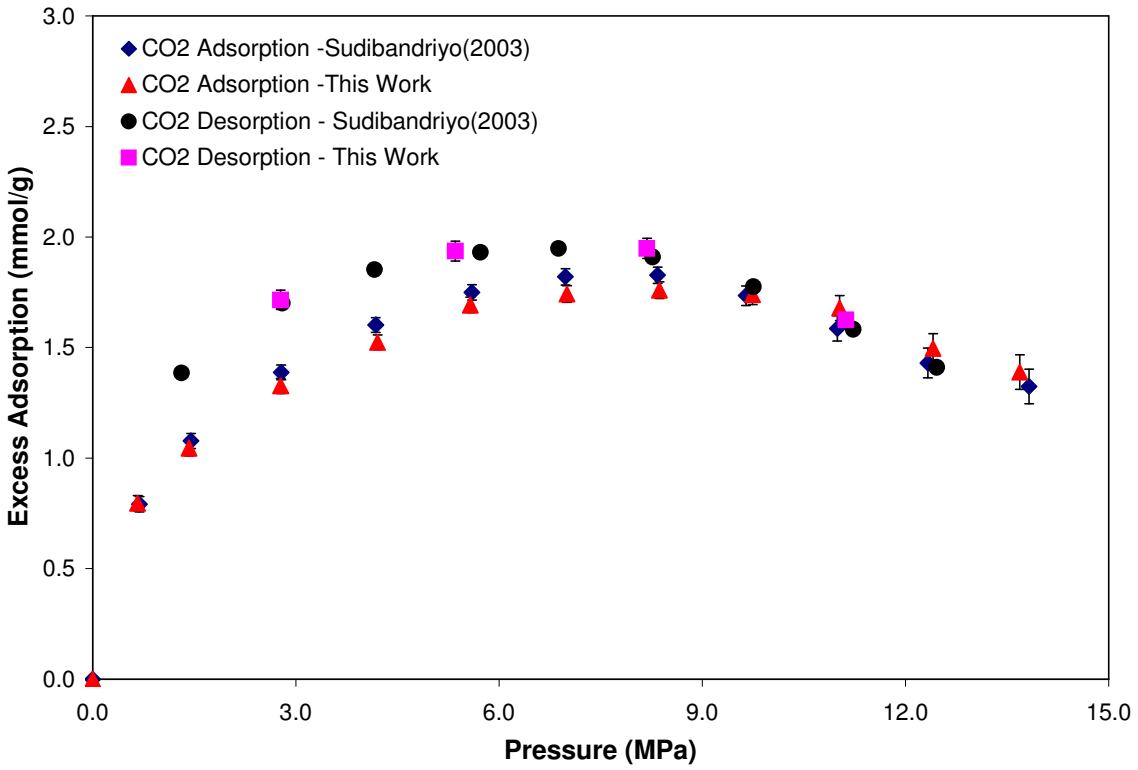

Figure 9: Excess Adsorption of Pure CO_2 on Dry Wyodak Coal at 328.2 K

The expected experimental uncertainty of the pure ethane adsorption data on Wyodak is about 11.8%. Figure 10 also shows that the adsorption and desorption data are comparable within the expected uncertainties, which indicates absence of hysteresis.

Figure 11 shows the excess adsorption of pure methane, nitrogen, CO_2 and ethane at 328.2 K (131 °F) and pressures to 13.8 MPa (2000 psia) on dry Wyodak Coal. At low to moderate pressures, an increasing order in the amount of gas adsorbed on this coal is observed for nitrogen, methane, ethane and CO_2, respectively. Specifically, the adsorption amount for CO_2 is 30% more than on Illinois #6. On the other hand, the adsorption amount for ethane is lower than on Illinois #6 below 7 MPa and equals that of Illinois #6 thereafter.

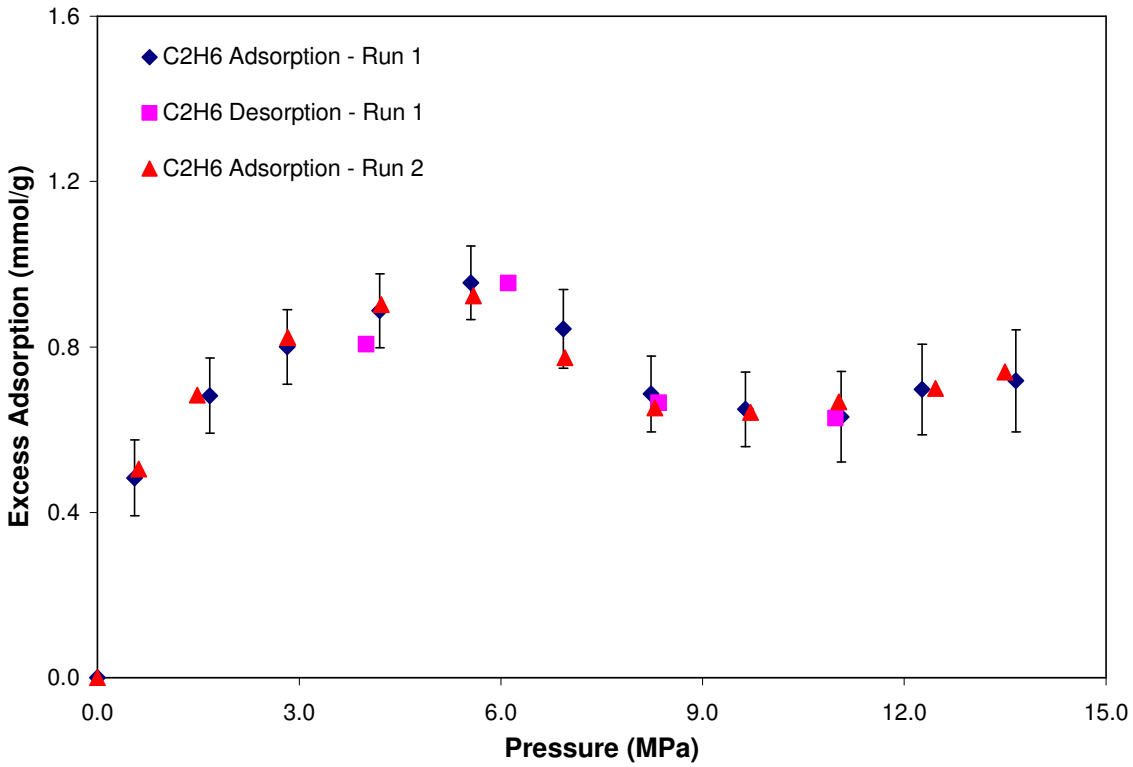

Figure 10: Excess Adsorption of Pure Ethane on Dry Wyodak Coal at 328.2 K

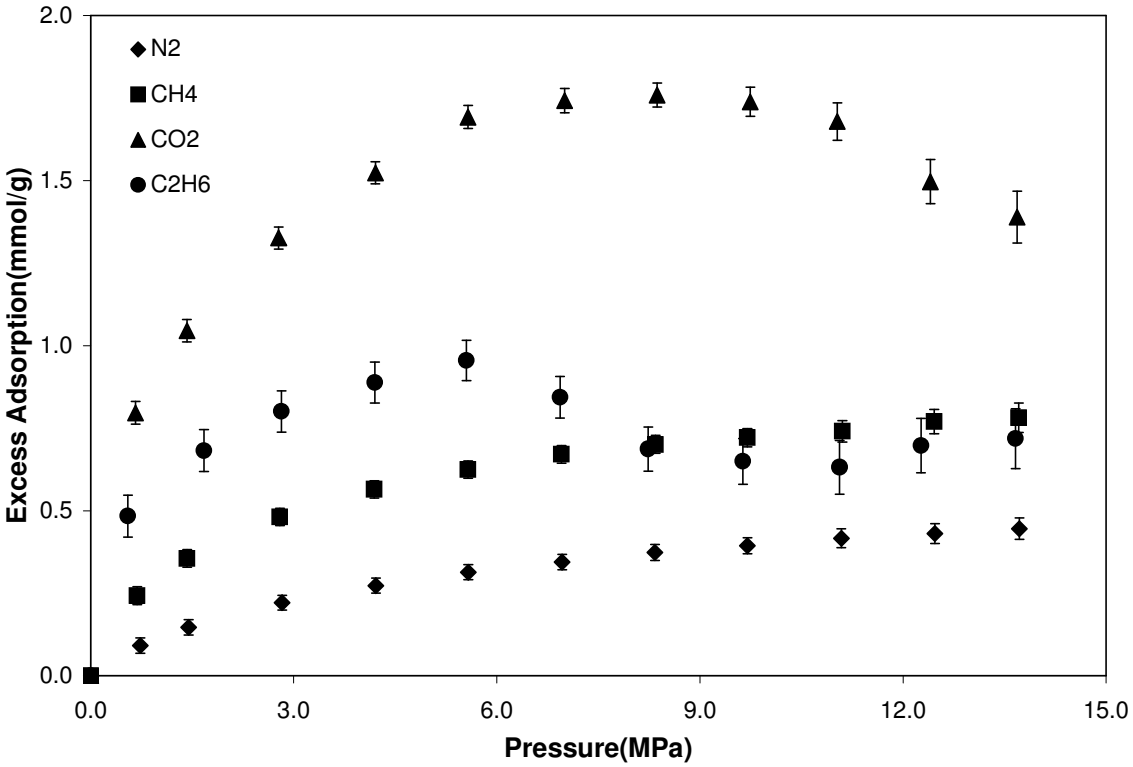

Figure 11: Excess Adsorption of Pure Coalbed Gases on Dry Wyodak Coal at 328.2 K

3.3 Adsorption on Dry Pocahontas #3 Coal

Adsorption of pure methane, nitrogen, CO_2 and ethane at 328.2 K (131°F) and pressures to 13.8 MPa (2000 psia) were measured on dry Pocahontas #3 coal. Tables 15 through 21 present the gas adsorption measurements on this coal.

Figures 12 through 17 show the effect of pressure on the Gibbs excess adsorption of pure methane, nitrogen, CO_2 and ethane on dry Pocahontas #3 coal. Figures 12 and 13 show the adsorption isotherms for pure nitrogen and methane, respectively. All the sorption measurements (adsorption and desorption) agree within the experimental uncertainty of about 3%. The adsorption amount increased by about 10% for both nitrogen and methane on Pocahontas #3 compared to the previously studied coals.

The CO_2 adsorption isotherm at 328.2 K is depicted in Figure 4. CO_2 adsorption isotherm exhibits a maximum in the amount adsorbed at 6.9 MPa (1000 psia). The expected experimental uncertainty of the pure CO_2 adsorption data on Pocahontas #3 is about 6.2%. Even though Pocahontas #3 has the maximum carbon content of the coals under study, the amount adsorbed for CO_2 is comparatively lower than Illinois #6 or Wyodak. This illustrates that the amount of adsorption does not depend entirely on the carbon content but also on other constituents of the coal such as oxygen, sulfur, ash and volatile matter.

Figure 14 also shows that the adsorption and desorption data are within the expected uncertainties, which indicates the absence of hysteresis. Further, comparison of the current adsorption measurements with comparable ones by Sudibandriyo (2003) shows agreement within 8% for most of the data. This level of agreement is well within the combined experimental uncertainty of both data sets.

Table 15:Adsorption of Pure Nitrogen on Dry Pocahontas #3 Coal at 328.2 K(Run 1)

SI Units

Void Volume (m^3)	0.00008288
Pump Press. (MPa)	6.90
Pump T (K)	328.2
Cell T (K)	328.2
Adsorbent mass (g)	59.5
Moist.content (%)	0.0
Ads.Phase Density (g/cm^3)	0.808

Pressure (MPa)	Gibbs Ads. (mmol/g)	Abs. Ads. (mmol/g)	Err.Gibbs (mmol/g)	Err.Abs. (mmol/g)
0.76	0.101	0.102	0.018	0.018
1.46	0.167	0.171	0.018	0.018
2.84	0.255	0.265	0.018	0.018
4.23	0.318	0.336	0.018	0.019
5.61	0.360	0.388	0.018	0.019
6.99	0.397	0.435	0.018	0.020
8.36	0.422	0.472	0.019	0.021
9.72	0.441	0.502	0.019	0.022
11.13	0.460	0.534	0.020	0.023
12.51	0.475	0.561	0.021	0.025
13.79	0.483	0.581	0.022	0.026
Desorption				
11.03	0.456	0.529	-	-
8.29	0.413	0.461	-	-
5.54	0.356	0.382	-	-
2.80	0.246	0.255	-	-

British Units

Void Volume (ft^3)	0.002927
Pump Press. (psia)	1000.9
Pump T (°F)	131.0
Cell T (°F)	131.0
Adsorbent mass (lb)	0.1312
Moist.content (%)	0.0
Ads.Phase Density (lb/ft^3)	50.44

Pressure (psia)	Gibbs Ads. (SCF/ton)	Abs. Ads. (SCF/ton)	Err.Gibbs (SCF/ton)	Err.Abs. (SCF/ton)
110.8	77.0	77.8	13.8	14.0
211.7	127.0	129.4	13.7	13.9
412.2	193.8	201.1	13.5	14.0
614.0	241.6	255.3	13.4	14.2
814.2	273.5	294.3	13.6	14.6
1014.0	301.3	330.4	13.8	15.1
1213.2	320.6	358.1	14.2	15.9
1410.1	334.5	380.7	14.7	16.7
1613.7	349.1	405.0	15.3	17.7
1814.3	360.3	426.0	15.9	18.8
2000.0	366.6	441.2	16.6	20.0
Desorption				
1600.1	346.2	401.1	-	-
1201.7	313.7	350.0	-	-
803.9	269.8	290.1	-	-
406.6	186.8	193.7	-	-

Table 16:Adsorption of Pure Nitrogen on Dry Pocahontas #3 Coal at 328.2 K(Run 2)

SI Units

Void Volume (m^3)	0.00008280
Pump Press. (MPa)	6.91
Pump T (K)	328.2
Cell T (K)	328.2
Adsorbent mass (g)	59.5
Moist.content (%)	0.0
Ads.Phase Density (g/cm^3)	0.808

Pressure (MPa)	Gibbs Ads. (mmol/g)	Abs. Ads. (mmol/g)	Err.Gibbs (mmol/g)	Err.Abs. (mmol/g)
1.61	0.179	0.183	0.017	0.017
4.21	0.319	0.337	0.017	0.018
6.99	0.397	0.435	0.018	0.020

British Units

Void Volume (ft^3)	0.002924
Pump Press. (psia)	1002.1
Pump T (°F)	131.0
Cell T (°F)	131.0
Adsorbent mass (lb)	0.1312
Moist.content (%)	0.0
Ads.Phase Density (lb/ft^3)	50.44

Pressure (psia)	Gibbs Ads. (SCF/ton)	Abs. Ads. (SCF/ton)	Err.Gibbs (SCF/ton)	Err.Abs. (SCF/ton)
233.3	136.0	138.8	12.9	13.2
610.8	242.0	255.7	13.1	13.9
1013.9	301.0	330.0	13.7	15.0

Table 17:Adsorption of Pure Methane on Dry Pocahontas #3 Coal at 328.2 K(Run 1)

SI Units

Void Volume (m^3)	0.00008280
Pump Press. (MPa)	6.92
Pump T (K)	328.2
Cell T (K)	328.2
Adsorbent mass (g)	59.5
Moist.content (%)	0.0
Ads.Phase Density (g/cm^3)	0.421

Pressure (MPa)	Gibbs Ads. (mmol/g)	Abs. Ads. (mmol/g)	Err.Gibbs (mmol/g)	Err.Abs. (mmol/g)
0.71	0.311	0.314	0.022	0.022
1.46	0.451	0.461	0.021	0.022
2.85	0.601	0.627	0.021	0.022
4.22	0.679	0.723	0.021	0.022
5.61	0.729	0.796	0.021	0.023
7.01	0.756	0.845	0.021	0.024
8.38	0.779	0.893	0.022	0.025
9.73	0.796	0.937	0.022	0.026
11.12	0.802	0.970	0.023	0.028
12.48	0.808	1.004	0.025	0.031
13.80	0.810	1.035	0.026	0.033
Desorption				
11.03	0.800	0.966	-	-
8.30	0.780	0.893	-	-
5.56	0.730	0.796	-	-
2.80	0.613	0.639	-	-

British Units

Void Volume (ft^3)	0.002924
Pump Press. (psia)	1003.2
Pump T (°F)	131.0
Cell T (°F)	131.0
Adsorbent mass (lb)	0.1312
Moist.content (%)	0.0
Ads.Phase Density (lb/ft^3)	26.28

Pressure (psia)	Gibbs Ads. (SCF/ton)	Abs. Ads. (SCF/ton)	Err.Gibbs (SCF/ton)	Err.Abs. (SCF/ton)
102.5	236.0	238.4	16.3	16.5
212.1	342.6	349.8	16.1	16.5
413.7	456.2	475.7	15.8	16.5
612.2	515.1	549.0	15.7	16.8
813.0	553.6	603.8	15.8	17.3
1016.2	573.9	641.6	16.1	18.0
1214.7	591.4	677.9	16.5	18.9
1411.8	604.4	711.1	17.1	20.1
1612.3	608.9	736.1	17.8	21.5
1810.3	613.1	762.0	18.6	23.2
2000.8	615.0	785.6	19.5	25.0
Desorption				
1599.3	607.4	733.1	-	-
1204.5	592.2	678.0	-	-
806.1	554.1	603.9	-	-
406.6	465.5	485.0	-	-

Table 18:Adsorption of Pure Methane on Dry Pocahontas #3 Coal at 328.2 K(Run 2)

SI Units

Void Volume (m^3)	0.00008280
Pump Press. (MPa)	6.90
Pump T (K)	328.2
Cell T (K)	328.2
Adsorbent mass (g)	59.5
Moist.content (%)	0.0
Ads.Phase Density (g/cm^3)	0.421

Pressure (MPa)	Gibbs Ads. (mmol/g)	Abs. Ads. (mmol/g)	Err.Gibbs (mmol/g)	Err.Abs. (mmol/g)
1.45	0.441	0.450	0.021	0.021
4.21	0.661	0.705	0.020	0.022
6.97	0.738	0.825	0.021	0.023

British Units

Void Volume (ft^3)	0.002924
Pump Press. (psia)	1000.1
Pump T (°F)	131.0
Cell T (°F)	131.0
Adsorbent mass (lb)	0.1312
Moist.content (%)	0.0
Ads.Phase Density (lb/ft^3)	26.28

Pressure (psia)	Gibbs Ads. (SCF/ton)	Abs. Ads. (SCF/ton)	Err.Gibbs (SCF/ton)	Err.Abs. (SCF/ton)
210.1	334.6	341.6	15.8	16.2
610.6	502.0	534.9	15.5	16.5
1011.0	560.2	625.9	15.8	17.7

Table 19: Adsorption of Pure CO_2 on Dry Pocahontas #3 Coal at 328.2 K

SI Units

Void Volume (m^3)	0.00008271
Pump Press. (MPa)	6.85
Pump T (K)	328.2
Cell T (K)	328.2
Adsorbent mass (g)	59.5
Moist.content (%)	0.0
Ads.Phase Density (g/cm^3)	1.027

Pressure (MPa)	Gibbs Ads. (mmol/g)	Abs. Ads. (mmol/g)	Err.Gibbs (mmol/g)	Err.Abs. (mmol/g)
0.73	0.636	0.643	0.035	0.035
1.47	0.826	0.847	0.034	0.035
2.84	1.000	1.052	0.033	0.035
4.24	1.093	1.093	0.033	0.036
5.62	1.138	1.286	0.033	0.037
6.96	1.155	1.370	0.033	0.039
8.35	1.127	1.435	0.035	0.044
9.70	1.078	1.526	0.039	0.056
11.06	0.937	1.587	0.060	0.102
12.42	0.843	1.761	0.066	0.139
13.73	0.777	1.900	0.076	0.185
Desorption				
11.19	0.907	1.567	-	-
8.21	1.098	1.386	-	-
5.46	1.129	1.270	-	-
2.82	0.982	1.033	-	-

British Units

Void Volume (ft^3)	0.002921
Pump Press. (psia)	993.5
Pump T (°F)	131.0
Cell T (°F)	131.0
Adsorbent mass (lb)	0.1312
Moist.content (%)	0.0
Ads.Phase Density (lb/ft^3)	64.11

Pressure (psia)	Gibbs Ads. (SCF/ton)	Abs. Ads. (SCF/ton)	Err.Gibbs (SCF/ton)	Err.Abs. (SCF/ton)
105.6	482.5	488.2	26.5	26.8
213.0	626.9	642.6	25.7	26.3
412.1	758.7	798.7	25.2	26.5
614.8	829.2	829.2	24.8	27.0
815.4	863.4	976.0	24.8	28.0
1009.4	876.5	1040.1	25.1	29.8
1211.4	855.7	1089.4	26.4	33.5
1406.4	817.9	1158.1	30.0	42.4
1604.1	711.2	1204.4	45.9	77.7
1801.6	639.5	1336.3	50.4	105.3
1991.3	589.7	1442.2	57.5	140.7
Desorption				
1622.4	688.6	1189.5	-	-
1191.3	833.5	1052.3	-	-
792.3	856.9	963.9	-	-
409.3	745.1	784.1	-	-

Table 20: Adsorption of Pure Ethane on Dry Pocahontas #3 Coal at 328.2 K (Run 1)

SI Units

Void Volume (m^3)	0.00008267
Pump Press. (MPa)	8.63
Pump T (K)	328.2
Cell T (K)	328.2
Adsorbent mass (g)	59.5
Moist.content (%)	0.0
Ads.Phase Density (g/cm^3)	0.444

Pressure (MPa)	Gibbs Ads. (mmol/g)	Abs. Ads. (mmol/g)	Err.Gibbs (mmol/g)	Err.Abs. (mmol/g)
0.58	0.608	0.618	0.097	0.098
1.46	0.749	0.780	0.096	0.100
2.85	0.827	0.904	0.095	0.104
4.23	0.849	0.995	0.094	0.110
5.59	0.828	1.084	0.093	0.122
6.95	0.731	1.239	0.095	0.161
8.34	0.618	1.498	0.092	0.223
9.71	0.590	1.768	0.091	0.273
11.09	0.565	1.975	0.091	0.318
12.47	0.540	2.140	0.091	0.362
13.77	0.527	2.319	0.091	0.402
		Desorption		
11.04	0.550	1.911	-	-
8.33	0.593	1.434	-	-
5.69	0.813	1.078	-	-
2.79	0.825	0.901	-	-

British Units

Void Volume (ft^3)	0.002919
Pump Press. (psia)	1252.0
Pump T (°F)	131.0
Cell T (°F)	131.0
Adsorbent mass (lb)	0.1312
Moist.content (%)	0.0
Ads.Phase Density (lb/ft^3)	27.72

Pressure (psia)	Gibbs Ads. (SCF/ton)	Abs. Ads. (SCF/ton)	Err.Gibbs (SCF/ton)	Err.Abs. (SCF/ton)
84.8	461.8	468.9	73.5	74.6
212.4	568.3	591.8	73.0	76.0
412.8	627.7	686.5	72.2	79.0
613.2	644.6	755.0	71.4	83.7
811.1	628.3	823.1	70.8	92.8
1008.6	554.9	940.4	72.1	122.2
1209.4	469.3	1136.8	69.8	169.2
1408.7	447.8	1341.8	69.2	207.4
1609.0	428.9	1498.7	69.2	241.7
1809.2	409.7	1624.0	69.3	274.6
1996.9	400.0	1759.9	69.4	305.3
		Desorption		
1601.2	417.3	1450.1	-	-
1207.9	450.1	1088.1	-	-
825.8	617.1	818.1	-	-
405.3	626.5	683.7	-	-

Table 21: Adsorption of Pure Ethane on Dry Pocahontas #3 Coal at 328.2 K (Run 2)

SI Units

Void Volume (m^3)	0.00008267
Pump Press. (MPa)	8.77
Pump T (K)	328.2
Cell T (K)	328.2
Adsorbent mass (g)	59.5
Moist.content (%)	0.0
Ads.Phase Density (g/cm^3)	0.444

Pressure (MPa)	Gibbs Ads. (mmol/g)	Abs. Ads. (mmol/g)	Err.Gibbs (mmol/g)	Err.Abs. (mmol/g)
0.67	0.581	0.591	0.073	0.074
1.45	0.746	0.776	0.072	0.075
4.27	0.838	0.983	0.070	0.083
6.97	0.710	1.208	0.074	0.126

British Units

Void Volume (ft^3)	0.002919
Pump Press. (psia)	1272.1
Pump T (°F)	131.0
Cell T (°F)	131.0
Adsorbent mass (lb)	0.1312
Moist.content (%)	0.0
Ads.Phase Density (lb/ft^3)	27.72

Pressure (psia)	Gibbs Ads. (SCF/ton)	Abs. Ads. (SCF/ton)	Err.Gibbs (SCF/ton)	Err.Abs. (SCF/ton)
96.8	441.2	448.9	55.2	56.2
210.3	565.9	589.0	54.8	57.0
619.0	635.8	746.4	53.4	62.7
1010.3	539.1	916.7	56.3	95.7

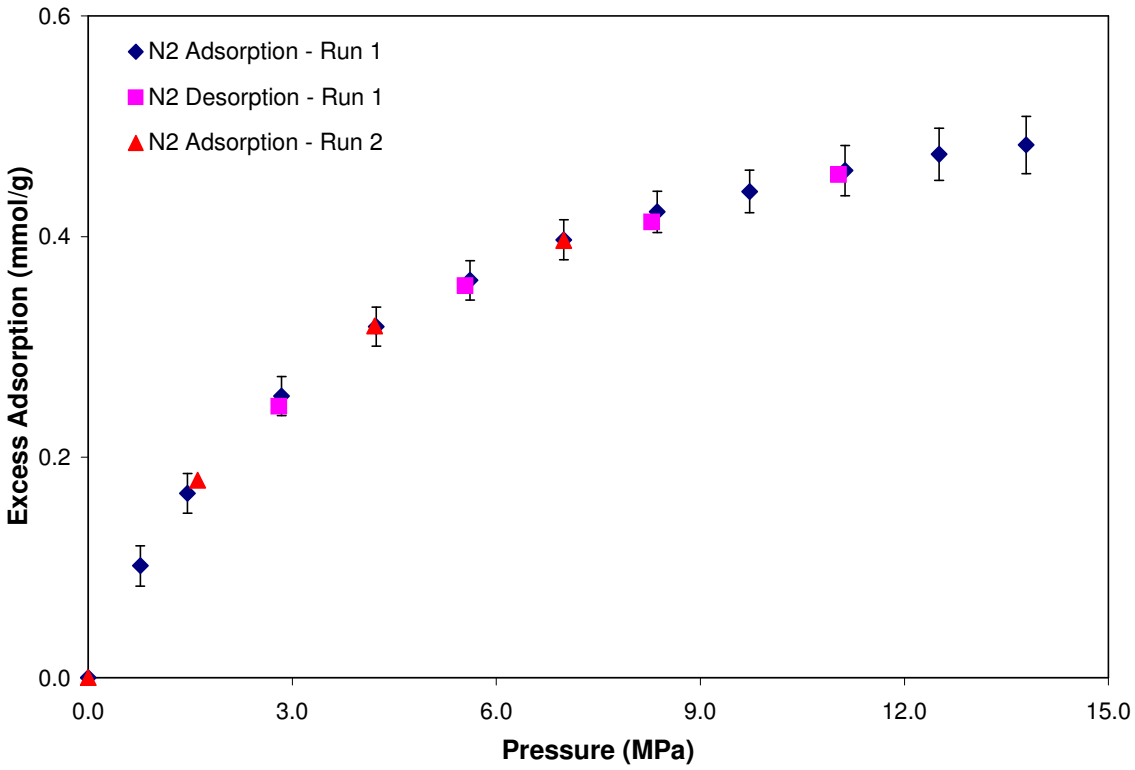

Figure 12: Excess Adsorption of Pure Nitrogen on Dry Pocahontas #3 Coal at 328.2 K

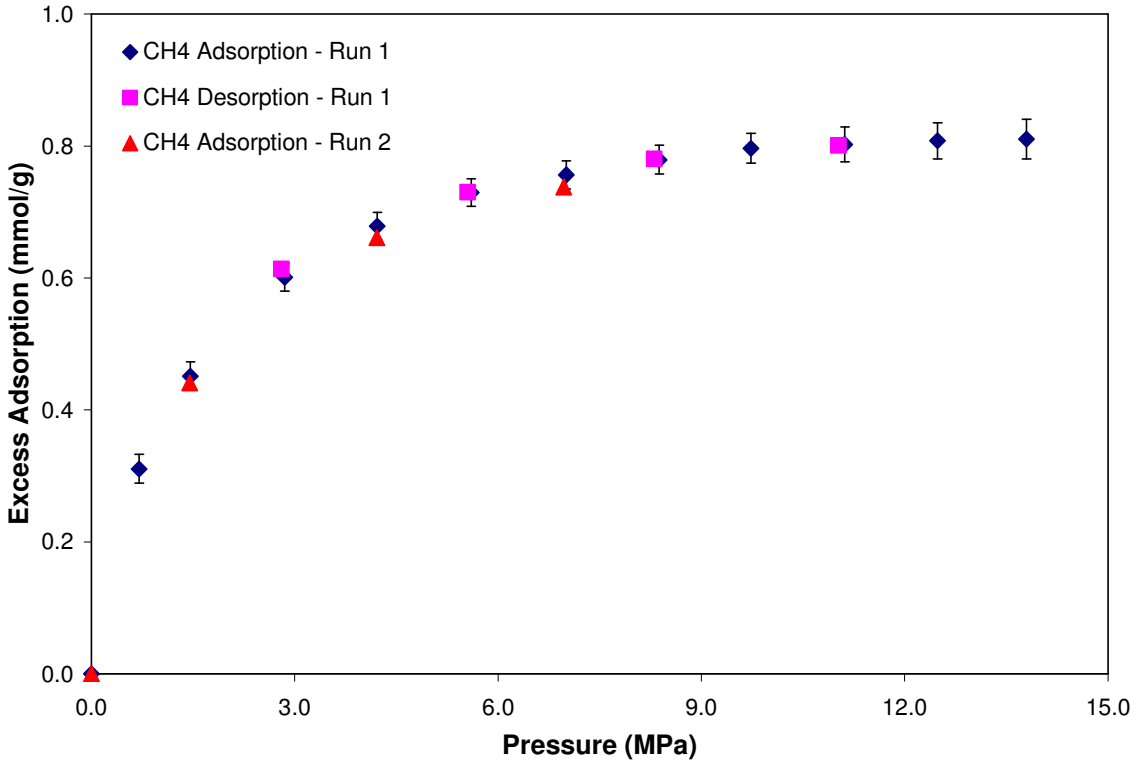

Figure 13: Excess Adsorption of Pure Methane on Dry Pocahontas #3 Coal at 328.2 K

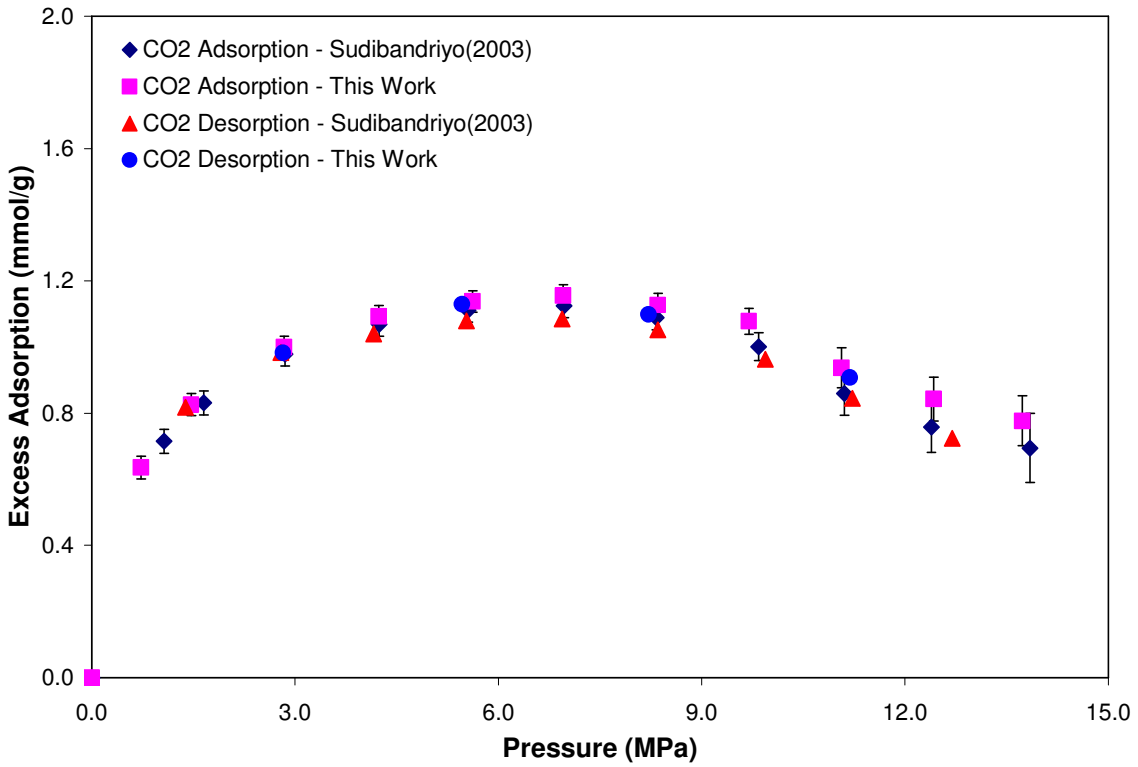

Figure 14: Excess Adsorption of Pure CO_2 on Dry Pocahontas #3 Coal at 328.2 K

Figure 15 depicts the adsorption isotherm for pure ethane at 328.2 K (131 °F) and pressures to 13.8 MPa (2000 psia). Similar to the CO_2 adsorption isotherm, ethane also exhibits a maximum in the adsorption amount at 4.2 MPa (613 psia). The expected experimental uncertainty of the pure ethane adsorption data on Illinois #6 is about 10.0%.

Figure 16 shows the excess adsorption of pure methane, nitrogen, CO_2 and ethane. Pocahontas #3 has the maximum amount of adsorption for both nitrogen and methane. However, the amount adsorbed for CO_2 and ethane were lowest compared to the other coals. This suggests that the adsorption is more on the low rank coals than on the high rank.

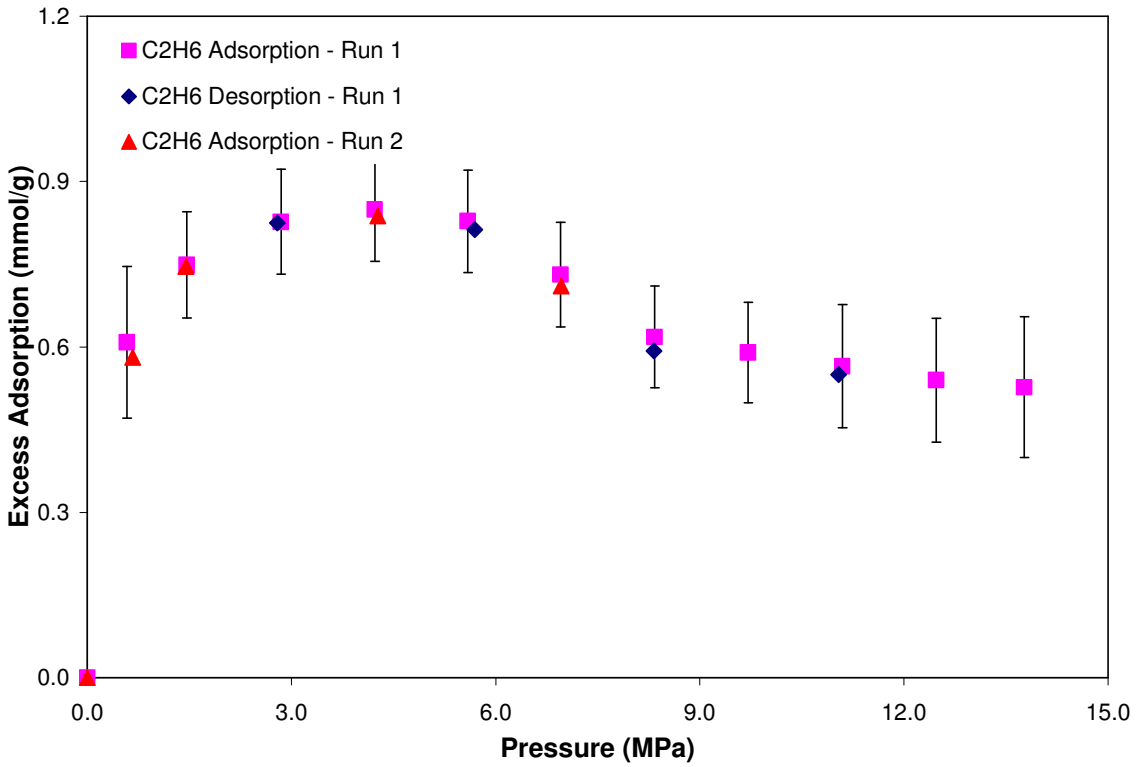

Figure 15: Excess Adsorption of Pure Ethane on Dry Pocahontas #3 Coal at 328.2 K

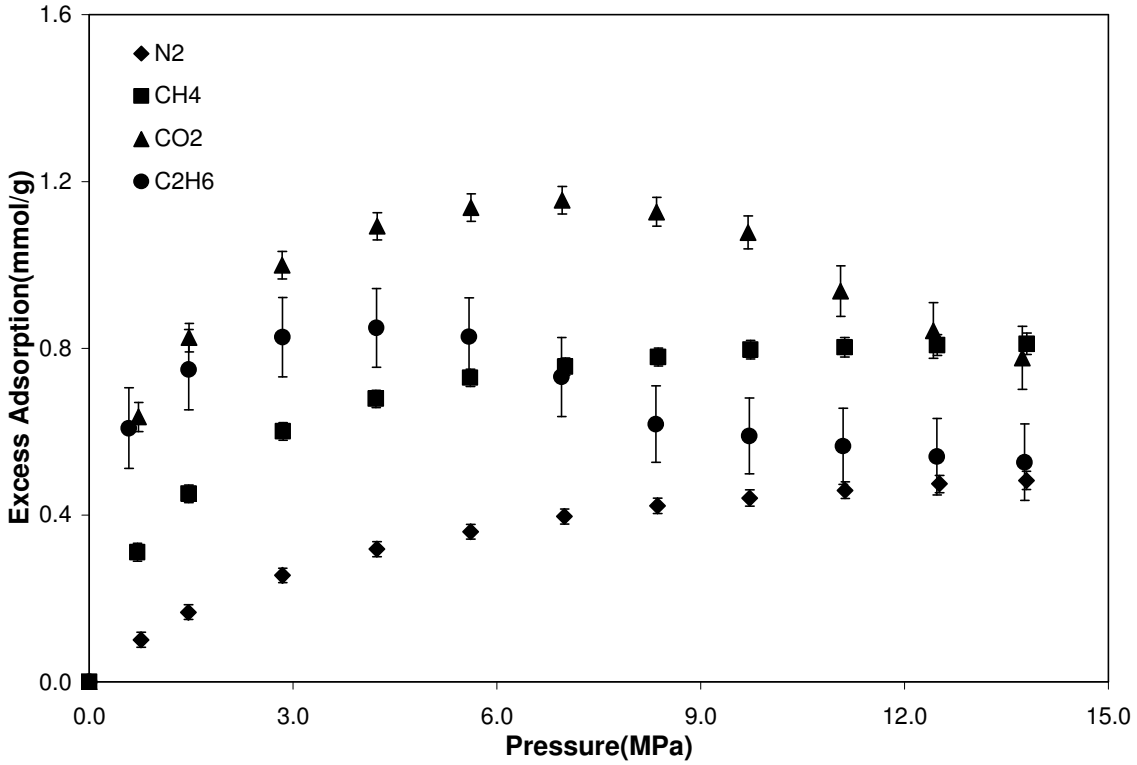

Figure 16: Excess Adsorption of Pure Coalbed Gases on Dry Pocahontas #3 Coal at 328.2 K

To study the effect of gas adsorption on the coal matrix (as indicated by adsorption capacity), repeated adsorption measurements were conducted in a selected sequence. Figures 17 depict measurements of methane adsorption on a fresh coal matrix, methane adsorption after CO_2 adsorption, and methane adsorption after both CO_2 and ethane adsorption. Little variation in isotherm reproducibility is shown. The methane adsorption isotherm on Pocahontas #3 is slightly outside expected uncertainties for some pressures after CO_2 adsorption. The methane adsorption after CO_2 and ethane adsorption, however, is comparable to the methane adsorption on the fresh matrix.

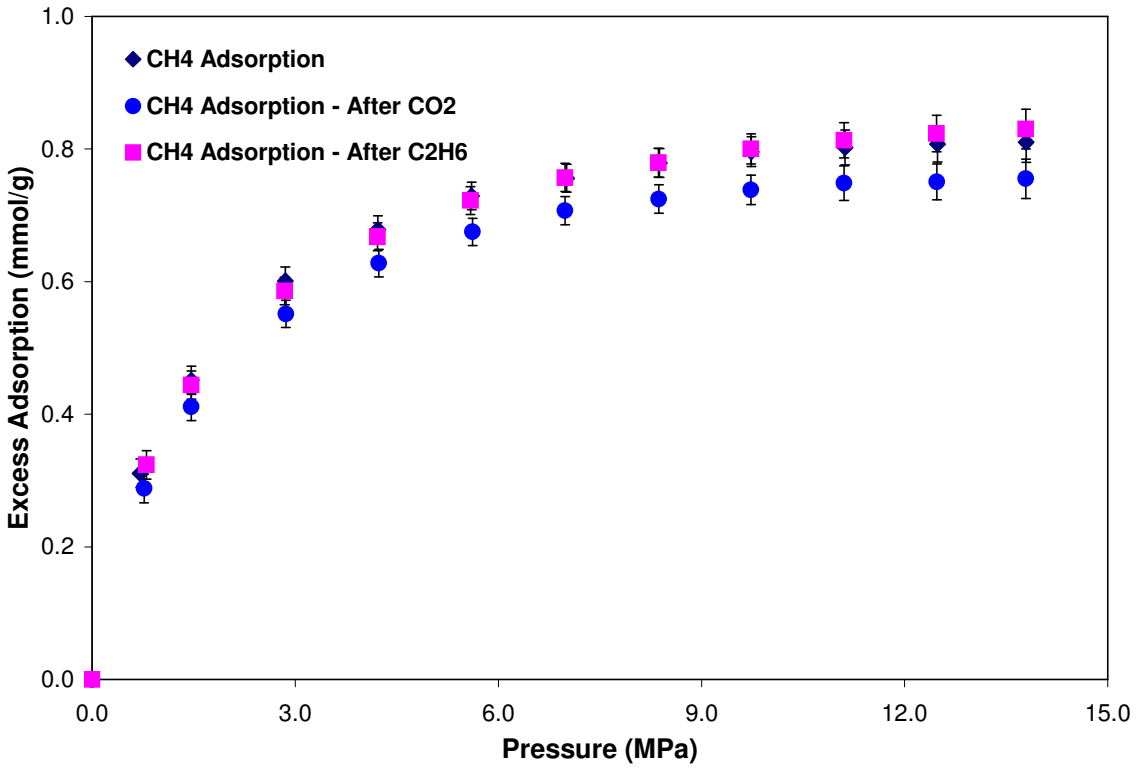

Figure 17: Excess Adsorption of Pure Methane on Dry Pocahontas #3 Before and After CO_2 and Ethane Gas Adsorption at 328.2 K

3.4 Adsorption on Dry Beulah Zap Coal

Adsorption of pure methane, nitrogen, CO_2 and ethane at 328.2 K (131 °F) and pressures to 13.8 MPa (2000 psia) were measured on dry Beulah Zap coal. Tables 22 through 28 present the gas adsorption measurements on this coal. Figures 18 through 24 depict the effect of pressure on Gibbs excess adsorption of pure methane, nitrogen, CO_2 and ethane on dry Beulah Zap coal.

Figures 18 and 19 present the adsorption isotherms for pure nitrogen and methane, respectively. As indicated by the figure, all the sorption measurements agree within the experimental uncertainty of about 5%.

The adsorption isotherm of CO_2 at 328.2 K is shown in Figure 20. As expected for a near-critical isotherm, CO_2 adsorption exhibits a maximum in the amount adsorbed at 8.3 MPa (1200 psia).

Figure 20 also shows some hysteresis for this coal during desorption. Since the current adsorption measurements agree with those of Sudibandriyo (2003) within 3% for most of the data, the desorption isotherm was expected to follow the same pattern. Therefore, the desorption measurements were forgone in favor of analyzing the composition of the desorbed gas to examine the possibility of CO_2 solvating (leaching) some of the coal constituents. Specifically, desorption gas samples were collected and analyzed using mass spectroscopy. As indicated by Figures 21a and 21b, the desorption gas contained mainly CO_2 as indicated by the single peak (Figure 21a). However, some insignificant impurities of less than 1% were found (Figure 21b) at mass numbers of 40, 45 and 46 (the first originating from impurity in the carrier gas helium). Hence, further analysis is needed to delineate the possibilities of CO_2 solvation.

Table 22: Adsorption of Pure Nitrogen on Dry Beulah Zap Coal at 328.2 K (Run 1)

SI Units

Void Volume (m^3)	0.00009904
Pump Press. (MPa)	6.89
Pump T (K)	328.2
Cell T (K)	328.2
Adsorbent mass (g)	39.4
Moist.content (%)	0.0
Ads.Phase Density (g/cm^3)	0.808

Pressure (MPa)	Gibbs Ads. (mmol/g)	Abs. Ads. (mmol/g)	Err.Gibbs (mmol/g)	Err.Abs. (mmol/g)
0.77	0.089	0.090	0.028	0.028
1.46	0.137	0.140	0.028	0.028
2.83	0.201	0.208	0.027	0.028
4.22	0.244	0.258	0.027	0.028
5.60	0.276	0.297	0.027	0.029
6.98	0.297	0.326	0.027	0.030
8.34	0.316	0.353	0.028	0.031
9.73	0.331	0.377	0.029	0.033
11.09	0.339	0.393	0.030	0.035
12.47	0.346	0.408	0.032	0.037
13.80	0.358	0.431	0.033	0.040
Desorption				
11.04	0.343	0.398	-	-
8.30	0.315	0.351	-	-
5.55	0.273	0.293	-	-
2.79	0.189	0.196	-	-

British Units

Void Volume (ft3)	0.003498
Pump Press. (psia)	999.5
Pump T (°F)	131.0
Cell T (°F)	131.0
Adsorbent mass (lb)	0.08686
Moist.content (%)	0.0
Ads.Phase Density (lb/ft3)	50.44

Pressure (psia)	Gibbs Ads. (SCF/ton)	Abs. Ads. (SCF/ton)	Err.Gibbs (SCF/ton)	Err.Abs. (SCF/ton)
111.1	67.8	68.4	21.2	21.4
211.8	104.2	106.1	20.9	21.3
409.9	152.3	157.9	20.5	21.3
611.9	185.4	195.9	20.4	21.6
812.3	209.8	225.8	20.5	22.1
1012.7	225.6	247.3	20.8	22.9
1209.7	240.1	268.1	21.4	23.9
1411.3	251.2	285.9	22.1	25.1
1608.4	257.0	298.0	23.0	26.6
1808.4	262.3	310.0	23.9	28.3
2001.7	271.6	327.0	25.0	30.1
Desorption				
1601.3	260.5	301.8	-	-
1203.3	238.9	266.6	-	-
805.4	206.9	222.5	-	-
404.6	143.7	148.9	-	-

Table 23: Adsorption of Pure Nitrogen on Dry Beulah Zap Coal at 328.2 K (Run 2)

SI Units

Void Volume (m^3)	0.00009904
Pump Press. (MPa)	6.89
Pump T (K)	328.2
Cell T (K)	328.2
Adsorbent mass (g)	39.4
Moist.content (%)	0.0
Ads.Phase Density (g/cm^3)	0.808

Pressure (MPa)	Gibbs Ads. (mmol/g)	Abs. Ads. (mmol/g)	Err.Gibbs (mmol/g)	Err.Abs. (mmol/g)
0.77	0.081	0.082	0.027	0.027
1.45	0.136	0.139	0.027	0.027
4.23	0.255	0.270	0.026	0.028
6.97	0.316	0.346	0.027	0.029

British Units

Void Volume (ft^3)	0.003498
Pump Press. (psia)	999.7
Pump T (°F)	131.0
Cell T (°F)	131.0
Adsorbent mass (lb)	0.08686
Moist.content (%)	0.0
Ads.Phase Density (lb/ft^3)	50.44

Pressure (psia)	Gibbs Ads. (SCF/ton)	Abs. Ads. (SCF/ton)	Err.Gibbs (SCF/ton)	Err.Abs. (SCF/ton)
111.5	61.6	62.2	20.6	20.8
210.3	103.2	105.2	20.3	20.7
613.8	193.7	204.7	19.9	21.0
1010.8	239.8	262.8	20.4	22.3

Table 24: Adsorption of Pure Methane on Dry Beulah Zap Coal at 328.2 K (Run 1)

SI Units

Void Volume (m^3)	0.00009898
Pump Press. (MPa)	6.90
Pump T (K)	328.2
Cell T (K)	328.2
Adsorbent mass (g)	39.4
Moist.content (%)	0.0
Ads.Phase Density (g/cm^3)	0.421

Pressure (MPa)	Gibbs Ads. (mmol/g)	Abs. Ads. (mmol/g)	Err.Gibbs (mmol/g)	Err.Abs. (mmol/g)
0.72	0.257	0.260	0.033	0.033
1.44	0.361	0.369	0.032	0.033
2.83	0.476	0.496	0.032	0.033
4.22	0.544	0.580	0.031	0.033
5.60	0.591	0.644	0.031	0.034
6.97	0.621	0.694	0.032	0.036
8.33	0.651	0.745	0.033	0.037
9.71	0.664	0.780	0.034	0.040
11.09	0.681	0.822	0.035	0.043
12.48	0.695	0.864	0.037	0.046
13.78	0.708	0.904	0.042	0.054
Desorption				
11.06	0.696	0.841	-	-
8.30	0.669	0.766	-	-
5.54	0.605	0.659	-	-
2.78	0.468	0.488	-	-

British Units

Void Volume (ft^3)	0.003495
Pump Press. (psia)	1001.3
Pump T (°F)	131.0
Cell T (°F)	131.0
Adsorbent mass (lb)	0.08686
Moist.content (%)	0.0
Ads.Phase Density (lb/ft^3)	26.28

Pressure (psia)	Gibbs Ads. (SCF/ton)	Abs. Ads. (SCF/ton)	Err.Gibbs (SCF/ton)	Err.Abs. (SCF/ton)
103.9	195.3	197.3	24.8	25.1
209.4	274.0	279.8	24.5	25.0
410.3	361.0	376.3	24.1	25.1
611.7	412.8	439.9	23.8	25.4
811.9	448.4	489.0	23.9	26.0
1010.6	471.4	526.6	24.2	27.0
1208.4	493.8	565.7	24.8	28.4
1408.3	503.7	592.3	25.6	30.1
1609.1	516.5	624.2	26.7	32.3
1809.8	527.4	655.5	28.0	34.8
1998.7	537.4	686.2	32.0	40.9
Desorption				
1603.5	528.6	638.3	-	-
1203.2	507.9	581.4	-	-
803.0	458.9	499.9	-	-
403.0	355.5	370.3	-	-

Table 25: Adsorption of Pure Methane on Dry Beulah Zap Coal at 328.2 K (Run 2)

SI Units

Void Volume (m^3)	0.00009898
Pump Press. (MPa)	6.91
Pump T (K)	328.2
Cell T (K)	328.2
Adsorbent mass (g)	39.4
Moist.content (%)	0.0
Ads.Phase Density (g/cm^3)	0.421

Pressure (MPa)	Gibbs Ads. (mmol/g)	Abs. Ads. (mmol/g)	Err.Gibbs (mmol/g)	Err.Abs. (mmol/g)
1.44	0.343	0.350	0.031	0.032
5.61	0.576	0.629	0.031	0.033
9.76	0.642	0.756	0.033	0.039

British Units

Void Volume (ft^3)	0.003495
Pump Press. (psia)	1002.6
Pump T (°F)	131.0
Cell T (°F)	131.0
Adsorbent mass (lb)	0.08686
Moist.content (%)	0.0
Ads.Phase Density (lb/ft^3)	26.28

Pressure (psia)	Gibbs Ads. (SCF/ton)	Abs. Ads. (SCF/ton)	Err.Gibbs (SCF/ton)	Err.Abs. (SCF/ton)
208.7	260.4	265.8	23.8	24.2
813.9	437.5	477.3	23.2	25.3
1415.2	487.6	573.9	25.1	29.5

Table 26: Adsorption of Pure CO_2 on Dry Beulah Zap Coal at 328.2 K

SI Units

Void Volume (m^3)	0.00009891
Pump Press. (MPa)	6.74
Pump T (K)	328.2
Cell T (K)	328.2
Adsorbent mass (g)	39.4
Moist.content (%)	0.0
Ads.Phase Density (g/cm^3)	1.027

Pressure (MPa)	Gibbs Ads. (mmol/g)	Abs. Ads. (mmol/g)	Err.Gibbs (mmol/g)	Err.Abs. (mmol/g)
0.98	0.975	0.991	0.072	0.073
1.45	1.107	1.134	0.071	0.073
2.80	1.348	1.418	0.069	0.073
4.18	1.525	1.655	0.067	0.073
5.54	1.693	1.909	0.066	0.075
6.98	1.721	2.044	0.066	0.079
8.31	1.752	2.225	0.069	0.088
9.73	1.621	2.304	0.103	0.147
11.10	1.431	2.438	0.122	0.207
12.46	1.270	2.670	0.143	0.301
13.72	1.220	2.981	0.177	0.431

British Units

Void Volume (ft^3)	0.003493
Pump Press. (psia)	978.0
Pump T (°F)	131.0
Cell T (°F)	131.0
Adsorbent mass (lb)	0.08686
Moist.content (%)	0.0
Ads.Phase Density (lb/ft^3)	64.11

Pressure (psia)	Gibbs Ads. (SCF/ton)	Abs. Ads. (SCF/ton)	Err.Gibbs (SCF/ton)	Err.Abs. (SCF/ton)
142.3	740.0	752.1	54.3	55.2
210.2	840.1	860.8	53.8	55.1
406.0	1023.4	1076.4	52.4	55.1
606.7	1157.2	1256.2	51.2	55.6
804.2	1285.0	1449.0	50.4	56.8
1012.9	1306.3	1551.6	50.4	59.8
1205.9	1329.8	1689.0	52.4	66.6
1411.7	1230.5	1748.7	78.3	111.2
1609.7	1086.3	1850.6	92.3	157.3
1807.6	964.2	2026.3	108.8	228.7
1990.0	926.0	2262.3	134.0	327.4

Table 27: Adsorption of Pure Ethane on Dry Beulah Zap Coal at 328.2 K (Run 1)

SI Units

Void Volume (m^3)	0.00009889
Pump Press. (MPa)	8.96
Pump T (K)	328.2
Cell T (K)	328.2
Adsorbent mass (g)	39.4
Moist.content (%)	0.0
Ads.Phase Density (g/cm^3)	0.444

Pressure (MPa)	Gibbs Ads. (mmol/g)	Abs. Ads. (mmol/g)	Err.Gibbs (mmol/g)	Err.Abs. (mmol/g)
0.62	0.470	0.478	0.151	0.154
1.45	0.601	0.626	0.151	0.157
2.79	0.742	0.810	0.149	0.163
4.30	0.789	0.928	0.147	0.173
5.60	0.764	1.002	0.146	0.191
6.95	0.544	0.921	0.150	0.254
8.30	0.481	1.157	0.144	0.346
9.73	0.517	1.553	0.142	0.426
11.10	0.522	1.827	0.141	0.495
12.47	0.524	2.077	0.142	0.561
13.76	0.528	2.323	0.142	0.623
Desorption				
11.03	0.528	1.832	-	-
8.33	0.451	1.091	-	-
6.06	0.745	1.039	-	-
2.92	0.853	0.936	-	-

British Units

Void Volume (ft^3)	0.003492
Pump Press. (psia)	1299.1
Pump T (°F)	131.0
Cell T (°F)	131.0
Adsorbent mass (lb)	0.08686
Moist.content (%)	0.0
Ads.Phase Density (lb/ft^3)	27.72

Pressure (psia)	Gibbs Ads. (SCF/ton)	Abs. Ads. (SCF/ton)	Err.Gibbs (SCF/ton)	Err.Abs. (SCF/ton)
90.2	357.1	362.9	115.0	116.8
210.3	456.2	474.9	114.2	118.9
405.4	563.1	614.6	113.0	123.3
623.6	598.9	704.5	111.6	131.3
812.5	579.9	760.5	110.8	145.3
1008.1	412.8	698.8	114.0	192.9
1204.4	364.9	877.9	109.2	262.8
1410.8	392.6	1178.4	107.6	323.0
1610.6	396.4	1386.7	107.4	375.6
1808.6	397.8	1576.5	107.4	425.8
1996.4	400.8	1763.2	107.6	473.1
Desorption				
1599.2	400.6	1390.2	-	-
1208.9	342.2	828.3	-	-
878.7	565.7	788.4	-	-
423.9	647.2	710.1	-	-

Table 28: Adsorption of Pure Ethane on Dry Beulah Zap Coal at 328.2 K (Run 2)

SI Units

Void Volume (m^3)	0.00009889
Pump Press. (MPa)	9.01
Pump T (K)	328.2
Cell T (K)	328.2
Adsorbent mass (g)	39.4
Moist.content (%)	0.0
Ads.Phase Density (g/cm^3)	0.444

Pressure (MPa)	Gibbs Ads. (mmol/g)	Abs. Ads. (mmol/g)	Err.Gibbs (mmol/g)	Err.Abs. (mmol/g)
1.50	0.716	0.747	0.149	0.155
5.65	0.806	1.062	0.145	0.191
9.64	0.548	1.628	0.141	0.418

British Units

Void Volume (ft^3)	0.003492
Pump Press. (psia)	1306.1
Pump T (°F)	131.0
Cell T (°F)	131.0
Adsorbent mass (lb)	0.08686
Moist.content (%)	0.0
Ads.Phase Density (lb/ft^3)	27.72

Pressure (psia)	Gibbs Ads. (SCF/ton)	Abs. Ads. (SCF/ton)	Err.Gibbs (SCF/ton)	Err.Abs. (SCF/ton)
216.9	543.6	566.6	113.1	117.9
818.8	611.4	806.0	109.9	144.8
1398.5	416.2	1235.8	106.8	317.1

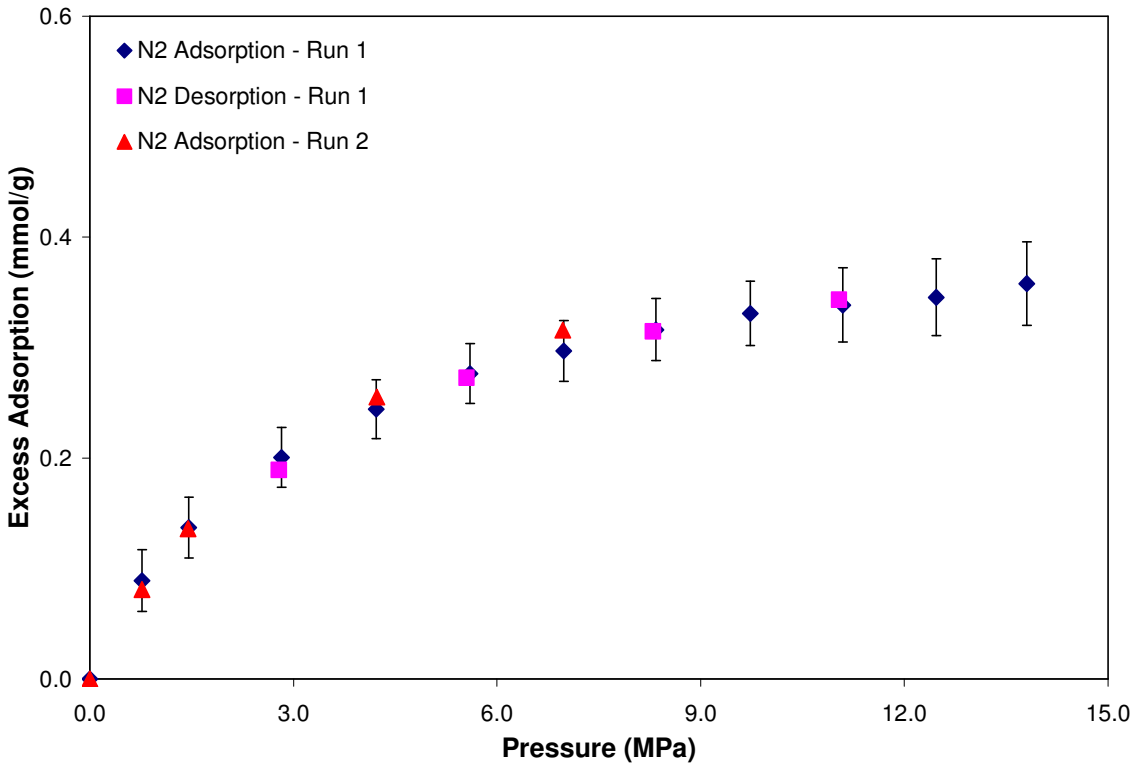

Figure 18: Excess Adsorption of Pure Nitrogen on Dry Beulah Zap Coal at 328.2 K

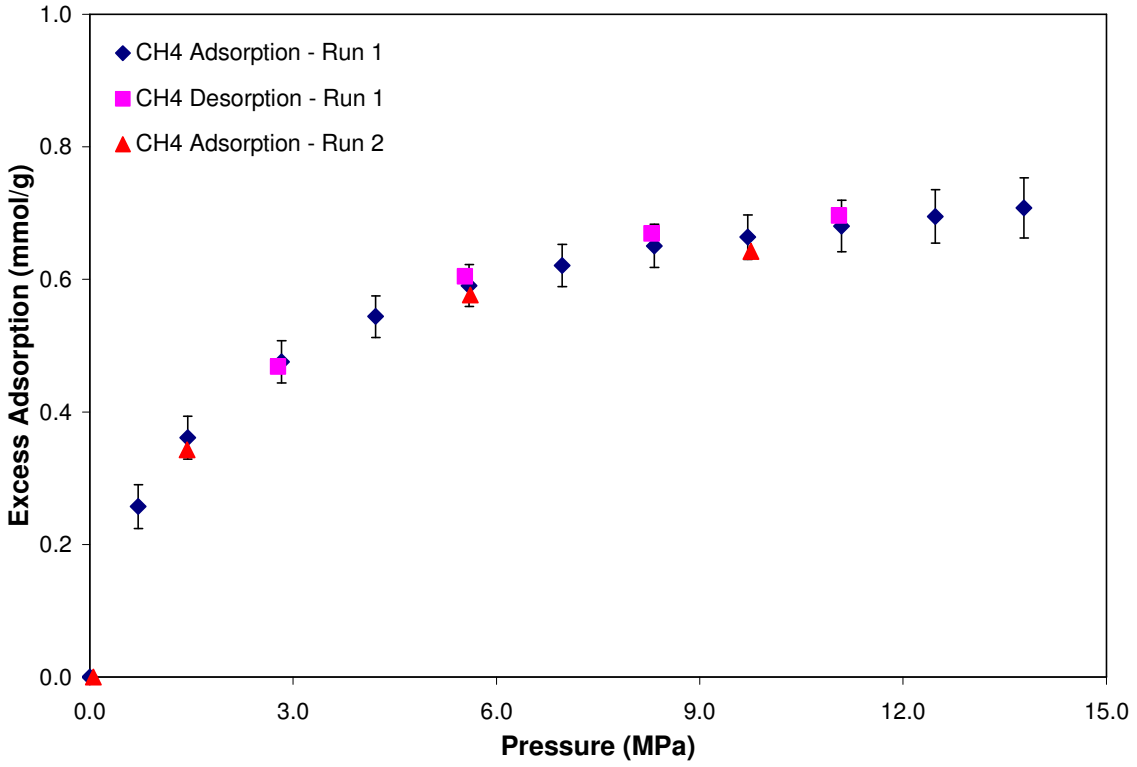

Figure 19: Excess Adsorption of Pure Methane on Dry Beulah Zap Coal at 328.2 K

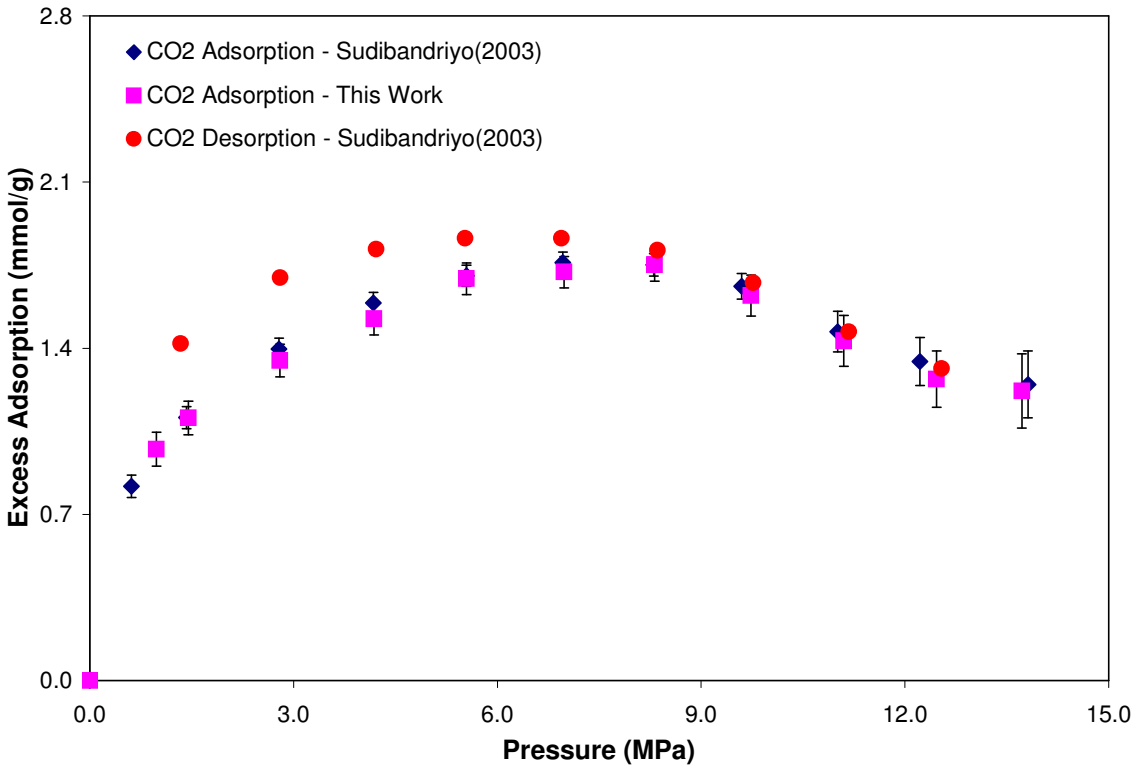

Figure 20: Excess Adsorption of Pure CO_2 on Dry Beulah Zap Coal at 328.2 K

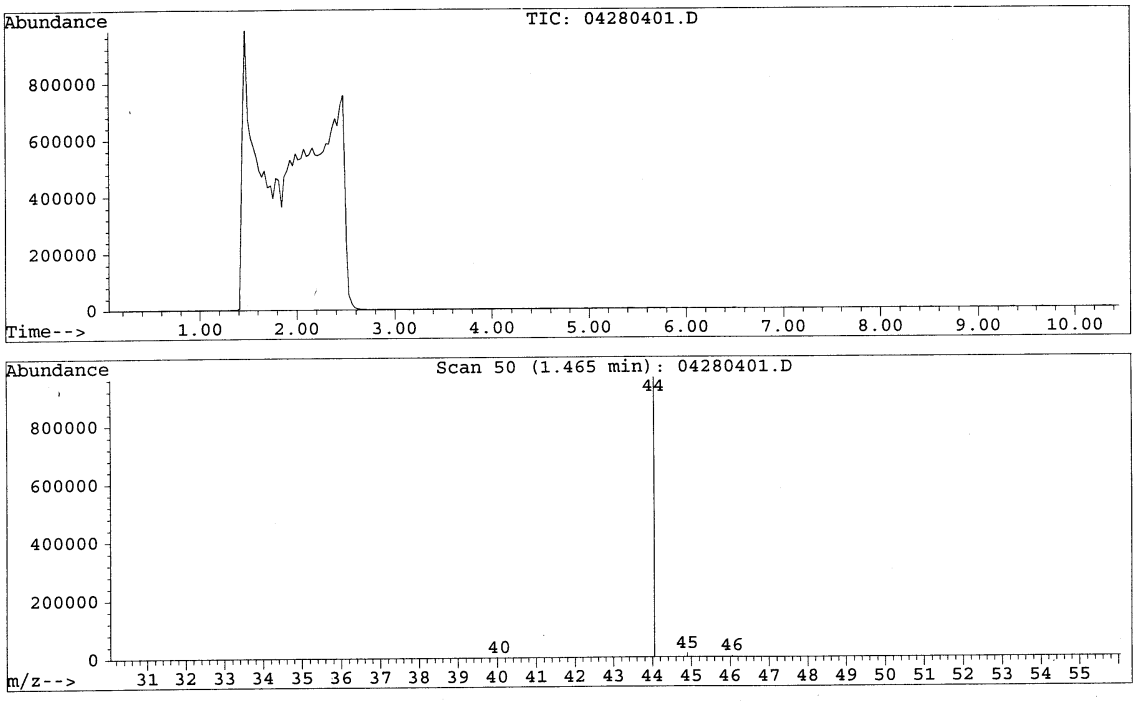

Figures 21a: Mass Spectroscopy Analysis of Desorbed Gas from Dry Beulah Zap Coal

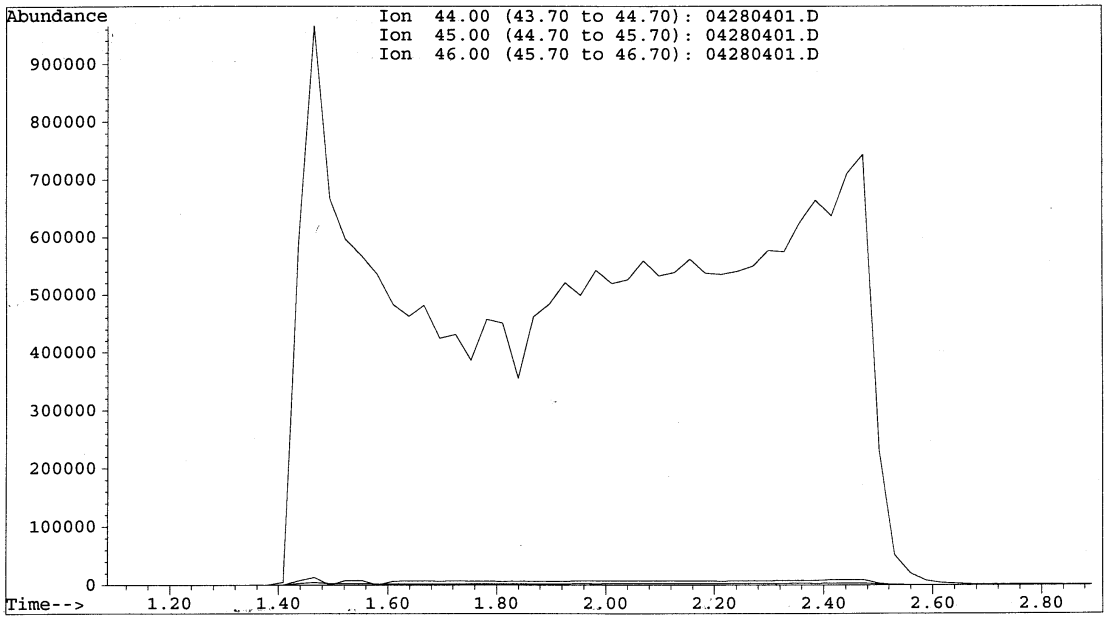

Figures 21b: Mass Spectroscopy Analysis of Desorbed Gas from Dry Beulah Zap Coal

Figure 22 depicts the adsorption isotherm for pure ethane at 328.2 K (131 °F) and pressures to 13.8 MPa (2000 psia). Similar to CO_2, ethane also exhibits a maximum in the adsorption amount at 4.3 MPa (623 psia). However, a minimum in the amount adsorbed is obtained after the observed maximum. This feature, however, might be due to measurement uncertainties. The expected experimental uncertainty of the pure ethane adsorption data on Beulah Zap is about 8.7%. The adsorption and desorption data are within experimental uncertainties.

Figure 23 shows the excess adsorption of pure methane, nitrogen, CO_2 and ethane on dry Beulah Zap coal. Specifically, the relative ratio in the amount adsorbed of CO_2 to ethane was the maximum among the coals studied so far. This behavior, however, might be due to higher percentage of oxygen content or the equilibrium moisture content compared to other coals.

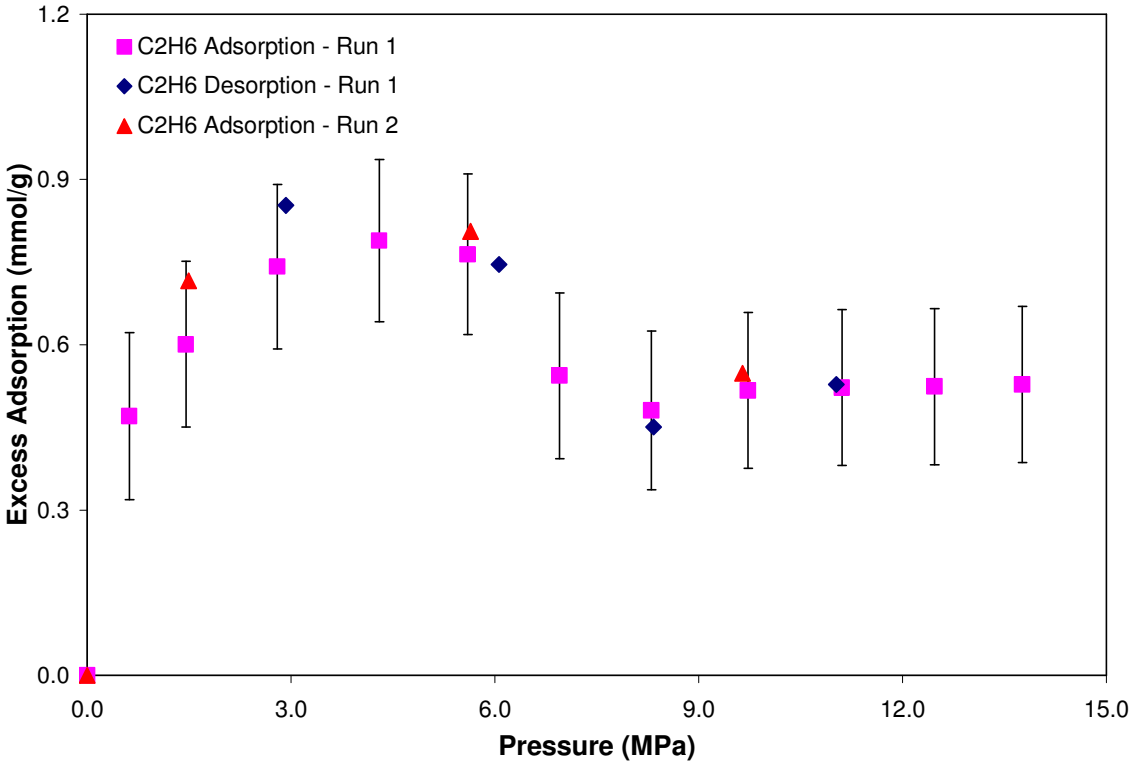

Figure 22: Excess Adsorption of Pure Ethane on Dry Beulah Zap Coal at 328.2 K

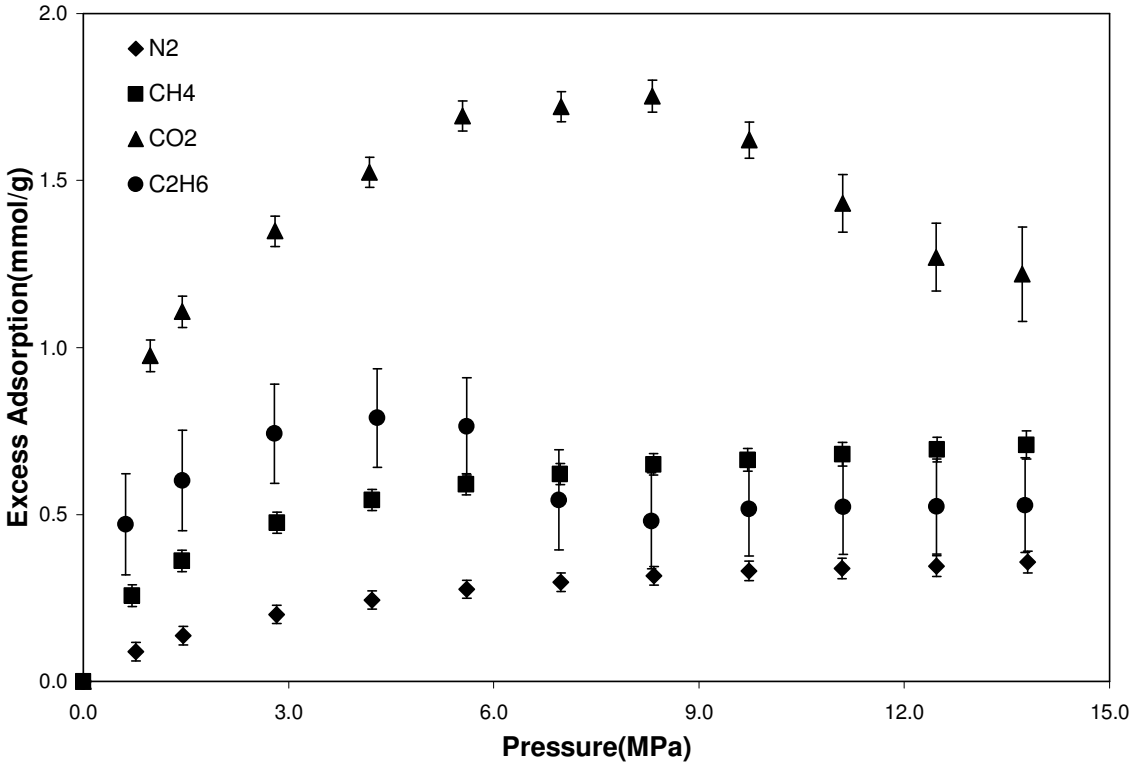

Figure 23: Excess Adsorption of Pure Coalbed Gases on Dry Beulah Zap Coal at 328.2 K

Figure 24 depict measurements of methane adsorption on a fresh coal matrix, methane adsorption after CO_2 adsorption, and methane adsorption after both CO_2 and ethane adsorption. Little variation in isotherm reproducibility is shown.

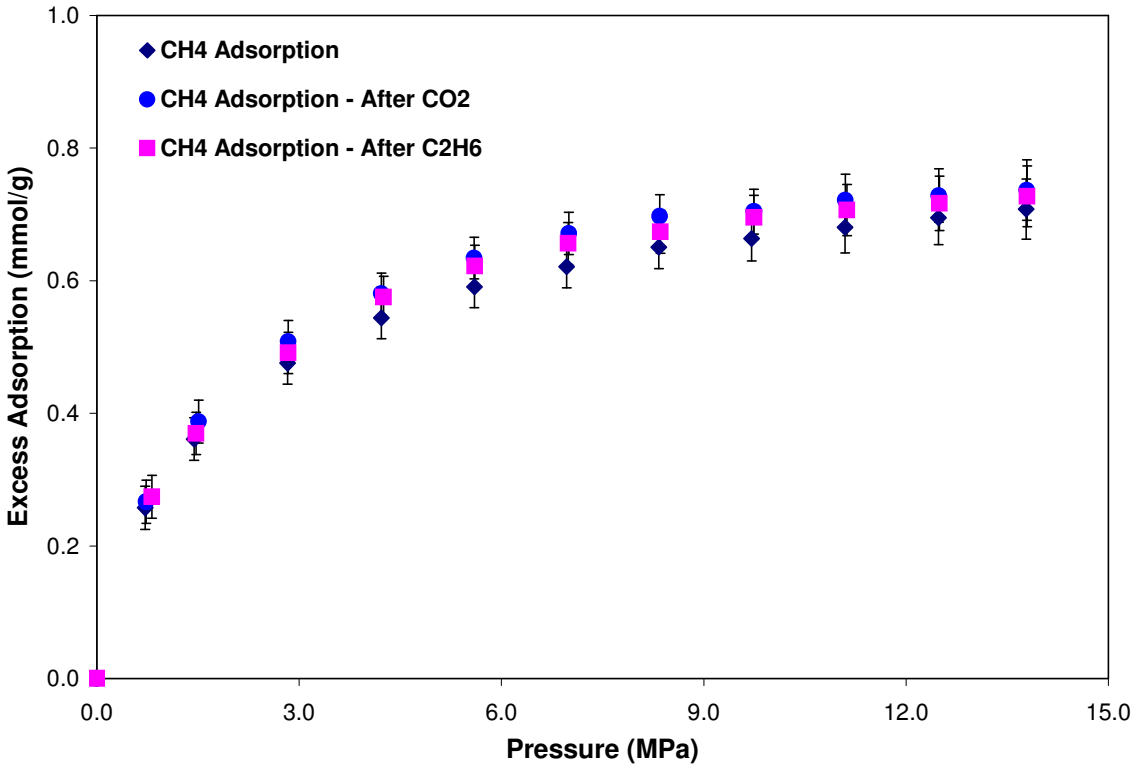

Figure 24: Adsorption of Pure Methane on Dry Beulah Zap Before and After CO_2 and Ethane Gas Adsorption at 328.2 K

3.5 Adsorption on Dry Upper Freeport Coal

Adsorption of pure methane, nitrogen, CO_2 and ethane at 328.2 K (131 °F) and pressures to 13.8 MPa (2000 psia) were measured on dry Upper Freeport coal. Tables 29 through 35 present the gas adsorption measurements on this coal. Figures 25 through 30 depict the effect of pressure on the Gibbs excess adsorption of pure methane, nitrogen, CO_2 and ethane on dry Upper Freeport coal.

Figures 25 and 26 present the adsorption isotherms for pure nitrogen and methane, respectively. The adsorption and desorption data were identical indicating no discernable change in the structure of the coal.

Table 29: Adsorption of Pure Nitrogen on Dry Upper Freeport Coal at 328.2 K (Run 1)

SI Units

Void Volume (m^3)	0.00007920
Pump Press. (MPa)	6.92
Pump T (K)	328.2
Cell T (K)	328.2
Adsorbent mass (g)	67.2
Moist.content (%)	0.0
Ads.Phase Density (g/cm^3)	0.808

Pressure (MPa)	Gibbs Ads. (mmol/g)	Abs. Ads. (mmol/g)	Err.Gibbs (mmol/g)	Err.Abs. (mmol/g)
0.77	0.079	0.080	0.016	0.016
1.44	0.124	0.126	0.016	0.016
2.83	0.193	0.200	0.016	0.016
4.25	0.237	0.251	0.016	0.017
5.61	0.273	0.294	0.016	0.017
7.03	0.300	0.329	0.016	0.018
8.41	0.319	0.357	0.017	0.019
9.74	0.335	0.382	0.017	0.020
11.11	0.349	0.404	0.018	0.021
12.50	0.360	0.426	0.019	0.022
13.77	0.371	0.446	0.019	0.023
		Desorption		
11.07	0.347	0.402	-	-
8.31	0.315	0.352	-	-
5.56	0.270	0.291	-	-
2.83	0.197	0.204	-	-

British Units

Void Volume (ft^3)	0.002797
Pump Press. (psia)	1003.6
Pump T (°F)	131.0
Cell T (°F)	131.0
Adsorbent mass (lb)	0.1482
Moist.content (%)	0.0
Ads.Phase Density (lb/ft^3)	50.44

Pressure (psia)	Gibbs Ads. (SCF/ton)	Abs. Ads. (SCF/ton)	Err.Gibbs (SCF/ton)	Err.Abs. (SCF/ton)
112.1	59.9	60.5	12.3	12.4
208.5	94.0	95.7	12.2	12.4
410.8	146.5	152.0	12.0	12.4
616.6	180.0	190.2	12.0	12.7
813.5	207.3	223.1	12.1	13.0
1019.0	227.9	250.0	12.3	13.5
1220.1	242.3	270.9	12.7	14.2
1413.2	254.5	289.7	13.1	14.9
1611.4	264.6	306.9	13.6	15.8
1812.8	273.3	323.2	14.2	16.8
1997.5	281.3	338.5	14.8	17.8
		Desorption		
1605.4	263.3	305.3	-	-
1204.9	239.0	266.8	-	-
806.1	205.3	220.7	-	-
410.1	149.3	154.9	-	-

Table 30: Adsorption of Pure Nitrogen on Dry Upper Freeport Coal at 328.2 K (Run 2)

SI Units

Void Volume (m^3)	0.00007920
Pump Press. (MPa)	6.90
Pump T (K)	328.2
Cell T (K)	328.2
Adsorbent mass (g)	67.2
Moist.content (%)	0.0
Ads.Phase Density (g/cm^3)	0.808

Pressure (MPa)	Gibbs Ads. (mmol/g)	Abs. Ads. (mmol/g)	Err.Gibbs (mmol/g)	Err.Abs. (mmol/g)
1.45	0.125	0.127	0.014	0.015
5.63	0.273	0.294	0.014	0.015
9.75	0.334	0.380	0.016	0.018

British Units

Void Volume (ft^3)	0.002797
Pump Press. (psia)	1000.7
Pump T (°F)	131.0
Cell T (°F)	131.0
Adsorbent mass (lb)	0.1482
Moist.content (%)	0.0
Ads.Phase Density (lb/ft^3)	50.44

Pressure (psia)	Gibbs Ads. (SCF/ton)	Abs. Ads. (SCF/ton)	Err.Gibbs (SCF/ton)	Err.Abs. (SCF/ton)
209.6	94.7	96.4	10.9	11.1
817.2	207.1	223.0	10.9	11.7
1413.7	253.2	288.2	12.1	13.8

Table 31: Adsorption of Pure Methane on Dry Upper Freeport Coal at 328.2 K (Run 1)

SI Units

Void Volume (m^3)	0.00007920
Pump Press. (MPa)	6.93
Pump T (K)	328.2
Cell T (K)	328.2
Adsorbent mass (g)	67.2
Moist.content (%)	0.0
Ads.Phase Density (g/cm^3)	0.421

Pressure (MPa)	Gibbs Ads. (mmol/g)	Abs. Ads. (mmol/g)	Err.Gibbs (mmol/g)	Err.Abs. (mmol/g)
0.73	0.241	0.243	0.019	0.019
1.46	0.340	0.347	0.019	0.019
2.84	0.448	0.468	0.019	0.019
4.23	0.512	0.545	0.018	0.020
5.62	0.549	0.599	0.019	0.020
6.98	0.576	0.643	0.019	0.021
8.37	0.593	0.680	0.019	0.022
9.74	0.603	0.710	0.020	0.024
11.12	0.612	0.740	0.021	0.025
12.47	0.617	0.767	0.022	0.027
13.76	0.617	0.788	0.023	0.029
Desorption				
11.06	0.609	0.735	-	-
8.30	0.587	0.672	-	-
5.53	0.548	0.597	-	-
2.80	0.456	0.476	-	-

British Units

Void Volume (ft^3)	0.002797
Pump Press. (psia)	1005.0
Pump T (°F)	131.0
Cell T (°F)	131.0
Adsorbent mass (lb)	0.1482
Moist.content (%)	0.0
Ads.Phase Density (lb/ft^3)	26.28

Pressure (psia)	Gibbs Ads. (SCF/ton)	Abs. Ads. (SCF/ton)	Err.Gibbs (SCF/ton)	Err.Abs. (SCF/ton)
105.3	182.7	184.6	14.5	14.6
211.6	258.2	263.7	14.3	14.6
412.2	340.3	354.9	14.1	14.7
613.3	388.3	413.9	14.0	14.9
814.6	416.9	454.9	14.1	15.4
1012.9	437.0	488.3	14.3	16.0
1214.5	450.3	516.3	14.7	16.8
1412.5	457.8	538.7	15.2	17.9
1612.2	464.5	561.6	15.8	19.1
1809.0	468.2	581.9	16.6	20.6
1995.9	468.4	597.8	17.3	22.1
Desorption				
1604.5	461.9	557.9	-	-
1203.8	445.8	510.4	-	-
801.5	416.0	453.1	-	-
405.6	346.4	360.9	-	-

Table 32: Adsorption of Pure Methane on Dry Upper Freeport Coal at 328.2 K (Run 2)

SI Units

Void Volume (m^3)	0.00007920
Pump Press. (MPa)	6.93
Pump T (K)	328.2
Cell T (K)	328.2
Adsorbent mass (g)	67.2
Moist.content (%)	0.0
Ads.Phase Density (g/cm^3)	0.421

Pressure (MPa)	Gibbs Ads. (mmol/g)	Abs. Ads. (mmol/g)	Err.Gibbs (mmol/g)	Err.Abs. (mmol/g)
1.32	0.315	0.321	0.015	0.016
4.21	0.497	0.529	0.015	0.016
7.01	0.562	0.628	0.016	0.018

British Units

Void Volume (ft^3)	0.002797
Pump Press. (psia)	1005.0
Pump T (°F)	131.0
Cell T (°F)	131.0
Adsorbent mass (lb)	0.1482
Moist.content (%)	0
Ads.Phase Density (lb/ft^3)	26.29

Pressure (psia)	Gibbs Ads. (SCF/ton)	Abs. Ads. (SCF/ton)	Err.Gibbs (SCF/ton)	Err.Abs. (SCF/ton)
191.9	238.9	243.5	11.6	11.8
610.0	377.0	401.7	11.5	12.2
1016.4	426.6	477.0	12.0	13.5

Table 33: Adsorption of Pure CO_2 on Dry Upper Freeport Coal at 328.2 K

SI Units

Void Volume (m^3)	0.00007917
Pump Press. (MPa)	6.70
Pump T (K)	328.2
Cell T (K)	328.2
Adsorbent mass (g)	67.2
Moist.content (%)	0.0
Ads.Phase Density (g/cm^3)	1.027

Pressure (MPa)	Gibbs Ads. (mmol/g)	Abs. Ads. (mmol/g)	Err.Gibbs (mmol/g)	Err.Abs. (mmol/g)
0.74	0.491	0.497	0.042	0.042
1.47	0.636	0.652	0.041	0.042
2.82	0.775	0.815	0.040	0.042
4.22	0.853	0.927	0.039	0.043
5.60	0.896	1.013	0.039	0.044
6.98	0.911	1.082	0.039	0.046
8.33	0.896	1.140	0.040	0.050
9.72	0.841	1.194	0.043	0.061
10.97	0.729	1.219	0.065	0.109
12.34	0.649	1.341	0.067	0.139
13.69	0.599	1.457	0.079	0.191
Desorption				
11.17	0.734	1.264	-	-
8.12	0.888	1.115	-	-
5.46	0.887	0.998	-	-
2.76	0.763	0.802	-	-

British Units

Void Volume (ft^3)	0.002796
Pump Press. (psia)	972.3
Pump T (°F)	131.0
Cell T (°F)	131.0
Adsorbent mass (lb)	0.1482
Moist.content (%)	0.0
Ads.Phase Density (lb/ft^3)	64.11

Pressure (psia)	Gibbs Ads. (SCF/ton)	Abs. Ads. (SCF/ton)	Err.Gibbs (SCF/ton)	Err.Abs. (SCF/ton)
107.6	372.5	377.0	31.7	32.0
212.7	482.7	494.8	31.2	32.0
409.7	588.1	618.9	30.5	32.1
612.6	647.7	703.9	30.0	32.6
811.7	680.4	768.5	29.6	33.4
1011.9	691.6	821.2	29.5	35.0
1208.3	680.3	865.0	30.1	38.2
1409.8	638.5	906.2	32.9	46.6
1591.8	553.5	924.9	49.6	82.9
1790.2	492.6	1017.9	51.0	105.4
1985.0	454.4	1106.2	59.7	145.2
Desorption				
1619.8	556.7	959.1	-	-
1177.5	673.8	846.0	-	-
792.3	673.4	757.5	-	-
399.9	579.3	608.8	-	-

Table 34: Adsorption of Pure Ethane on Dry Upper Freeport Coal at 328.2 K (Run 1)

SI Units

Void Volume (m^3)	0.00007928
Pump Press. (MPa)	8.68
Pump T (K)	328.2
Cell T (K)	328.2
Adsorbent mass (g)	67.2
Moist.content (%)	0.0
Ads.Phase Density (g/cm^3)	0.444

Pressure (MPa)	Gibbs Ads. (mmol/g)	Abs. Ads. (mmol/g)	Err.Gibbs (mmol/g)	Err.Abs. (mmol/g)
0.56	0.441	0.447	0.083	0.084
1.44	0.578	0.601	0.083	0.086
2.85	0.629	0.688	0.082	0.089
4.25	0.641	0.752	0.081	0.095
5.64	0.605	0.797	0.080	0.106
6.97	0.495	0.843	0.082	0.140
8.34	0.399	0.966	0.080	0.194
9.73	0.401	1.204	0.079	0.238
11.11	0.371	1.297	0.079	0.278
12.48	0.400	1.588	0.080	0.316
13.72	0.357	1.567	0.080	0.350
Desorption				
11.00	0.380	1.315	-	-
8.31	0.377	0.908	-	-
5.87	0.596	0.808	-	-
2.73	0.634	0.690	-	-

British Units

Void Volume (ft^3)	0.00280
Pump Press. (psia)	1258.2
Pump T (°F)	131.0
Cell T (°F)	131.0
Adsorbent mass (lb)	0.1482
Moist.content (%)	0.0
Ads.Phase Density (lb/ft^3)	27.72

Pressure (psia)	Gibbs Ads. (SCF/ton)	Abs. Ads. (SCF/ton)	Err.Gibbs (SCF/ton)	Err.Abs. (SCF/ton)
80.5	334.4	339.2	63.1	64.0
209.1	438.4	456.2	62.7	65.2
413.5	477.3	522.1	62.1	67.9
616.0	486.6	570.6	61.5	72.1
818.3	459.2	605.0	61.0	80.4
1011.2	375.5	639.6	62.4	106.3
1209.0	302.8	733.1	60.7	147.0
1411.6	304.3	914.0	60.2	180.9
1611.8	281.3	984.7	60.3	211.0
1810.4	303.9	1205.4	60.4	239.5
1990.0	271.3	1189.3	60.5	265.3
Desorption				
1595.8	288.4	998.4	-	-
1204.6	286.4	689.2	-	-
851.2	452.1	613.0	-	-
396.2	481.4	524.1	-	-

Table 35: Adsorption of Pure Ethane on Dry Upper Freeport Coal at 328.2 K (Run 2)

SI Units

Void Volume (m^3)	0.00007928
Pump Press. (MPa)	8.83
Pump T (K)	328.2
Cell T (K)	328.2
Adsorbent mass (g)	67.2
Moist.content (%)	0.0
Ads.Phase Density (g/cm^3)	0.444

Pressure (MPa)	Gibbs Ads. (mmol/g)	Abs. Ads. (mmol/g)	Err.Gibbs (mmol/g)	Err.Abs. (mmol/g)
1.53	0.610	0.637	0.076	0.080
5.65	0.648	0.854	0.074	0.098
9.68	0.421	1.255	0.074	0.219

British Units

Void Volume (ft^3)	0.00280
Pump Press. (psia)	1280.0
Pump T (°F)	131.0
Cell T (°F)	131.0
Adsorbent mass (lb)	0.1482
Moist.content (%)	0.0
Ads.Phase Density (lb/ft^3)	27.72

Pressure (psia)	Gibbs Ads. (SCF/ton)	Abs. Ads. (SCF/ton)	Err.Gibbs (SCF/ton)	Err.Abs. (SCF/ton)
222.6	463.1	483.3	57.9	60.4
819.0	491.8	648.4	56.4	74.3
1403.5	319.4	952.7	55.8	166.6

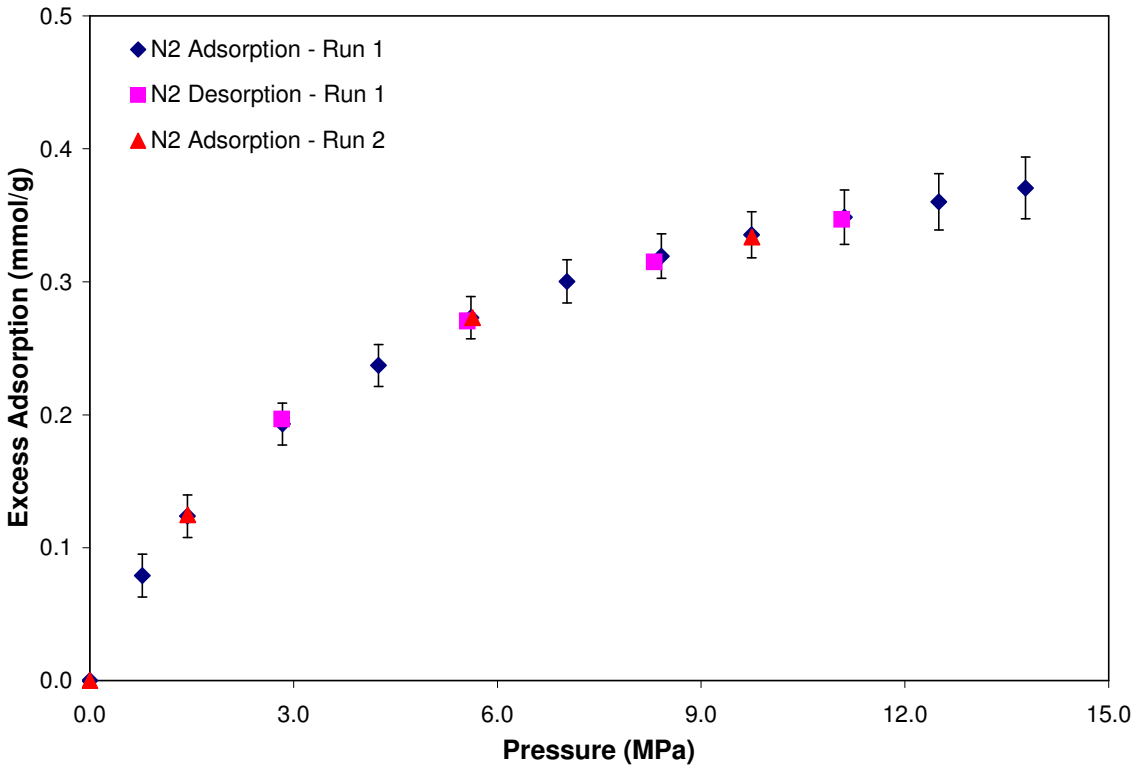

Figure 25: Excess Adsorption of Pure Nitrogen on Dry Upper Freeport Coal at 328.2 K

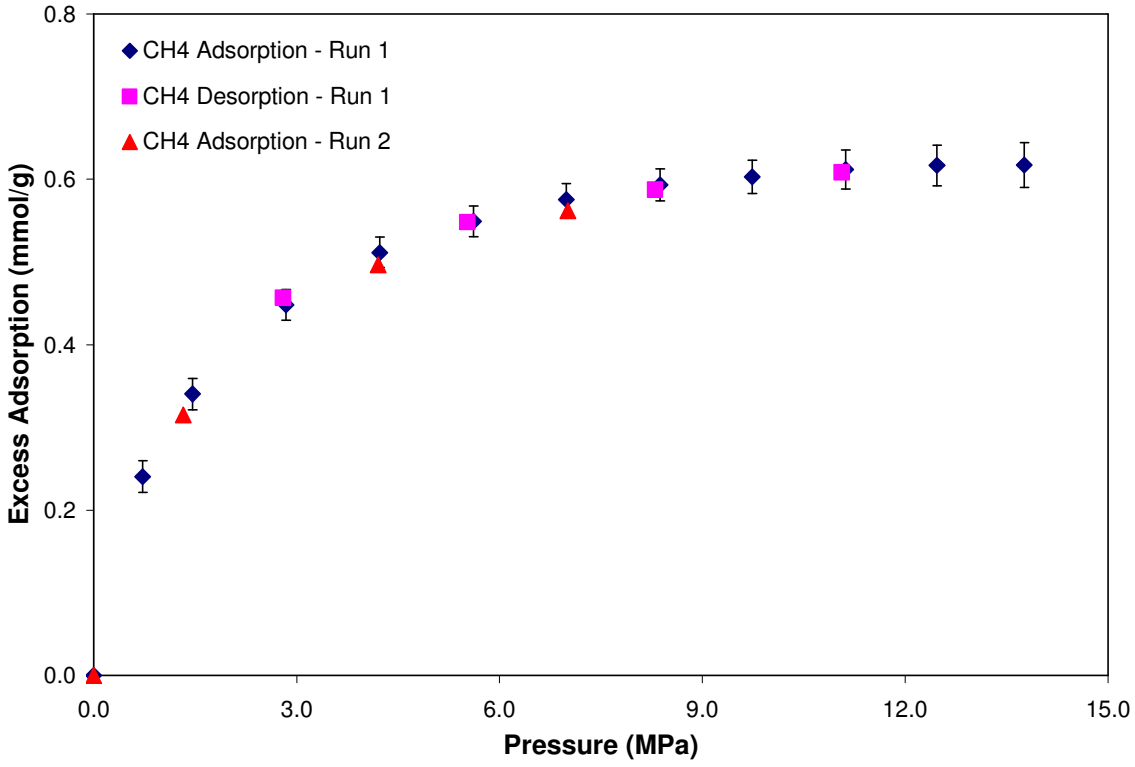

Figure 26: Excess Adsorption of Pure Methane on Dry Upper Freeport Coal at 328.2 K

The adsorption isotherm of CO_2 at 318.2 K is shown in Figure 27. Figure 27 also shows that the adsorption and desorption data are in agreement within the expected uncertainties, which indicates absence of hysteresis. Further, comparison of the current adsorption measurements with those by Sudibandriyo (2003) shows agreement within 3% for most of the data. This level of agreement is well within the combined experimental uncertainty of two data sets.

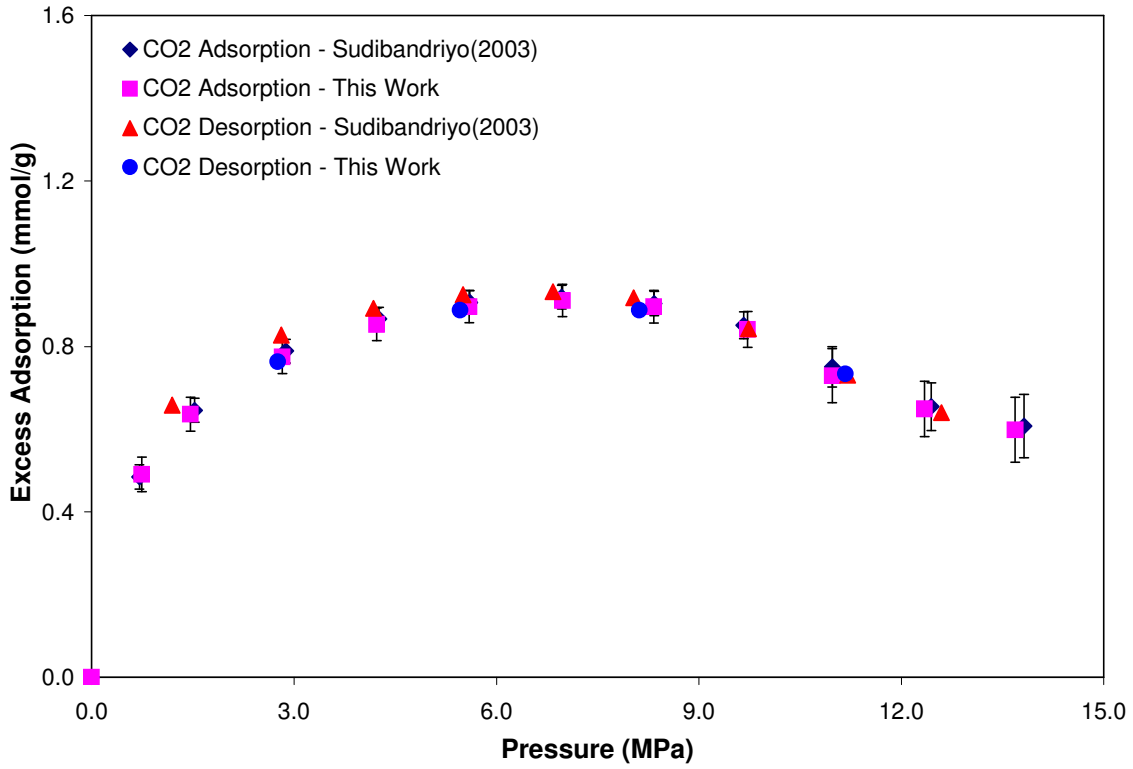

Figure 27: Excess Adsorption of Pure CO_2 on Dry Upper Freeport Coal at 328.2 K

Figure 28 depicts the adsorption isotherm for pure ethane at 328.2 K (131 °F) and pressures to 13.8 MPa (2000 psia). The expected experimental uncertainty of the pure ethane adsorption data on Upper Freeport is about 8.7%. Figure 28 also indicates there are little "bumps" observed above 9 MPa (1200 psia). This might be due to uncertainties in the measurement.

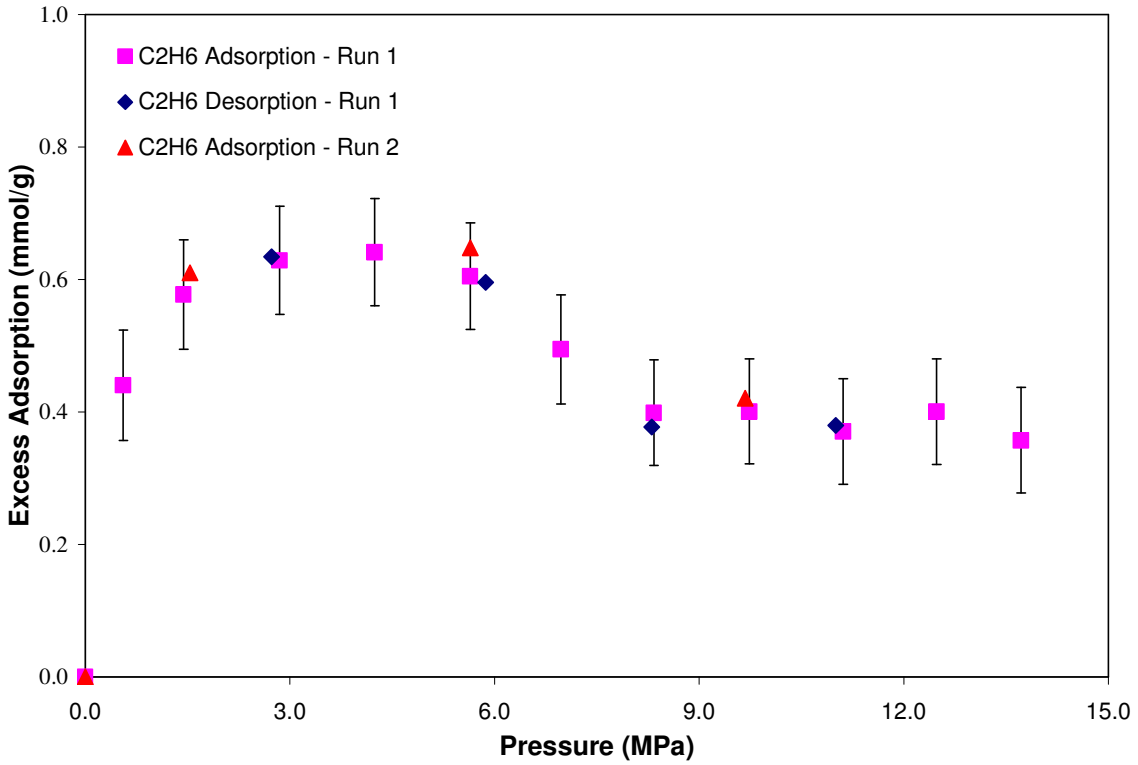

Figure 28: Excess Adsorption of Pure Ethane on Dry Upper Freeport Coal at 328.2 K

Figure 29 shows the excess adsorption of pure methane, nitrogen, CO_2 and ethane at 328.2 K (131 °F) and pressures to 13.8 MPa (2000 psia) on dry Upper Freeport coal. The amount adsorbed in the lowest for most of the gases when compared to the other coals. This suggests that the high ranked coals have lower adsorption than the lower ranked coals.

Figures 30 depict measurements of methane adsorption on a fresh coal matrix, methane adsorption after CO_2 adsorption, and methane adsorption after both CO_2 and ethane adsorption. Little variation in isotherm reproducibility is shown.

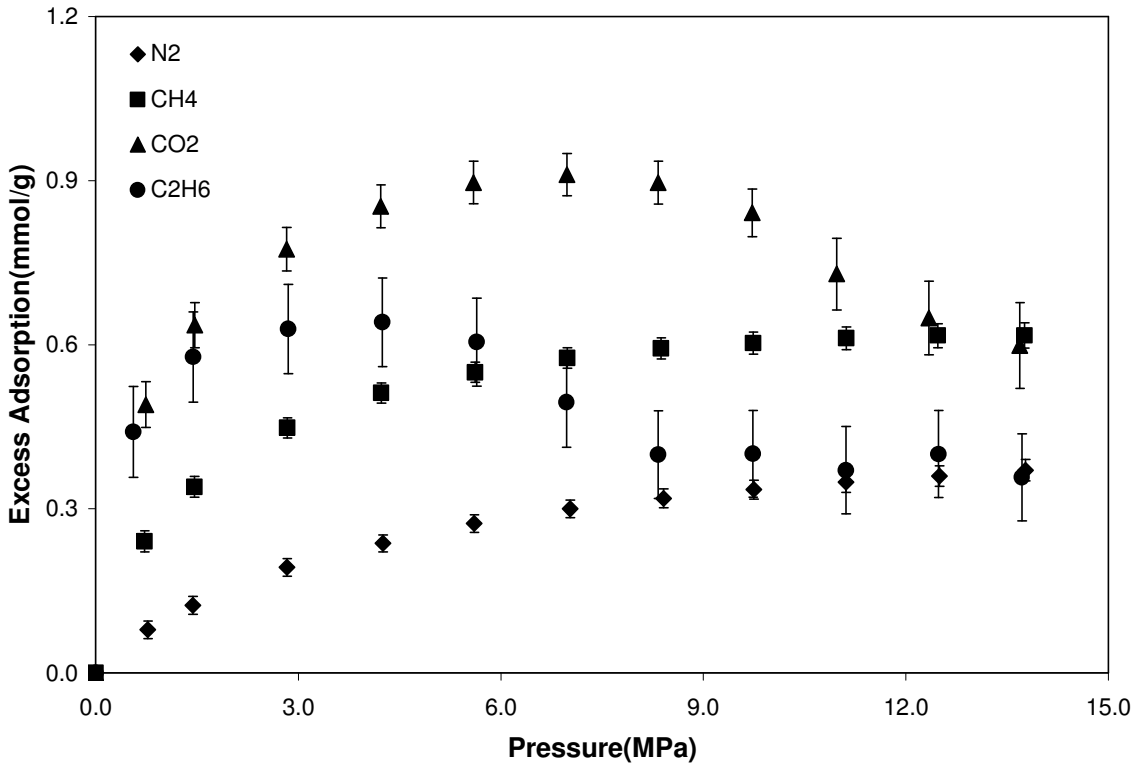

Figure 29: Excess Adsorption of Pure Coalbed Gases on Dry Upper Freeport Coal at 328.2 K

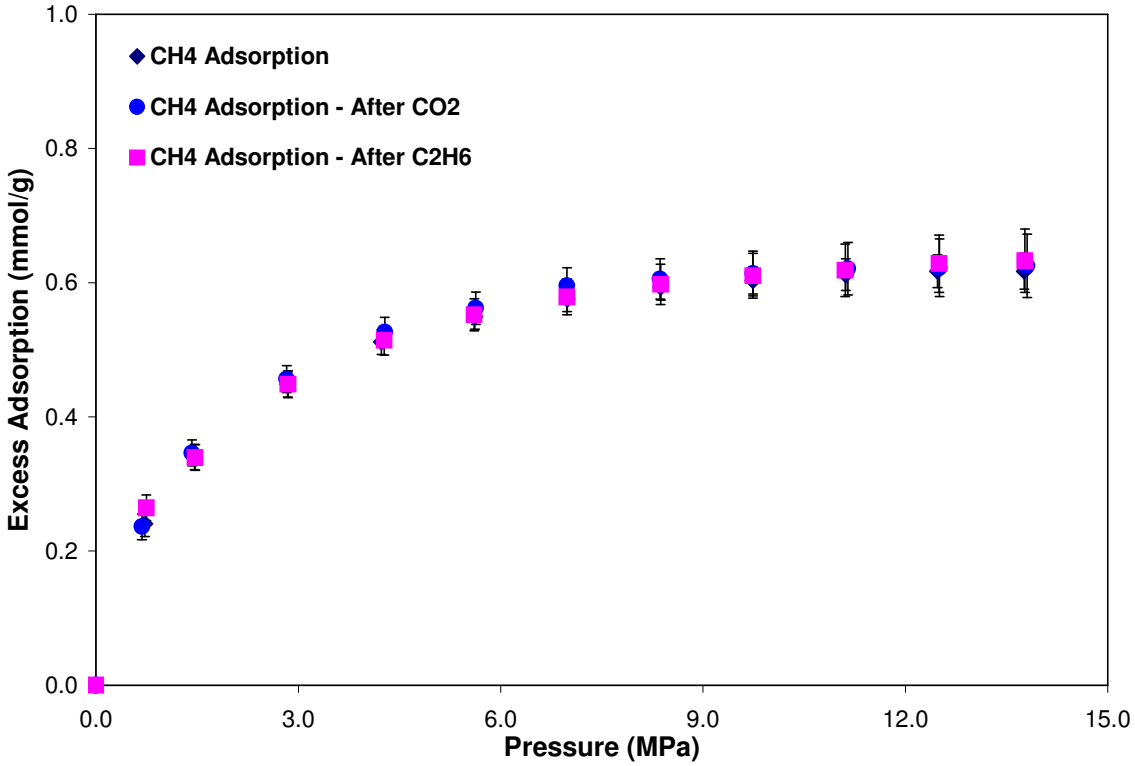

Figure 30: Adsorption of Pure Methane on Dry Upper Freeport Before and After CO_2 and Ethane Gas Adsorption at 328.2 K

3.6 Adsorption of Pure-Gases on Different Dry Coals

The gas adsorption isotherms on all the coals considered in this study have some general characteristics. At low to moderate pressures, an increasing order in the amount of gas adsorbed on this coal is observed for nitrogen, methane, ethane and CO_2, respectively. Ethane isotherms have excess adsorption maximums between 4 and 6 MPa and CO_2 isotherms have excess adsorption maximums between 6 and 8.5 MPa.

Figures 31-34 depict the excess adsorption of each gas for all the five coals. The excess adsorption of methane on these coals varies no more than 35% at pressures from 10 MPa to 14 MPa; however, qualitative differences in isotherm shape are apparent. The excess adsorption isotherm of methane on Upper Freeport and Pocahontas #3 appears flat at pressures higher than 10 MPa. Methane adsorption on the other coals is increasing slightly with pressure at 10 MPa. The order in the increasing amount of methane adsorbed among the coals has the following trend: Pocahontas #3, Illinois #6, Wyodak, Beulah Zap, and Upper Freeport.

Nitrogen adsorption varied no more than 45% in the amount adsorbed between any of the coals at pressures of 10 MPa to 14 MPa. The order in the increasing amount of nitrogen adsorbed among the coals is respectively, Pocahontas #3, Wyodak and Illinois #6 (tied), and Upper Freeport and Beulah Zap (tied).

The order of increasing CO_2 adsorption among the coals is Wyodak, Beulah Zap, Illinois #6, Pocahontas #3, and Upper Freeport. The CO_2 adsorption on Wyodak and Beulah Zap are almost indistinguishable below 10 MPa. These two coals have similar ultimate and proximate analyses. At the maximum excess adsorption pressure, the amount of adsorption for CO_2 varies by no more than 110% between any of the coals.

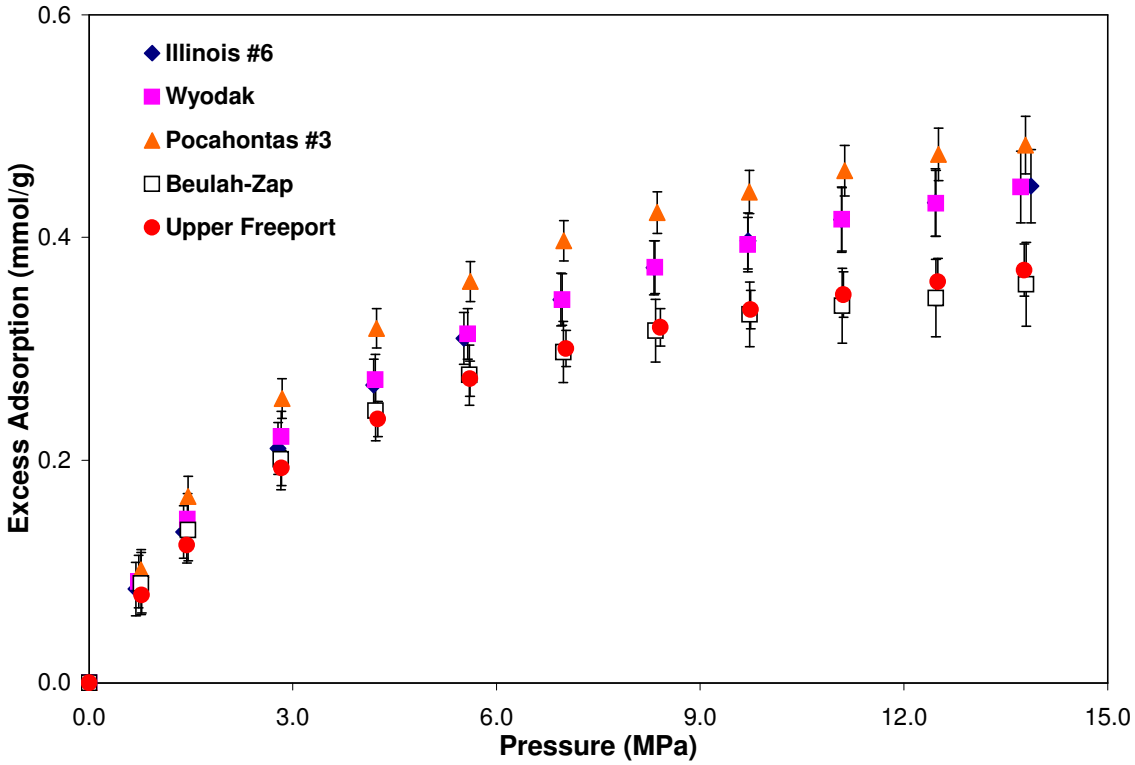

Figure 31: Excess Adsorption of Pure Nitrogen on Different Dry Coal Matrices at 328.2 K

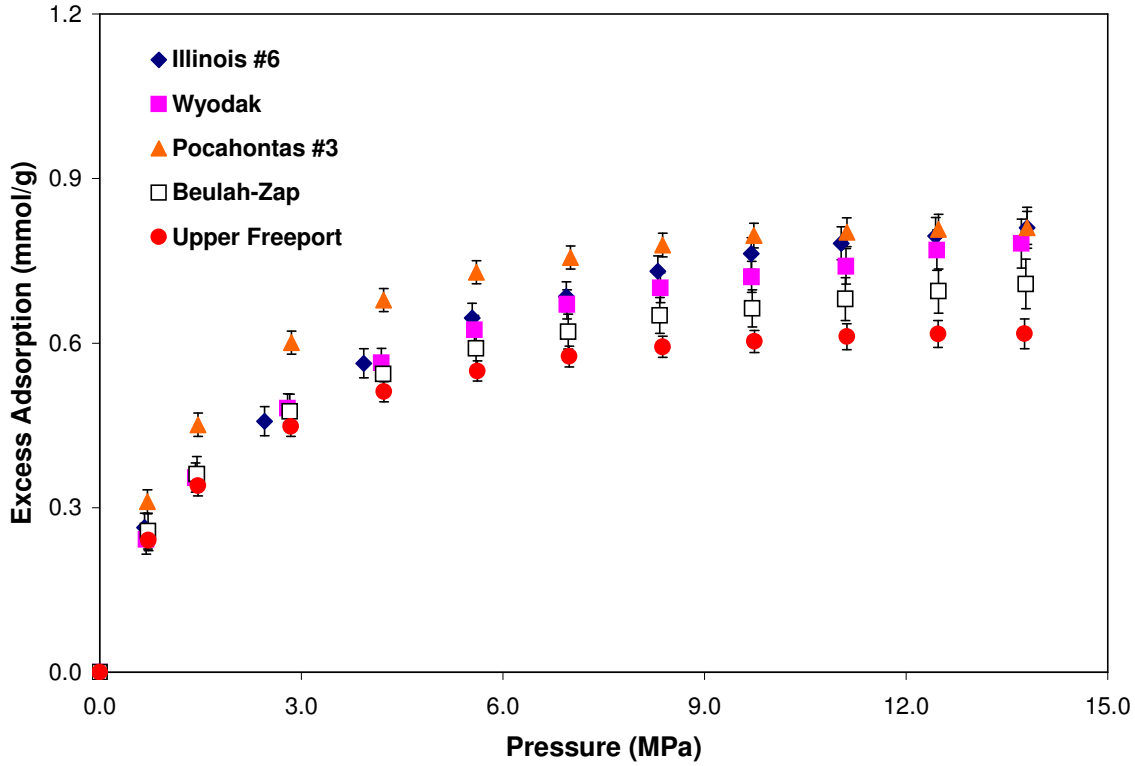

Figure 32: Excess Adsorption of Pure Methane on Different Dry Coal Matrices at 328.2 K

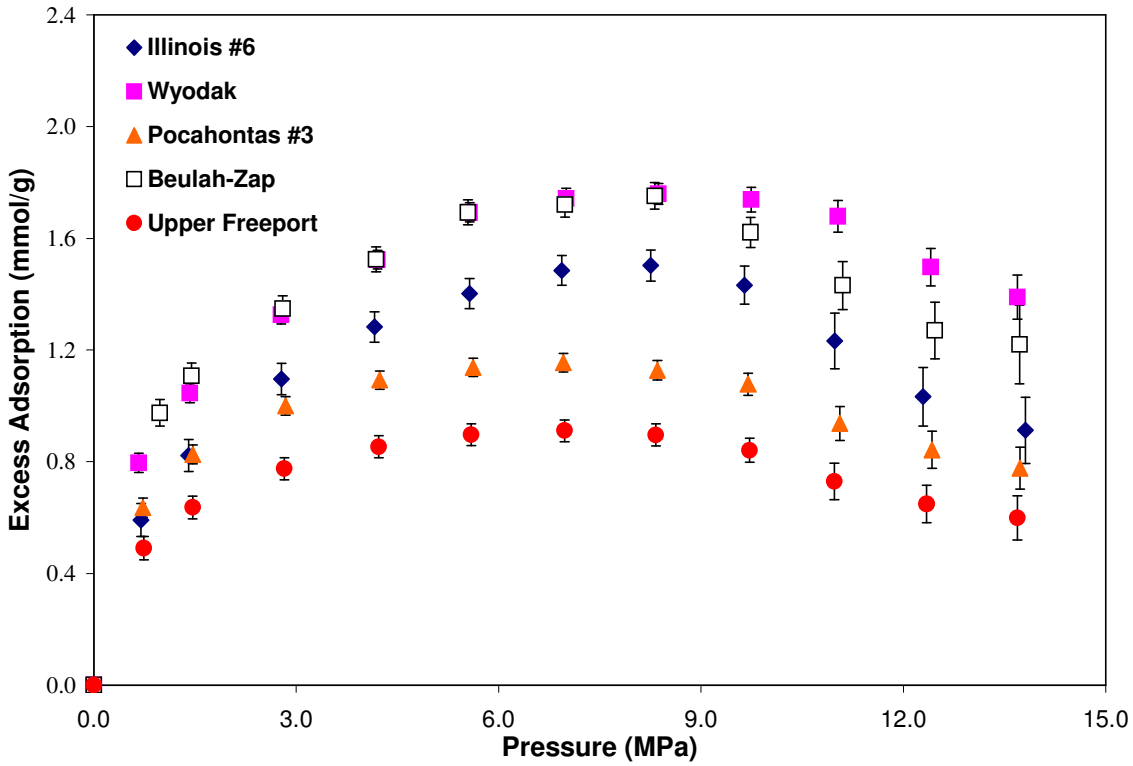

Figure 33: Excess Adsorption of Pure CO_2 on Different Dry Coal Matrices at 328.2 K

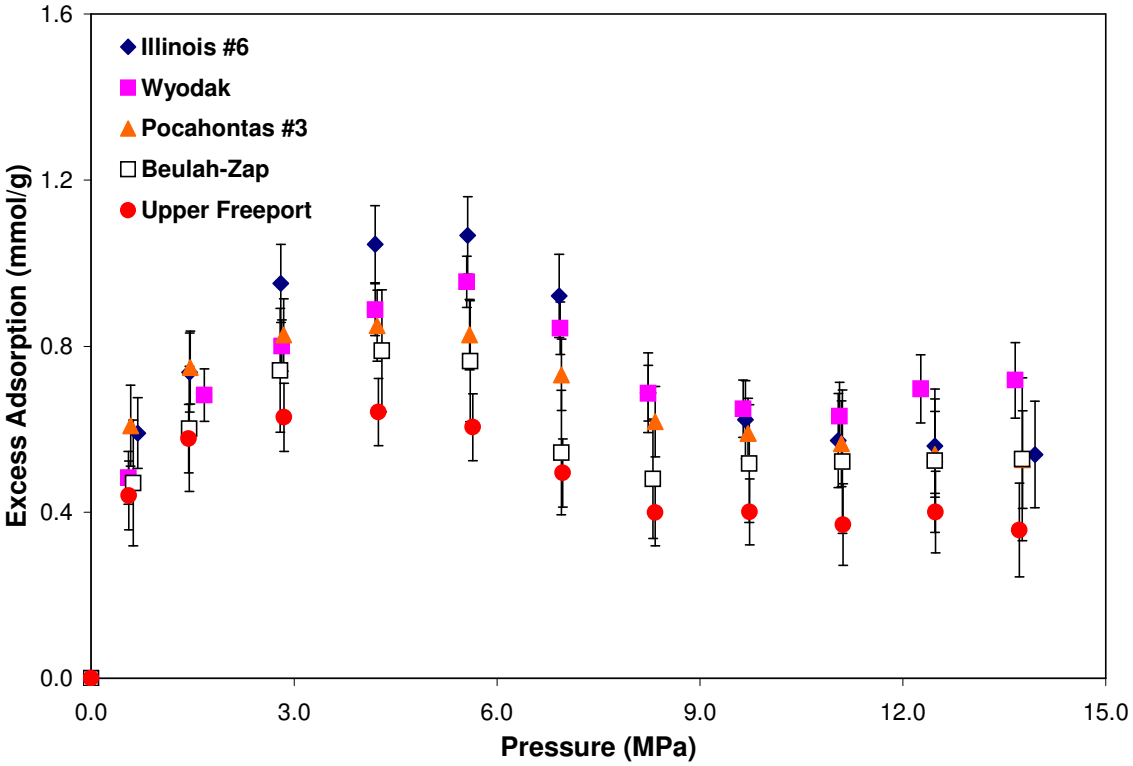

Figure 34: Excess Adsorption of Pure Ethane on Different Dry Coal Matrices at 328.2 K

The acquired adsorption data for CO_2 was also compared with adsorption measurements conducted at pressures to 7 MPa as part of the DOE-NETL Inter-Laboratory Study [Goodman et al., 2004]. The data were in good agreement for most of the coals, except, for the Wyodak coal. Specifically, we report lower adsorption for Wyodak than observed in another laboratory

Ethane adsorption exhibits unique features on some of the coals. Adsorption isotherms on Wyodak and Beulah Zap have a *minimum* after the adsorption maximum. These features, however, remain suspect due to measurement uncertainties.

The ratio of CO_2 to ethane adsorption varies notably among the coals. Beulah Zap has the largest ratio, with Wyodak close behind. Pocahontas #3 has the smallest ratio. The CO_2/ethane adsorption ratio appears to increase qualitatively with the natural equilibrium moisture content of the coal, and decrease qualitatively with oxygen content.

3.7 Effect of Moisture Content

In general coalbed methane recovery operations are carried out at super-saturated water conditions. Nevertheless, the percentage of moisture present in the coal has an impact on the pure-gas adsorption behavior. Specifically, the moisture content may affect significantly the adsorption capacity, adsorbed-phase density, gas-mixture adsorption behavior and may lead to incorrect data interpretation and reconciliation.

A comparison between the adsorption of dry and wet Illinois #6 coal is shown in Figure 35. As expected the moisture content affects the amount of adsorption on coals. Figure 35 also demonstrates how an increase in the coal moisture content, below the equilibrium saturation level, decreases the amount of gas adsorbed. Specifically, the

amount of adsorption at 6.9 MPa (1197.2 psia) ranges from 0.6 mmol/g for the wet coal (8% moisture content) to 1.5 mmol/g for the dry coal.

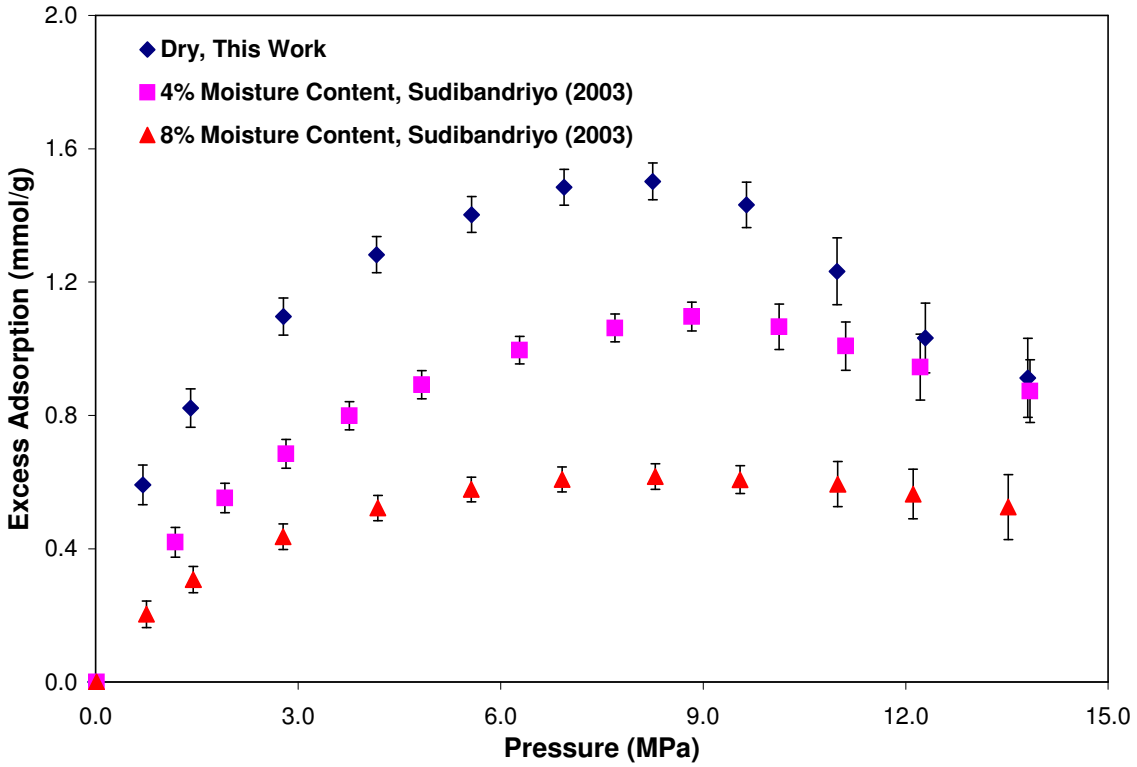

Figure 35: Moisture Effects on CO_2 Excess Adsorption on Illinois #6 Coal at 328.2 K

These preliminary data indicate the need for additional experimental measurements (involving both pure and gas mixtures) to delineate the effect of moisture content on coalbed gas adsorption.

CHAPTER 4

LOADING-RATIO CORRELATION MODEL FOR ADSORPTION

4.1 The Langmuir Model

The Langmuir model is one of several models commonly used to represent the adsorption behavior of gases on adsorbents. The model, which was presented in 1918, expresses the dynamic equilibrium between the rates of evaporation and condensation occurring at a gas-solid interface [Yang, 1987].

The Langmuir model may be written in terms of fractional loading as:

$$\theta = \frac{\omega}{L} = \frac{BP}{1+BP} \quad \text{or} \quad BP = \frac{\theta}{1-\theta} \tag{4-1}$$

where θ is the fraction of monolayer coverage, ω is the amount of gas adsorbed per unit of adsorbent, (1/B) is the Langmuir pressure, and L is the amount adsorbed per unit of adsorbent at complete monolayer adsorption.

As shown in Figure 36, several types of adsorptions have been identified [Brunauer, 1940]. Type I is roughly characterized by a monotonic approach to a limiting adsorption that corresponds to a complete monolayer. Type II is very common in the case of physical adsorption with multilayer formation. Type III is relatively rare and seems to be characterized by a heat of adsorption equal to or less than the heat of liquefaction of the adsorbate. Type IV and V are considered to reflect capillary condensation phenomena, which may show hysteresis effects.

The Langmuir model can only represent Type I (Figure 36) adsorption and is commonly applied to physical adsorption of gases where multilayer adsorption occurs [Yang, 1987].

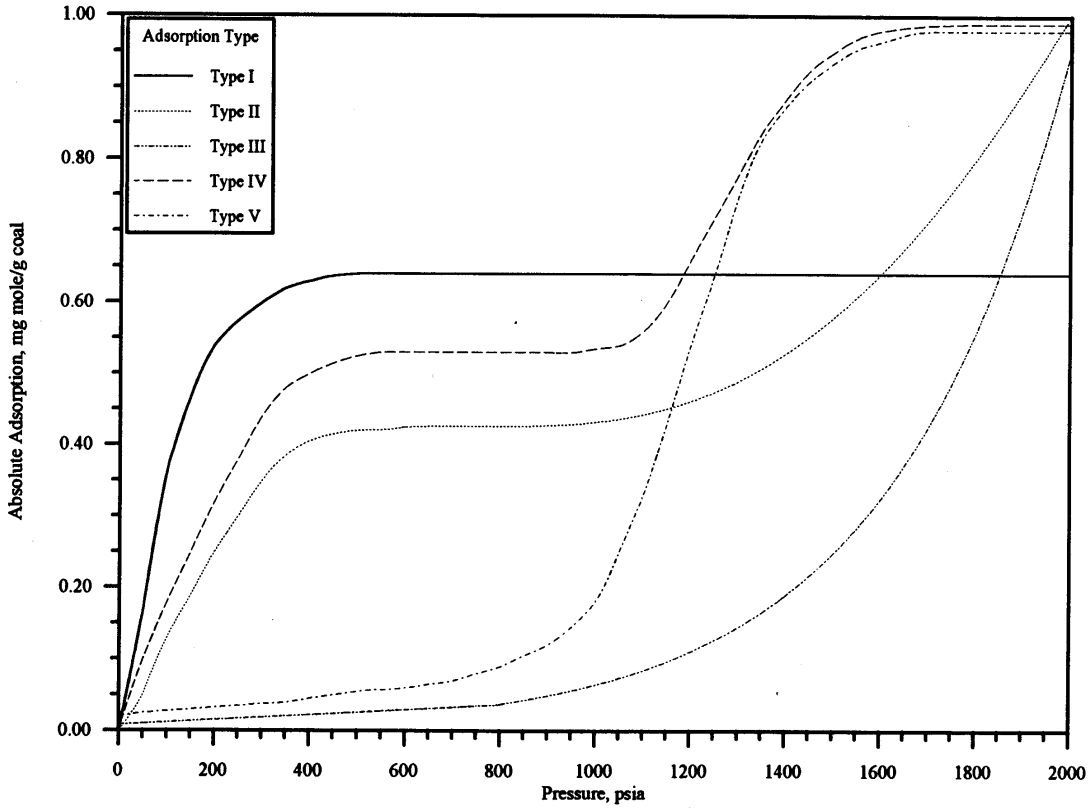

Figure 36: Types of Adsorption Isotherms [Brunauer, 1940]

In this study, the newly-acquired gas adsorption data for pure methane, nitrogen, CO_2 and ethane on dry Beulah-Zap, Wyodak, Illinois #6, Upper Freeport, Pocahontas #3 were correlated using the Langmuir model and its extension, the Loading-Ratio Correlation (LRC).

Table 36 presents a summary of the model evaluation results for the Langmuir model. The model parameters (L and B), were determined by minimizing the sum of the squares of weighted absolute deviations in the absolute adsorption, for the pure gas of interest.

Measures for the quality of the fit, expressed in terms of absolute average percentage deviation (%AAD) and weighted average absolute deviations (WAAD), are also given in Table 36. The amount adsorbed per unit of adsorbent at complete monolayer adsorption, L, is given in both SI and English units for convenience.

The effectiveness of the model, however, depends on the shape of the absolute adsorption. Therefore, the choice of the adsorbed-phase density may affect the quality of the Langmuir representation, especially at high pressures. Figure 37 and 38 illustrate the impact of various adsorbed-phase density estimates on CO_2 and ethane on dry Illinois #6 coal. In this study, the experimental Gibbs excess adsorption data are converted to absolute adsorption using the adsorbed-phase density obtained from the Ono-Kondo model.

At high pressures, the apparent order in the amount adsorbed forming a complete monolayer is nitrogen, methane, ethane and CO_2. The ratio in the amount adsorbed for CO_2/nitrogen, CO_2/methane and CO2/ethane is comparatively higher for Beulah Zap coal, which is correlative to the percentage of oxygen or equilibrium moisture content in that coal.

The maximum capacity, L, for all the gases increases with that of oxygen content. The increase in amount for the maximum capacity is smaller for nitrogen when compared to other gases. As the oxygen content increases, the Langmuir pressure drops or decreases linearly as the fixed carbon content increases.

Overall, the Langmuir model using two regressed parameters (L and B) is capable of representing the adsorption data considered within the expected experimental uncertainties, which corresponds to 5.9% AAD on average (WAAD = 0.7).

Table 36: Langmuir Model Parameters for the Dry Coals at 328.2 K

Coals	Gases	L		1/B	%AAD	WAAD
		mmol/g	SCF/Ton	psia		
Illinois #6	N_2	0.8	637	1195	4.7	0.3
	CH_4	1.4	1066	763	5.5	0.8
	CO_2	2.9	2213	614	6.5	0.9
	C_2H_6	2.0	1532	387	6.9	0.4
Wyodak	N_2	0.8	621	1112	4.9	0.4
	CH_4	1.2	885	543	5.4	0.8
	CO_2	2.5	1924	285	7.0	1.9
	C_2H_6	1.4	1052	235	6.8	0.5
Pocahontas	N_2	0.8	633	898	2.6	0.3
	CH_4	1.4	1039	471	5.4	1.4
	CO_2	1.7	1260	217	6.8	1.2
	C_2H_6	1.2	909	117	7.7	0.4
Beulah-Zap	N_2	0.6	457	768	3.4	0.2
	CH_4	1.1	847	502	6.3	0.8
	CO_2	3.0	2270	452	6.6	1.3
	C_2H_6	1.1	850	169	8.4	0.2
Upper Freeport	N_2	0.7	499	990	3.4	0.3
	CH_4	1.0	789	482	6.0	1.3
	CO_2	1.3	1008	220	7.3	0.9
	C_2H_6	0.8	609	66	5.8	0.2
Overall					5.9	0.7

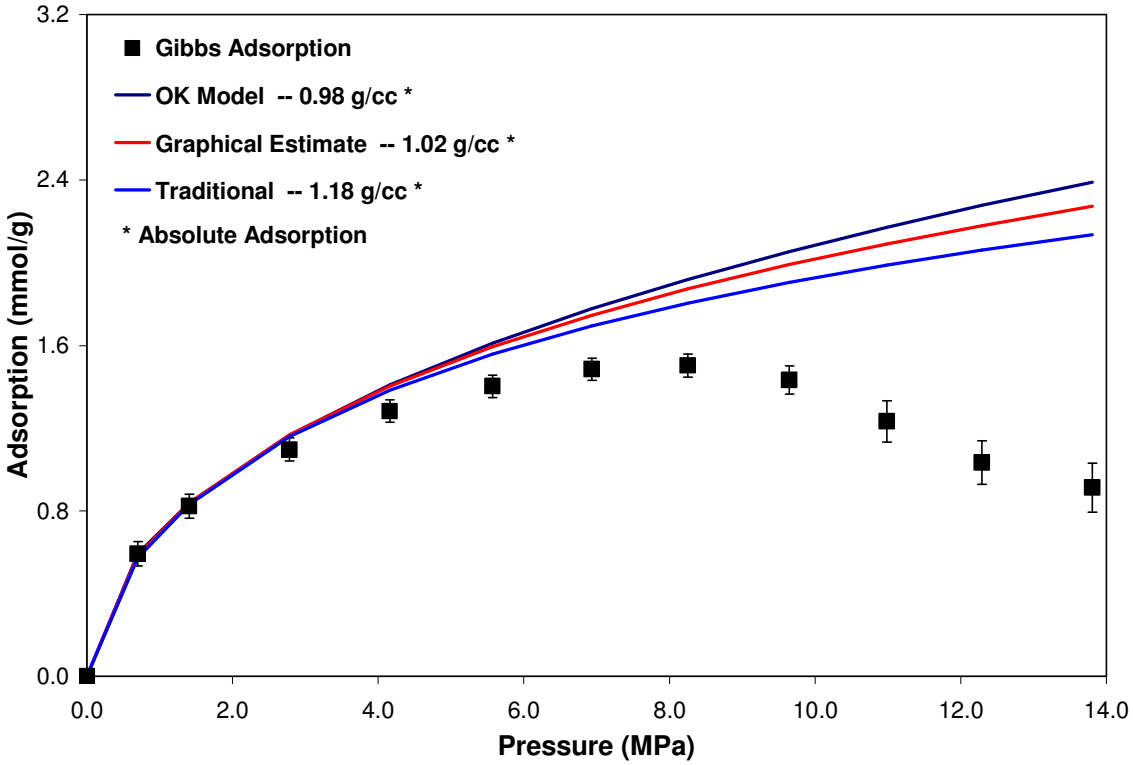

Figure 37: Impact of Adsorbed-Phase Density for CO_2 on Dry Illinois #6 Coal at 328.2 K

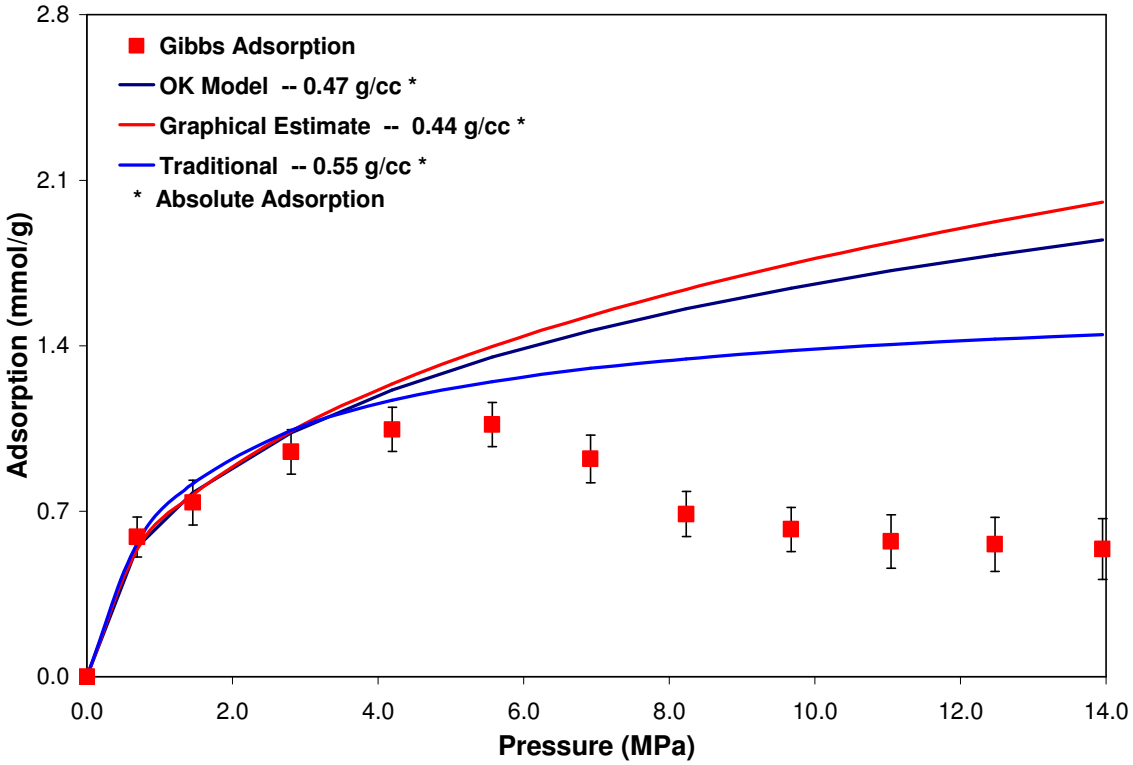

Figure 38: Impact of Adsorbed-Phase Density for Ethane on Dry Illinois #6 Coal at 328.2 K

4.2 The Loading-Ratio Correlation (LRC)

The combined Langmuir-Freundlich adsorption isotherm yields the Loading-Ratio Correlation (LRC) expressed as

$$n^{Abs} = \frac{LBP^{\eta}}{1 + BP^{\eta}} \qquad (4\text{-}2)$$

The additional parameter in the LRC (η) gives the Langmuir model more flexibility. Nevertheless, this Langmuir type model can only handle absolute adsorption as monotonic functions of pressure, and when η equals to one, the LRC expression reduces to simple Langmuir model.

Table 37 presents a summary of the model evaluation results for the LRC model. The model parameters (L, B, and η), listed in Table 37, were determined in the same manner as for the Langmuir model. To establish a model of equivalent form for all components, regressions were also performed on all pure substances simultaneously, specifying a common value for the model constant η. The optimum value for η was taken on the basis of average for all the five coals. Model constants for the LRC with η = 0.8 are tabulated in Table 38.

The simplification of the LRC made by fixing the model constant (η) is justified by the fact that changes in the weighted average absolute deviation (WAAD) are within the average expected experimental uncertainty; albeit, the error (AAD, WAAD) in representing ethane adsorption increased by as much as two-fold when the fixed exponent (η) was used. This was expected since the optimum value for ethane (around 0.6) is smaller than the fixed value (0.8).

Table 37: Loading-Ratio Correlation Model Parameters for Dry Coals at 328.2 K

Coals	Gases	L		1/B	η	%AAD	WAAD
		mmol/g	SCF/ton	psia			
Illinois #6	N_2	1.0	765	800	0.9	2.6	0.1
	CH_4	1.7	1279	320	0.8	3.6	0.5
	CO_2	3.8	2876	255	0.8	3.9	0.5
	C_2H_6	2.6	1992	117	0.7	3.8	0.2
Wyodak	N_2	0.9	683	712	0.9	3.3	0.1
	CH_4	1.3	974	280	0.9	3.8	0.1
	CO_2	3.2	2419	106	0.7	4.3	1.1
	C_2H_6	1.8	1367	59	0.7	5.1	0.4
Pocahontas	N_2	1.0	728	530	0.9	0.7	0.1
	CH_4	1.8	1403	112	0.7	1.7	0.6
	CO_2	1.9	1449	57	0.7	4.8	0.8
	C_2H_6	1.4	1045	20	0.6	5.8	0.3
Beulah-Zap	N_2	0.7	503	466	0.9	1.9	0.1
	CH_4	1.2	932	238	0.8	4.6	0.6
	CO_2	3.9	2951	87	0.7	3.8	0.7
	C_2H_6	1.5	1105	28	0.6	6.6	0.2
Upper Freeport	N_2	0.7	549	523	0.9	1.0	0.2
	CH_4	1.2	947	183	0.8	3.6	0.8
	CO_2	1.7	1261	64	0.7	4.7	0.6
	C_2H_6	1.0	761	16	0.6	4.1	0.1
Overall						3.7	0.4

Table 38: Loading-Ratio Correlation Model Parameters with $\eta = 0.8$

Coals	Gases	L		1/B	η	%AAD	WAAD
		mmol/g	SCF/ton	psia			
Illinois #6	N_2	1.1	835	386	0.8	3.4	0.3
	CH_4	1.9	1429	282	0.8	3.1	0.4
	CO_2	3.9	2960	241	0.8	3.6	0.5
	C_2H_6	2.5	1918	147	0.8	4.2	0.2
Wyodak	N_2	1.4	1063	552	0.8	2.0	0.2
	CH_4	1.5	1110	196	0.8	2.6	0.4
	CO_2	3.3	2528	138	0.8	4.4	1.1
	C_2H_6	1.8	1367	114	0.8	6.4	0.4
Pocahontas	N_2	1.3	1023	432	0.8	1.5	0.2
	CH_4	1.4	1057	126	0.8	1.2	0.3
	CO_2	1.9	1421	76	0.8	4.8	0.8
	C_2H_6	1.3	979	41	0.8	6.3	0.3
Beulah-Zap	N_2	0.8	631	304	0.8	0.5	0.1
	CH_4	1.5	1161	222	0.8	4.3	0.5
	CO_2	3.6	2701	150	0.8	4.9	0.9
	C_2H_6	1.2	882	49	0.8	6.8	0.2
Upper Freeport	N_2	1.1	807	463	0.8	1.2	0.2
	CH_4	1.3	1012	185	0.8	3.3	0.8
	CO_2	1.7	1260	106	0.8	5.4	0.6
	C_2H_6	1.1	823	63	0.8	8.2	0.4
Overall						3.9	0.4

Figures 39 through 43 illustrate the Langmuir and LRC model representation on dry coals. As indicated in the figures the adsorption amount for nitrogen is about half that of pure methane. The CO_2 adsorption is almost twice that of the methane and four-fold that of nitrogen.

Methane and nitrogen represent a monolayer Type I adsorption. The adsorption of CO_2 and ethane is not typical Type I monolayer adsorption. CO_2 and ethane exhibits monolayer adsorption up to approximately 8 MPa (1000 psia).

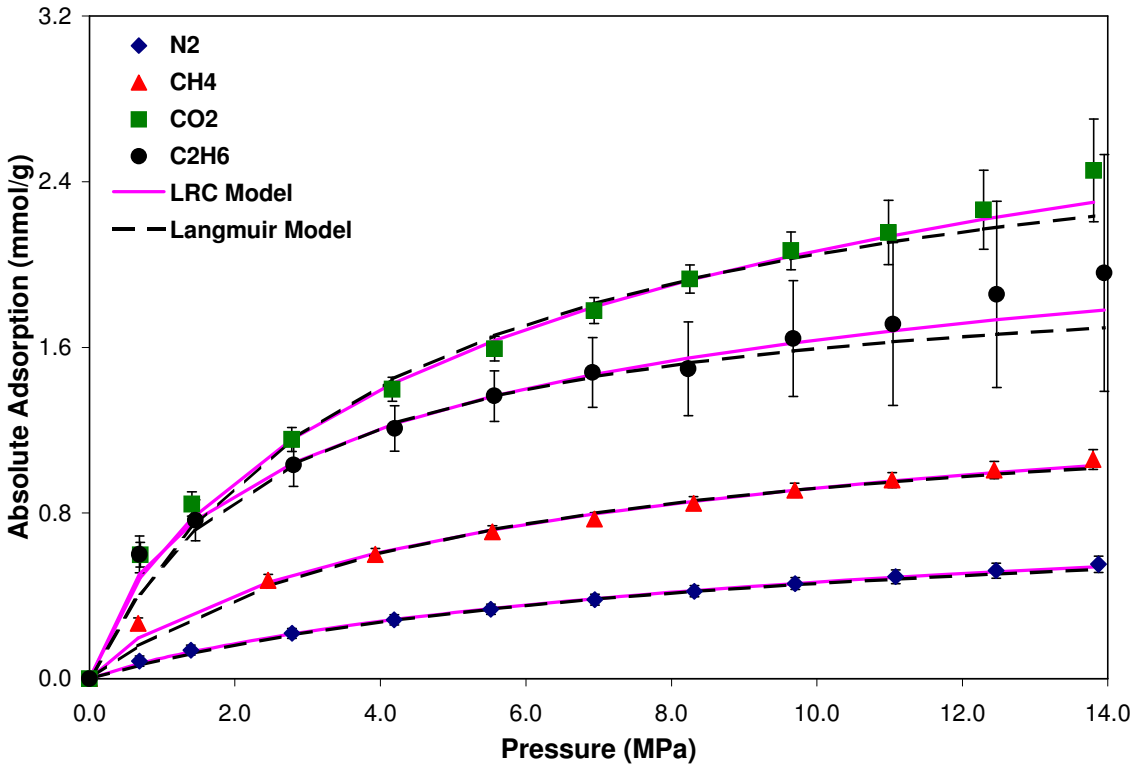

Figure 39: LRC and Langmuir Model Representation of Pure Coalbed Gases on Dry Illinois #6 Coal at 328.2 K

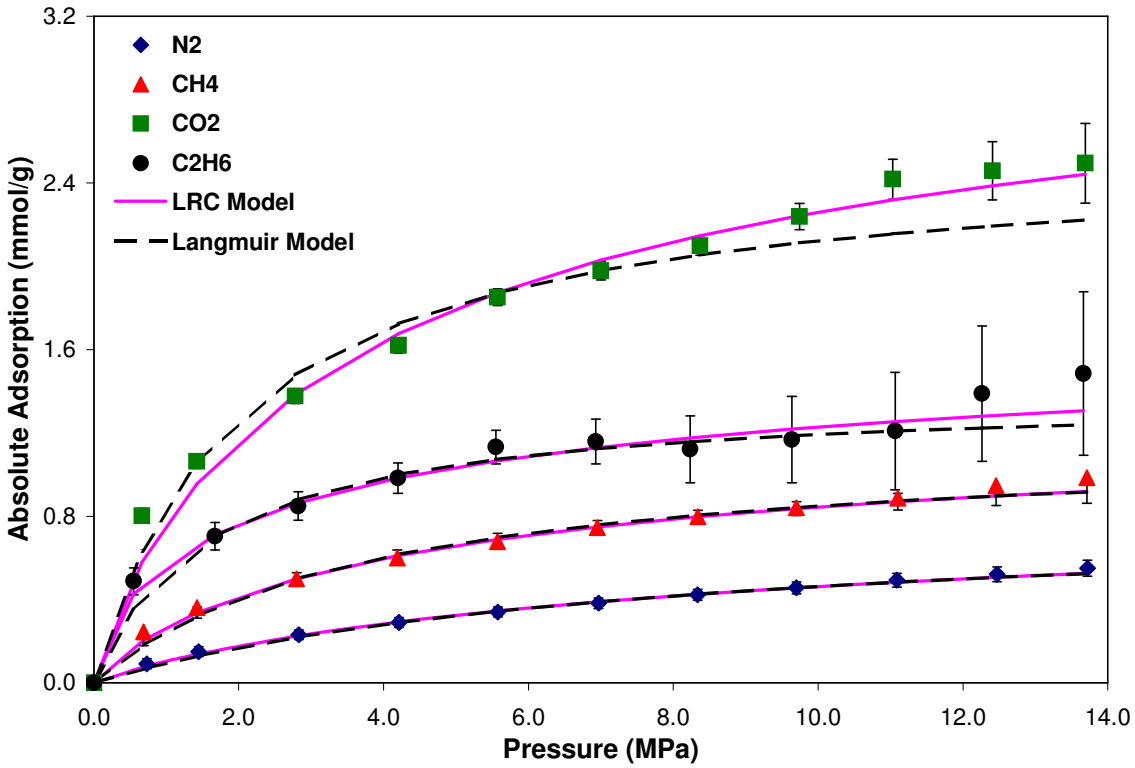

Figure 40: LRC and Langmuir Model Representation of Pure Coalbed Gases on Dry Wyodak Coal at 328.2 K

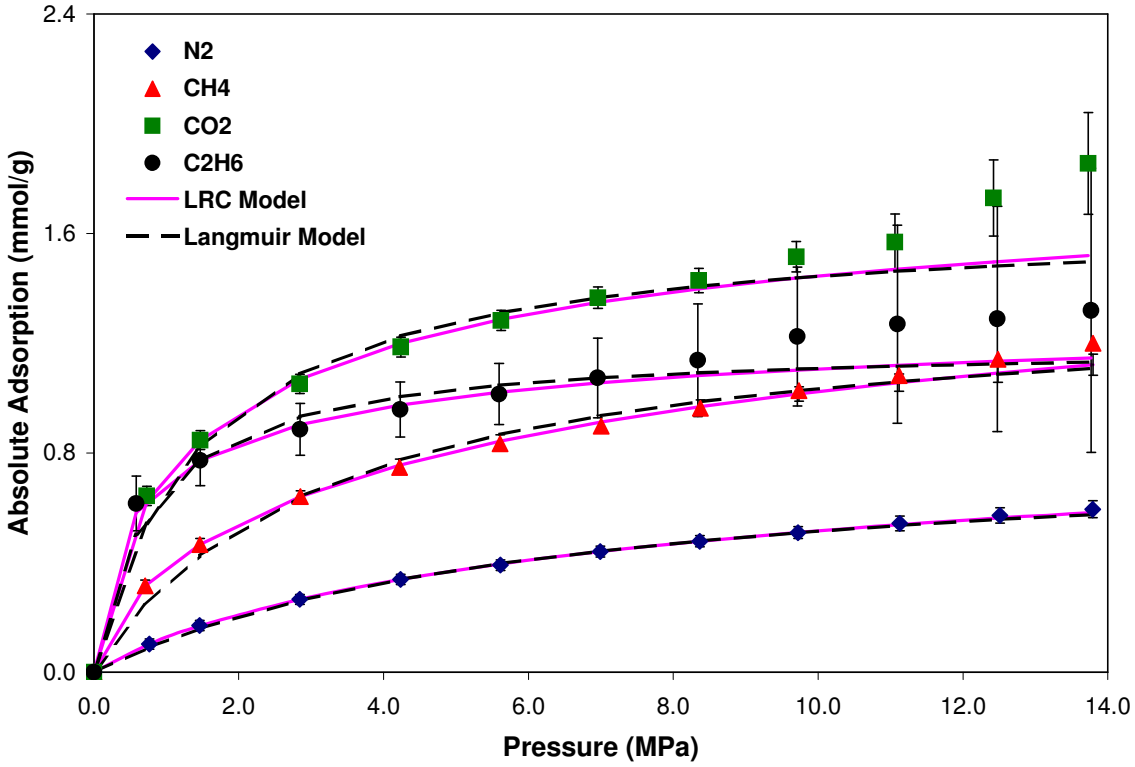

Figure 41: LRC and Langmuir Model Representation of Pure Coalbed Gases on Dry Pocahontas #3 Coal at 328.2 K

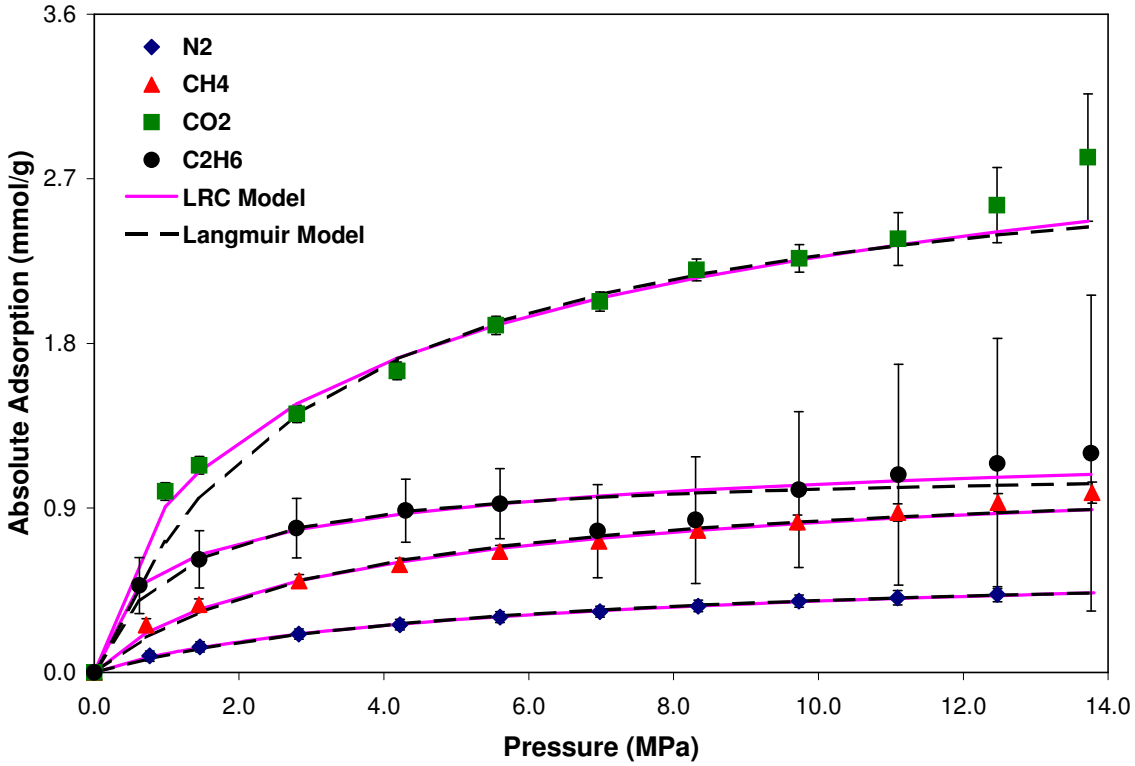

Figure 42: LRC and Langmuir Model Representation of Pure Coalbed Gases on Dry Beulah Zap Coal at 328.2 K

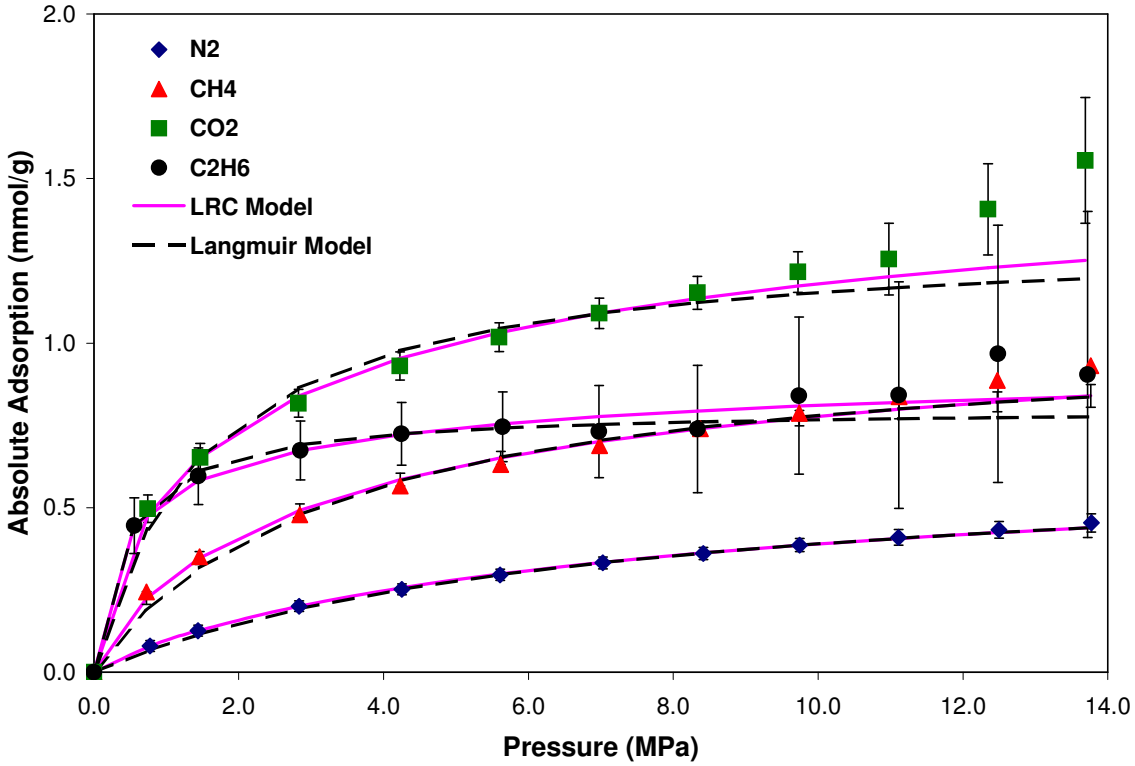

Figure 43: LRC and Langmuir Model Representation of Pure Coalbed Gases on Dry Upper Freeport Coal at 328.2 K

The LRC is capable of representing the adsorption data from low to mid-range pressures within two to three percent for both nitrogen and methane, but slightly under-predicts at higher pressure. On the other hand, the Langmuir model under-predicts the adsorption data at low pressure and at higher pressures, and over-predicts at mid-range pressures (especially for CO_2 isotherms). Both the LRC and Langmuir model appear to have more difficulty at low pressures, where the relative deviations are large.

Overall, the LRC model with two regressed parameters and a fixed exponent can represent the data within the expected experimental uncertainties, which corresponds to 3.9% AAD on average (WAAD = 0.4) as compared to Langmuir model with 5.9% AAD (WAAD = 0.7) on average.

CHAPTER 5

ONO-KONDO LATTICE MODEL FOR ADSORPTION

A lattice model was selected for modeling the newly-acquired data because of its sound theoretical framework, which employs a clear physical basis for modeling adsorption. Specifically the Ono-Kondo (OK) model:

- Describes monolayer and multilayer adsorption
- Has a potential to describe the adsorption behavior based on the physical properties of the adsorbates and the accessible characterization of the adsorbent
- Is structured to incorporate accurate density calculations, which may reduce the correlative burden of the adsorption modeling

5.1 Ono-Kondo Lattice Model

An adsorption model based on the lattice theory was proposed first by Ono and Kondo [Ono and Kondo, 1960]. A generalized form was developed further by Donohue and coworkers for the adsorption of solutes in liquid solutions [Aranovich et al., 1996 and 1997; Hocker et al., 1999]. Sudibandriyo (2003) further developed the OK model for application in high pressure gas adsorption. The assumptions for the lattice Ono-Kondo model are [Sudibandriyo, 2003]:

- The fluid system is assumed to be composed of layers of lattice cells that contain fluid molecules and vacancies.

- Molecular interactions are assumed to exist only between the nearest neighboring molecules.
- Chemical equilibrium between the adsorbed layers and the bulk is given by the equality of the chemical potential in each layer and the bulk.

A configuration of molecules in a mixture fluid in its equilibrium state can be represented by a square lattice, which is shown in Figure 44. In this condition, the total number of lattice cell sites, $M = \sum_{i}^{n} N_i$, is constant, where N_i is the particle number, including the empty cell sites and N_n represents the number of "holes" or empty cells present in the system. The shaded cells in Figure 44 are the primary nearest-neighbor cells around a cell filled with molecule *j*. Two more primary nearest-neighbor cells are on top of and under molecule *j*. Each primary nearest-neighbor cell may be filled by other species *i*, or may be an empty cell.

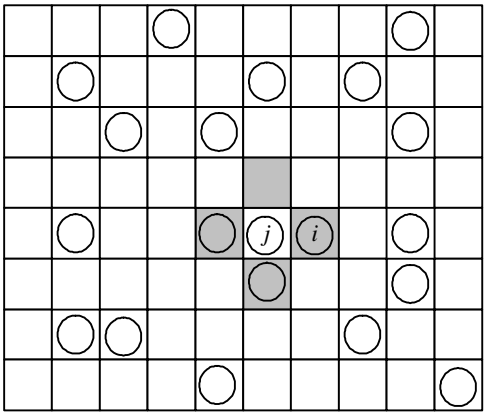

Figure 44: Fluid Mixture on a Square Lattice

Benard and Chahine (1997) assume that the adsorption process may be directly mapped on two parallel hexagonal graphite planes as shown in Figure 45. The figure also shows adsorbed molecules inside a slit between the planes, and Figure 46 shows the

adsorbed molecules positioned among the carbon atoms of the graphite planes. In this approach, the equilibrium equation becomes:

$$\ln\left[x_{ads}(1-x_b)/x_b(1-x_{ads})\right]+((z_1+1)x_{ads}-z_0x_b)\varepsilon_{ff}/kT+\varepsilon_{fs}/kT=0 \qquad (5\text{-}1)$$

where x_b is fractional coverage of a pure component in the bulk phase, x_{ads} is fractional coverage of a pure component in the monolayer lattice model, z_1 is the parallel coordination number representing the number of primary nearest-neighbor cells in parallel direction (z_l = 6), and z_0 is the lattice coordination number (z_0 = 8) for the hexagonal lattice cell. The interaction energy between molecule i and j is expressed by ε_{ff}, and ε_{fs} is the interaction energy between molecule *i* and the solid surface.

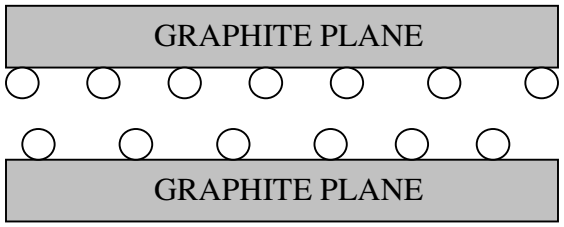

Figure 45: Monolayer Adsorption on Graphite Slit

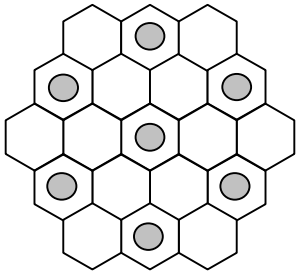

Figure 46: Adsorbed Molecules Positioned among the Carbon Atoms of the Graphite Planes

According to the lattice theory, the excess adsorption is defined as

$$n_i^{Ex} = C_i \sum_{t=1}^{m} (x_{i,t} - x_{i,b}) \tag{5-2}$$

where $x_{i,t}$ is the fraction of adsorbed molecules i that occupy the lattice cells at layer t (= $N_{i,t}$ /M_t), and $x_{i,b}$ is the fraction of gas molecules i occupying the same number of lattice cells as those at layer t (=$N_{i,b}$/M_t). This fractional coverage can also be expressed as $x_{i,t} = \rho_{i,t} / \rho_{i,mc}$ and $x_{i,b} = \rho_{i,b,} / \rho_{i,mc}$, where $\rho_{i,t}$ is the adsorbed density of component i at layer t, $\rho_{i,b}$ is the adsorbed density of component i at the gas phase, and $\rho_{i,mc}$ is the adsorbed density of component i at the maximum capacity. The prefactor C_i represents the maximum capacity of the adsorbent. For pure adsorption inside the slit, according to the approach by Benard and Chahine (1997), the number of layers, m, is equal to two, and Equation 5-2 becomes:

$$n^{Ex} = 2C\ (x_{ads} - x_b) = 2C \left(\frac{\rho_{ads}}{\rho_{mc}} - \frac{\rho_b}{\rho_{mc}} \right) \tag{5-3}$$

Here, the pre-factor C may be assumed to be a parameter taking into account the fraction of the active pores of the adsorbent and other structural properties of the adsorbent. C/ρ_{mc} represents the specific adsorbed-phase volume for the adsorbate-adsorbent system.

Equation 5-1 is used for monolayer adsorption equilibrium, and together with Equation 5-3 they can be used to correlate the experimental excess adsorption isotherm to obtain four parameters per gas, i.e., ε_{ff}/k, ε_{fs}/k, ρ_{mc} and C. In the present work, these four parameters were optimized using the following objective function:

$$OBJ = \sum_{i}^{npts} ((n_{i,calc}^{Ex} - n_i^{Ex})/\sigma_i)^2 \qquad (5\text{-}4)$$

where σ_i is the expected uncertainty in n_i^{Ex}.

5.2 Modeling of Pure-Gas Adsorption

The correlative capability of the Ono-Kondo (OK) model was evaluated. Model parameters (ε_{ff}/k, ε_{fs}/k, ρ_{mc} and C – Case 1) were regressed to obtain precise representations for pure-gas, high pressure adsorption on the five coals involving adsorbates in the near critical and supercritical regions.

Table 39 presents a summary of the model evaluation results for the monolayer OK model employed in this study. The model parameters, given in Table 39, were determined by minimizing the sum of squares of weighted absolute deviations in the calculated adsorption (Equation 5-4), for the pure gas of interest. Measures for the quality of the fit, expressed in terms of absolute average percentage deviation (%AAD) and weighted average absolute deviations (WAAD), are also given in Table 39.

As indicated by the tabulated results, the OK model using four regressed parameters can represent the data within their expected experimental uncertainties, which corresponds to 3.3% AAD on average.

5.3 Two-Parameter OK Model

To minimize the number of regressed parameters and move toward a generalized model, a two-parameter model (Case-2) was examined. In this case, generalized estimates for the adsorbed-phase density and the fluid-fluid energy parameter were used.

Table 39: Ono-Kondo Model Parameters for Dry Coals at 328.2 K – Case 1

Coals	Gases	ε_{fs} / k (K)	ε_{ff} / k (K)	C mg mole/g coal	ρ_{mc} mg mole/cm^3	%AAD	WAAD
Illinois #6	N_2	-690	50	0.57	25.5	2.4	0.1
	CH_4	-970	65	0.75	24.3	3.5	0.5
	CO_2	-1195	80	1.26	22.2	1.8	0.3
	C_2H_6	-1265	85	0.89	15.8	4.3	0.3
Wyodak	N_2	-760	50	0.53	27.4	2.7	0.2
	CH_4	-1075	70	0.68	27.5	2.4	0.4
	CO_2	-1425	85	1.33	31.0	1.7	0.5
	C_2H_6	-1445	65	0.66	22.1	6.1	0.6
Pocahontas	N_2	-805	50	0.53	26.0	0.4	0.1
	CH_4	-1000	60	0.75	17.6	2.7	0.7
	CO_2	-1520	85	0.84	23.7	2.4	0.3
	C_2H_6	-1545	80	0.62	19.0	6.4	0.5
Beulah-Zap	N_2	-840	45	0.37	23.1	1.5	0.1
	CH_4	-1000	65	0.64	20.4	3.6	0.5
	CO_2	-1365	85	1.35	24.1	3.0	0.6
	C_2H_6	-1645	85	0.51	20.4	8.9	0.3
Upper Freeport	N_2	-780	85	0.49	26.5	0.4	0.0
	CH_4	-990	75	0.59	17.0	2.5	0.4
	CO_2	-1510	100	0.68	22.4	2.3	0.1
	C_2H_6	-1700	85	0.43	18.9	6.3	0.3
Overall						3.3	0.3

Following the work of Sudibandriyo (2003), the adsorbed-phase density and the fluid-fluid energy parameter were estimated from the reciprocal van der Waals co-volume and the adjusted energy parameter of the Lennard-Jones 12-6 potential, respectively. Following is a brief description for these parameter generalizations.

A general approximation for the maximum adsorbed-phase density, ρ_{mc}, is the liquid density at the normal boiling point, as was done by Arri et al., (1992). However, examination of the results from the OK model reveals that the adsorbed-phase densities generated by the OK model, as presented in Table 40, are less than the boiling point estimates and are closer to the reciprocal van der Waals co-volume estimates [Sudibandriyo, 2003].

Table 40: Adsorbed-Phase Densities Estimated by Different Methods

Method	Adsorbed-Phase Density (g/cm^3)			
	Methane	Nitrogen	CO_2	Ethane
Ono-Kondo model	0.345	0.673	0.977	0.475
Zhou-Gasem-Robinson (ZGR) EOS	0.345	0.839	0.982	---
Liquid density estimate	0.421	0.808	---	0.546
Solid density estimate	---	---	1.18	---
Reciprocal van der Waals covolume	0.374	0.725	1.03	0.462
Graphical estimate from the Gibbs adsorption	---	---	1.02	0.444

The fluid-fluid energy parameter, ε_{ff}/k, was estimated to be proportional to the Lennard-Jones well depth energy parameter. For the Lennard-Jones 12-6 potential, the pair-wise interaction between two molecules separated by a distance *r* is given by

$$\Phi(r) = 4\varepsilon * \left[\left(\frac{\sigma}{r} \right)^{12} - \left(\frac{\sigma}{r} \right)^{6} \right] \qquad (5\text{–}5)$$

where $\Phi(r)$ is the potential energy, ε^* is the well depth of the potential, and σ is the collision diameter, which is defined as the distance at which the potential energy is zero. Equation 5-5 was simplified by Sudibandriyo (2003) to,

$$\varepsilon_{ff} = 0.432\varepsilon^* \tag{5-6}$$

The values for ε^* are obtained from Reid et al., (1987) and listed in the Table 41.

Table 41: Physical Properties of the Adsorbates [a]

Adsorbate	MW	Tc (K)	Pc (MPa)	Normal Boiling Point (K)	Reciprocal van der Waals co-volume (mol/L)	σ ($\times 10^{-10}$ m)	ε^*/k (K)
N_2	28.01	126.20	3.40	77.3	25.89	3.798	71.4
CO_2	44.01	304.21	7.38	216.6 [b]	23.34	3.941	195.2
CH_4	16.04	190.56	4.60	111.7	23.37	3.758	148.6
C_2H_6	30.07	305.32	4.87	184.6	15.41	4.443	215.7

[a] Reid et al., (1987)
[b] Triple point temperature

Table 42 presents the summary results for the two-parameter OK model. As indicated, the model can represent the adsorption data within twice the experimental uncertainties for all the coals considered with a maximum of 15.4% AAD for ethane on Beulah-Zap coal. These large errors are due to the under prediction of higher-pressure adsorption data. Apparently, the adsorbed-phase density estimate obtained from van der Waals reciprocal co-volume is not adequate for representing the adsorption data for ethane at higher pressures. Thus to correlate the adsorption data for ethane more precisely, a three-parameter OK model (ε_{fs}/k, ρ_{mc} and C) was examined.

Table 42: Two-parameter OK Model for Dry Coals at 328.2 K – Case 2

Coals	Gases	ε_{fs} / k (K)	ε_{ff} / k [a] (K)	C mg mole/g coal	ρ_{mc} [b] mg mole/cm^3	%AAD	WAAD
Illinois #6	N_2	-730	31	0.50	25.9	2.9	0.2
	CH_4	-935	64	0.79	23.4	3.5	0.5
	CO_2	-1250	84	1.23	23.3	2.0	0.3
	C_2H_6	-1265	93	0.91	15.4	5.4	0.3
Wyodak	N_2	-800	31	0.45	25.9	3.0	0.3
	CH_4	-1065	64	0.66	23.4	2.7	0.5
	CO_2	-1250	84	1.49	23.3	5.5	1.4
	C_2H_6	-1250	93	0.84	15.4	13.4	1.2
Pocahontas	N_2	-800	31	0.51	25.9	1.4	0.2
	CH_4	-1180	64	0.66	23.4	1.3	0.3
	CO_2	-1520	84	0.83	23.3	2.7	0.4
	C_2H_6	-1500	93	0.69	15.4	14.4	0.9
Beulah-Zap	N_2	-905	31	0.32	25.9	1.6	0.1
	CH_4	-1025	64	0.64	23.4	4.0	0.5
	CO_2	-1385	84	1.33	23.3	3.3	0.6
	C_2H_6	-1430	93	0.62	15.4	15.4	0.5
Upper Freeport	N_2	-890	31	0.33	25.9	2.9	0.4
	CH_4	-1180	64	0.50	23.4	1.3	0.3
	CO_2	-1500	84	0.66	23.3	2.0	0.2
	C_2H_6	-1520	93	0.46	15.4	13.3	0.6
Overall						5.1	0.5

[a] Calculated from Equation 5-6.

[b] Reciprocal of van der Waals co-volume listed in Table 38.

Table 43 lists the parameters for all the three forms of the OK model. Figure 47 shows the representation of the all the OK models on Beulah Zap coal. As projected, the three-parameter model represents the adsorption data better than the two-parameter model and within the expected experimental uncertainties of the data.

Table 43: Regressed OK model Parameters for Ethane on Dry Beulah Zap Coal

Beulah-Zap	Gas	ε_{ss} / k (K)	ε_{ff} / k (K)	C mg mole/g coal	ρ_{mc} mg mole/cm^3	%AAD	WAAD
4-Parameter	C2H6	-1700	85	0.43	18.9	6.3	0.3
3-Parameter	C2H6	-1500	93	0.56	20.2	9.0	0.3
2-Parameter	C2H6	-1520	93	0.46	15.4	13.3	0.6

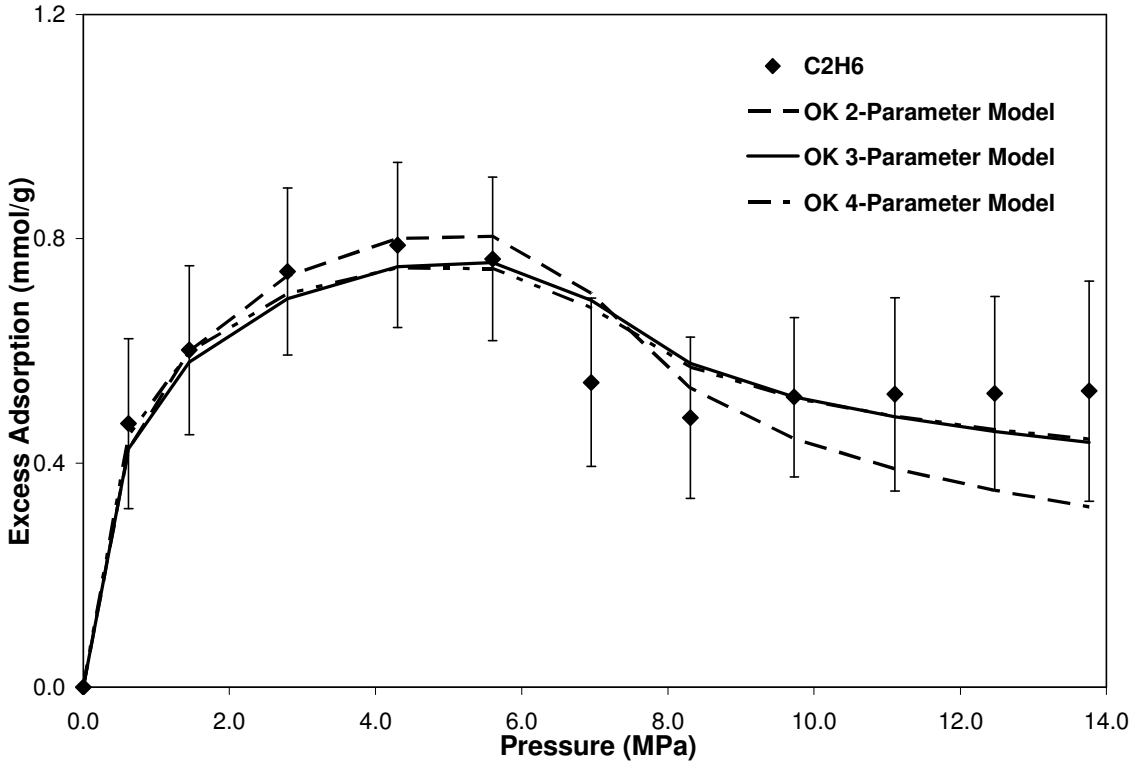

Figure 47: OK Model Representation of Ethane on Dry Beulah Zap Coal at 328.2 K

Figures 48 through 52 illustrate the quality of representation of both the two-parameter and four-parameter OK model. On average, the four-parameter OK model can represent the adsorption data within the expected experimental uncertainties. Nevertheless, some relatively large errors (maximum 8% AAD) were observed for ethane. These large errors are partly due to the high uncertainty in the ethane bulk density calculation. Also, the percentage deviation is exaggerated when the Gibbs excess adsorption becomes exceedingly small; i.e., at lower pressure, at high temperatures, or at nearly full coverage adsorption at higher pressures.

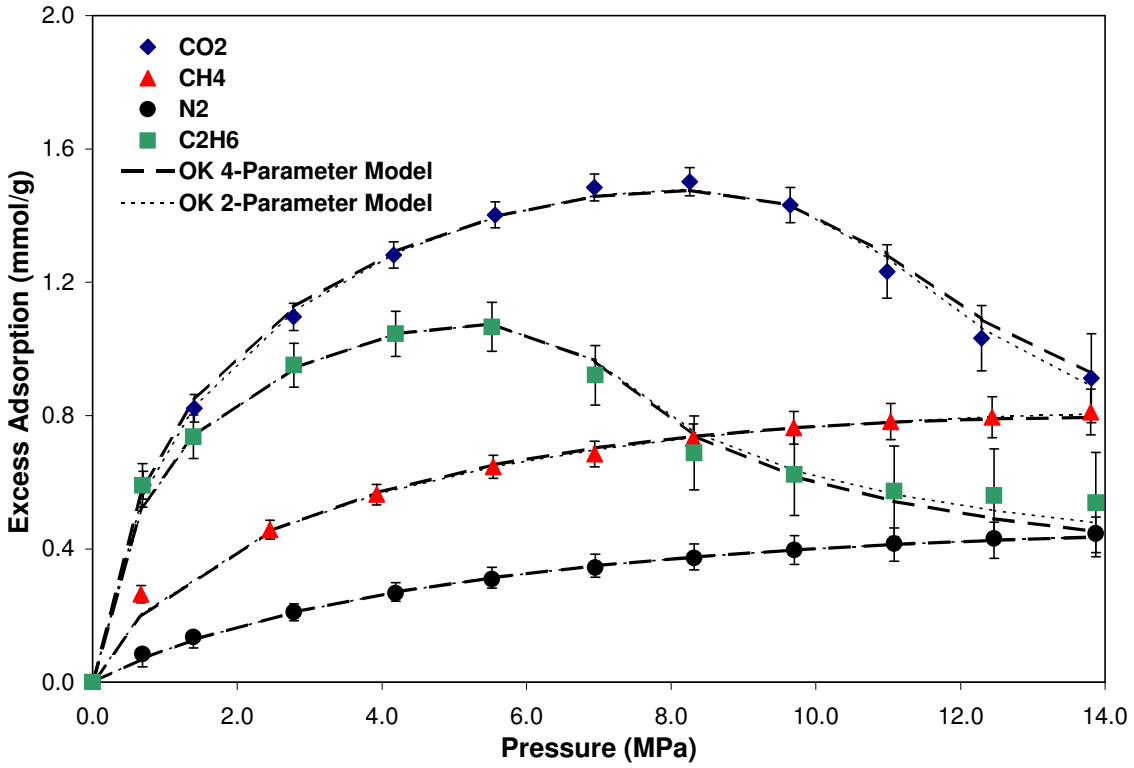

Figure 48: Ono-Kondo Representation of Pure Coalbed Gases on Dry Illinois #6 Coal at 328.2 K

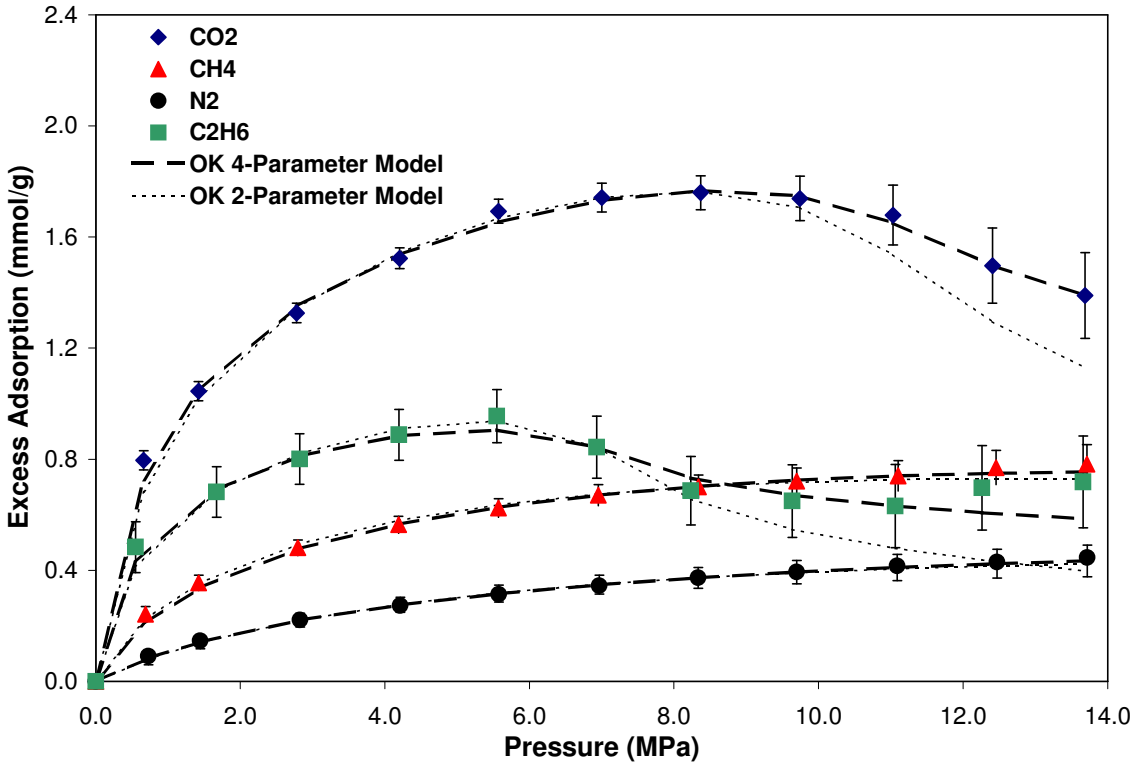

Figure 49: Ono-Kondo Representation of Pure Coalbed Gases on Dry Wyodak Coal at 328.2 K

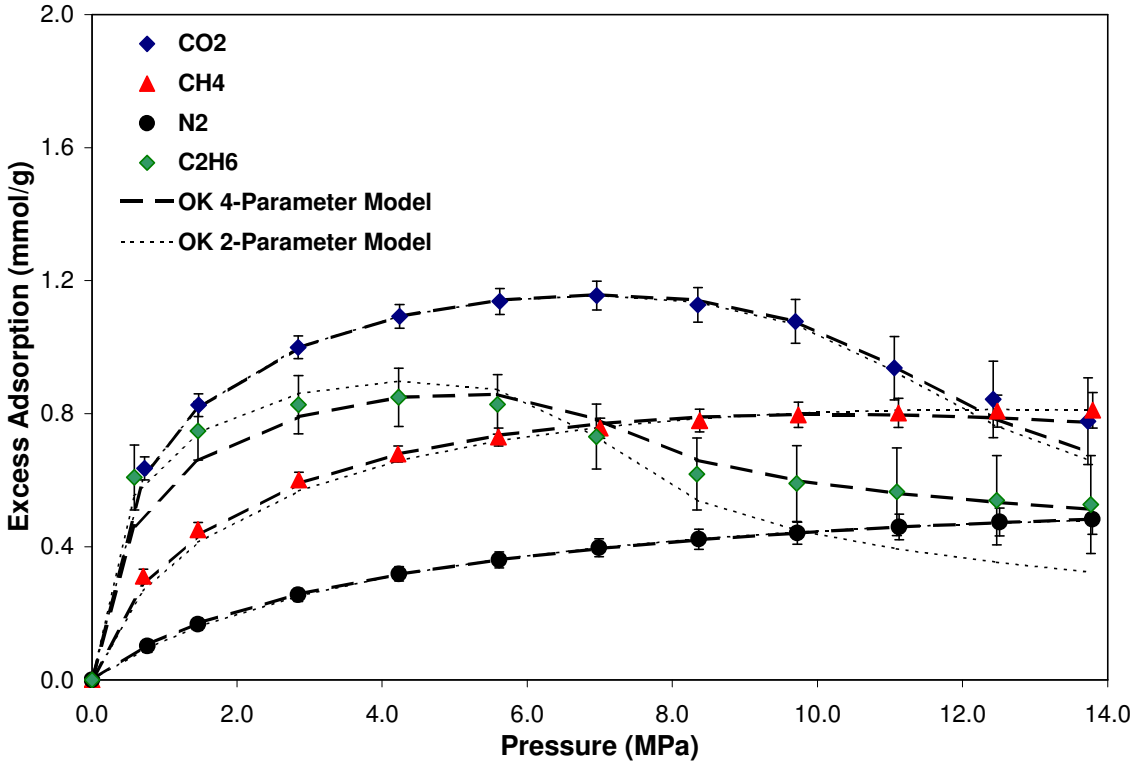

Figure 50: Ono-Kondo Representation of Pure Coalbed Gases on Dry Pocahontas #3 Coal at 328.2 K

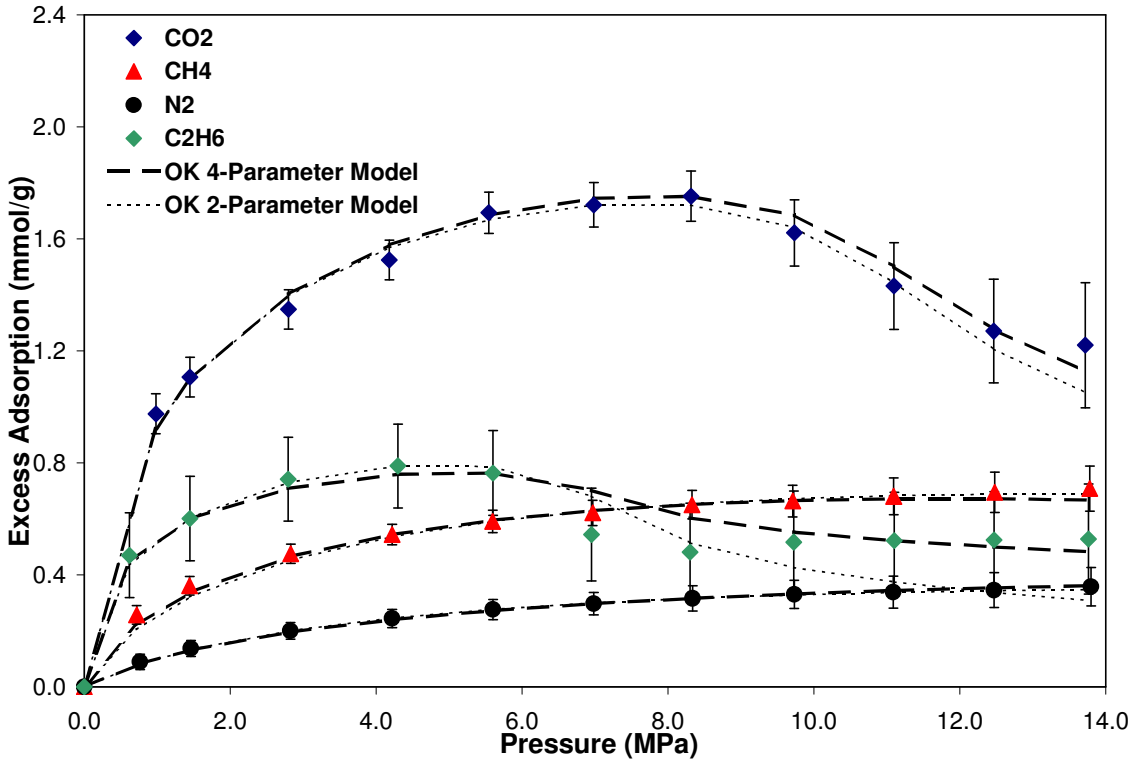

Figure 51: Ono-Kondo Representation of Pure Coalbed Gases on Dry Beulah Zap Coal at 328.2 K

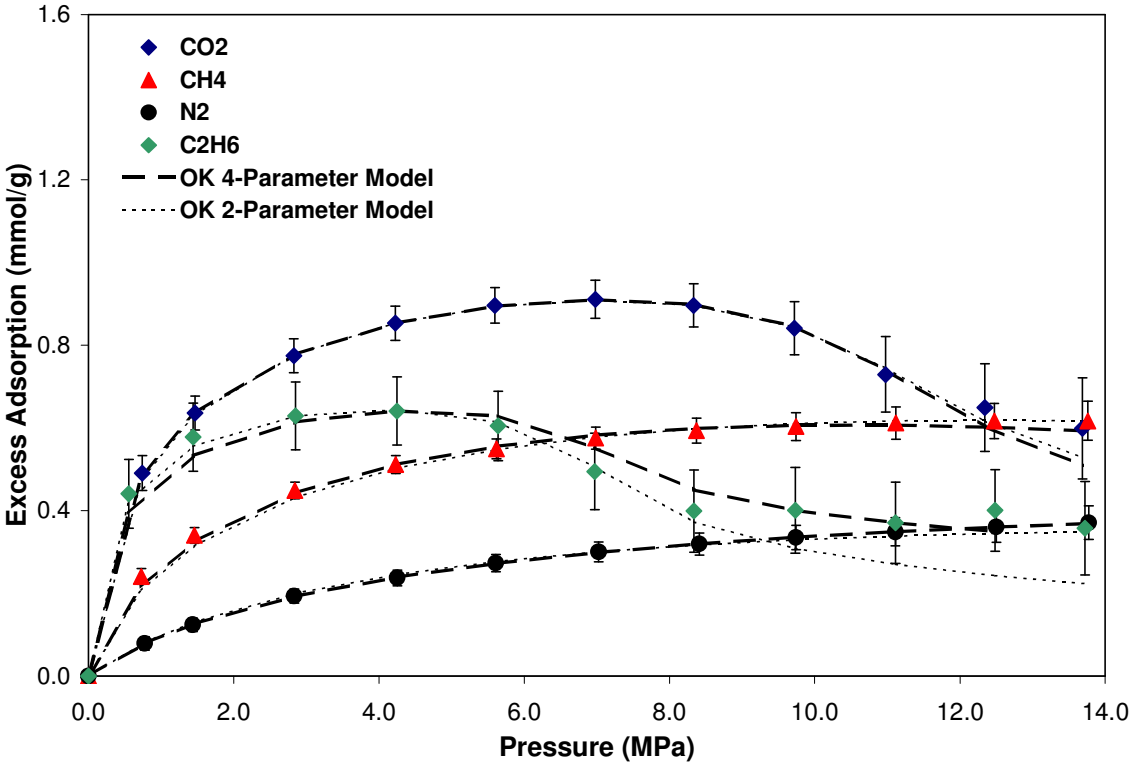

Figure 52: Ono-Kondo Representation of Pure Coalbed Gases on Dry Upper Freeport Coal at 328.2 K

5.4 Generalized OK Model

Although, Sudibandriyo (2003) generalized the OK model parameters based on molecular descriptors, an effort was made in this work to generalize the model parameters based on the composition of the adsorbent (fixed carbon content, oxygen content, etc.) and the critical properties of the adsorbates under study.

In Figure 53, we examined the trends in the regressed OK fluid-solid energy parameter ε_{fs}/k presented in Table 42. Both the coal fixed carbon and the gas critical temperature show reasonable correlation with energy parameter. Specifically, for all coal samples, the value of ε_{fs}/k decreases as the critical temperature increases. In addition, a linear correlation approximates the relation between the fixed carbon content [dry ash free (daf)] of each coal and the energy parameter.

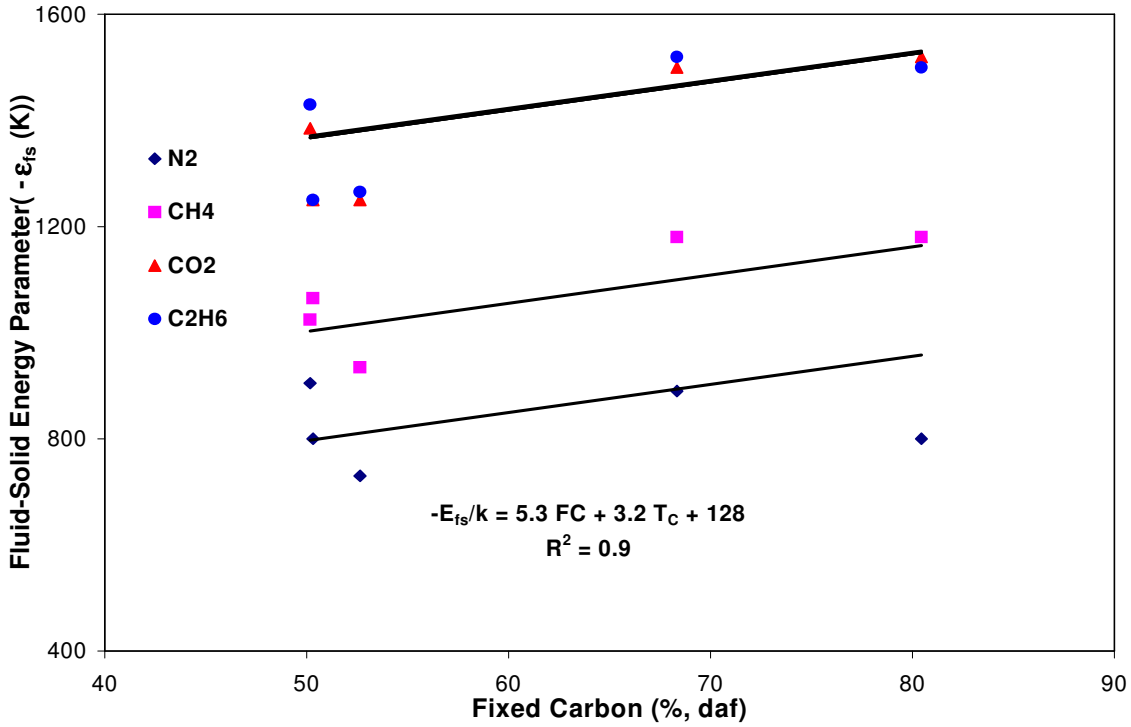

Figure 53: Variation of the Fluid-Solid Energy Parameter with Fixed Carbon and Critical Temperature.

A general correlation to describe the fluid-solid energy parameter in terms of adsorbent and adsorbate properties was obtained:

$$-\varepsilon_{fs}/k = 5.3\ FC + 3.2\ T_C + 128 \qquad (5\text{-}7)$$

where FC is the fixed carbon content (daf) of the coal and T_C (K) is the critical temperature of the pure-gas. In general, reasonably accurate predictions for the energy parameter, as indicated by the comparison presented in Figure 54, were obtained. Specifically, the generalized parameter predictions are within 11% of the regressed values given in Table 42.

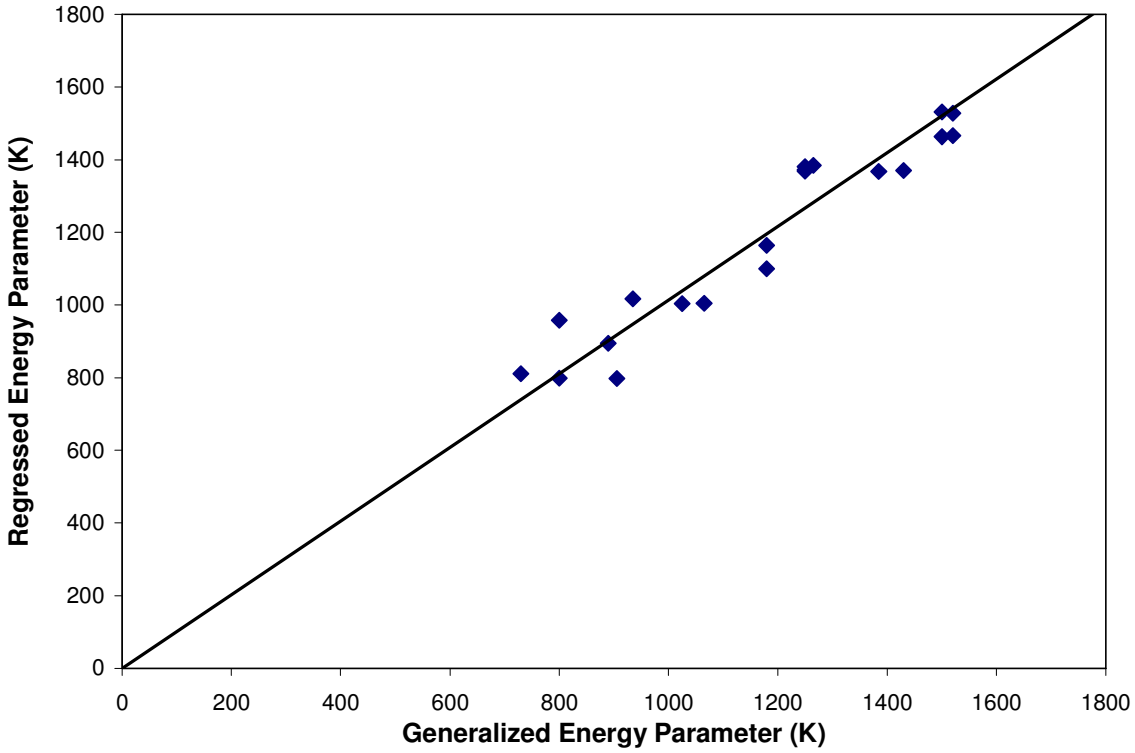

Figure 54: Comparison of Generalized and Regressed Fluid-Solid Energy Parameter

An attempt was made to correlate the maximum capacity parameter, C, with the oxygen content of the coals. Figure 55 illustrates the variation in the maximum capacity

with the oxygen content of the coals studied. Although clear trends are observed for each gas, significant scatter, attributable to coal structure, remains in these trends. The preliminary correlation obtained for the capacity parameter yielded poor results (AAD of 19%). Although further refinement of this correlation is possible, additional data would be required to justify the effort. Therefore, the one-parameter generalization of Case 3 (generalized ε_{ff}/k, ε_{fs}/k, ρ_{mc}, and regressed C) represents the extent of our generalization currently. Table 44 presents the results of this case, which indicates that the one-parameter OK model is capable of describing the adsorption behavior of the gases considered with an AAD of 6.1%.

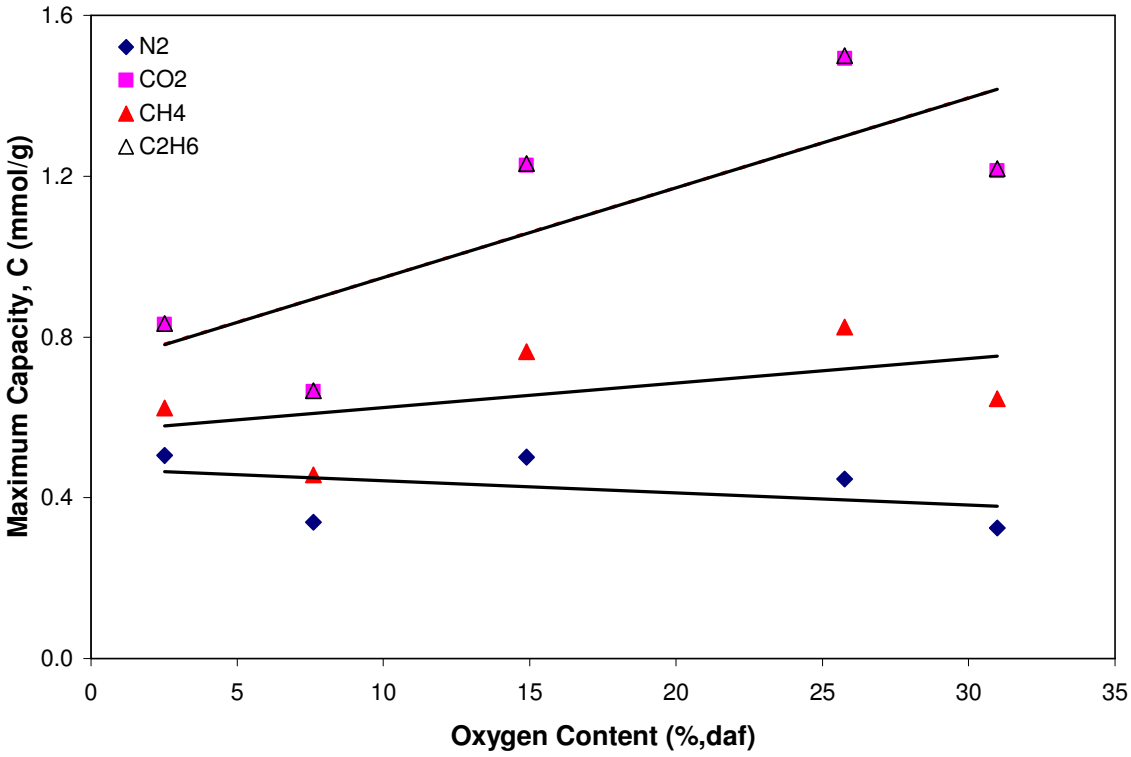

Figure 55: Variation of the Maximum Capacity with Oxygen Content of Coals

Table 45 presents the summary results of the OK model evaluation on three cases. As expected, the greater the number of regressed parameters, the higher is the precision of the OK model representations. Specifically, the OK four-parameter model (ε_{ff}/k, ε_{fs}/k, ρ_{mc} and C regressed for individual isotherm) represents the data with AAD of 3%. In comparison, the two-parameter and one-parameter models yield AAD of 5% and 6%, respectively.

Table 44: Generalized OK Model Parameters for Dry Coals – Case 3

Coals	Gases	ε_{fs} / k [c] (K)	ε_{ff} / k [a] (K)	C [d] mg mole/g coal	ρ_{mc} [b] mg mole/cm^3	%AAD	WAAD
Illinois #6	N_2	-811	31	0.44	25.9	3.3	0.3
	CH_4	-1017	64	0.72	23.4	4.1	0.7
	CO_2	-1380	84	1.13	23.3	5.0	0.8
	C_2H_6	-1384	93	0.84	15.4	6.4	0.4
Wyodak	N_2	-798	31	0.45	25.9	3.0	0.3
	CH_4	-1004	64	0.70	23.4	2.9	0.4
	CO_2	-1368	84	1.40	23.3	7.4	2.2
	C_2H_6	-1372	93	0.78	15.4	15.0	1.4
Pocahontas	N_2	-958	31	0.40	25.9	5.5	0.7
	CH_4	-1164	64	0.67	23.4	1.6	0.4
	CO_2	-1528	84	0.83	23.3	2.7	0.4
	C_2H_6	-1531	93	0.68	15.4	14.5	0.9
Beulah-Zap	N_2	-798	31	0.39	25.9	4.7	0.3
	CH_4	-1004	64	0.66	23.4	4.5	0.5
	CO_2	-1367	84	1.31	23.3	3.3	0.6
	C_2H_6	-1406	93	0.64	15.4	15.5	0.5
Upper Freeport	N_2	-894	31	0.33	25.9	3.1	0.4
	CH_4	-1100	64	0.54	23.4	3.0	0.6
	CO_2	-1464	84	0.68	23.3	2.4	0.3
	C_2H_6	-1467	93	0.51	15.4	13.5	0.7
Overall						6.1	0.6

[a] Calculated from Equation 5-6.

[b] Reciprocal of van der Waals co-volume listed in Table 38.

[c] Estimated from the Equation 5-7 .

[d] Regressed for each gas

Table 45: Summary Results of OK Modeling

Case No	Description	Overall %AAD	Overall WAAD
1	ε_{ff}/k, ε_{fs}/k, ρ_{mc} and C regressed for each gas and coal separately	3.3	0.3
2	Generalized ε_{ff}/k , ρ_{mc} ε_{ff}/k – adjusted Lennard-Jones parameter (Equation 5-6) ρ_{mc} - reciprocal van der Waals co-volume and ε_{fs}/k regressed for each gas C regressed for each gas separately	5.1	0.5
3	Generalized ε_{ff}/k, ρ_{mc} and ε_{fs}/k ε_{ff}/k – adjusted Lennard-Jones parameter (Equation 5-6) ρ_{mc} - reciprocal van der Waals co-volume ε_{fs}/k – fixed carbon and critical temperature correlation (Equation 5-7) and C regressed for each gas separately	6.1	0.6

CHAPTER 6

CONCLUSIONS AND RECOMMENDATIONS

6.1 Conclusions

High pressure adsorption of pure methane, nitrogen, CO_2 and ethane at 328.2 K (131 °F) and pressures to 13.8 MPa (2000 psia) were measured on dry Illinois #6, Wyodak, Pocahontas #3, Beulah Zap, and Upper Freeport coals. The Langmuir model, Loading-Ratio Correlation (LRC) and the Ono-Kondo (OK) lattice model were used to represent the newly-acquired pure-gas, high pressure adsorption data. Following are the conclusions drawn and the recommendation made based on this study:

- The average expected uncertainties for the methane, nitrogen, ethane, and CO_2 adsorption measurements are approximately 2.4% (0.02-0.03 mmol/g), 2.7% (0.03-0.04 mmol/g), 10.1% (0.09-0.13 mmol/g) and 5.4% (0.06-0.12 mmol/g), respectively.
- Nitrogen, methane, ethane, and CO_2 exhibit an increasing order in the amount of absolute gas adsorbed.
- At low to moderate pressures, the adsorption amount is greater for low rank coals (Beulah-Zap, Wyodak) than the higher ranked ones for CO_2 and ethane.
- Hysteresis is observed for low rank (Beulah-Zap, Wyodak) coals during desorption, especially for CO_2.
- Methane and nitrogen showed far less variation in adsorption amounts than either CO_2 or ethane.

- As expected, the near-critical isotherms of CO_2 and ethane exhibit maxima in the excess adsorption.
- The ratio (CO_2 /ethane) in the absolute amount of adsorption varies notably among the coals.
- Little variation in isotherm reproducibility is shown for methane after the coal has been subjected to CO_2 and ethane gas adsorption.
- The Langmuir model is adequate for describing pure-gas adsorption at low to moderate pressures (AAD of 5.9%).
- The Loading-Ratio Correlation is capable of representing each isotherm within the experimental uncertainties (AAD of 2.9%). Further, using this correlation with a common exponent (η of 0.8) proved sufficiently precise for the systems considered.
- The Ono-Kondo model with four regressed parameters per individual pure-gas isotherm is capable of representing all Gibbs excess adsorption isotherms within the experimental uncertainties (AAD of 3.0%).
- The one-parameter generalized Ono-Kondo model can represent the pure-gas adsorption data with 7% AAD or twice the experimental uncertainties.
- These newly-acquired data constitute a valuable addition to the existing high pressure adsorption database at Oklahoma State University.

6.2 Recommendations

- Adsorption measurements on wet Illinois #6, Wyodak, Pocahontas #3, Beulah Zap, and Upper Freeport coals should be acquired to investigate the effect of moisture content on coal adsorption.

- An expanded database, involving a variety of coals, should be used to fully generalize the Ono-Kondo model.
- A density meter should be utilized to measure in-situ the adsorbate densities and thus minimize the uncertainties associated with this variable.

REFERENCES

Angus, S., Armstrong, B., de Reuck, K.M., "International Thermodynamic Tables of the Fluid State-5: Methane," IUPAC Chemical Data Series 16, Pergamon Press, New York, 1978.

Angus, S., de Reuck, K.M., Armstrong, B., "International Thermodynamic Tables of the Fluid State-6: Nitrogen," IUPAC Chemical Data Series 20, Pergamon Press, New York, 1979.

Arri, L. E., Yee, D., *Modeling Coalbed Methane Production with Binary Gas Sorption*, SPE Paper 24363, presented at the SPE Rocky Mountain Regional Meeting, Casper, Wyoming, May, 18-21, 1992.

Aranovich, G.L., Donohue, M.D., *Adsorption of Supercritical Fluids*, J. Colloid and Interface Sci., 180, 537-541, 1996.

Aranovich, G.L., Donohue, M.D., *Predictions of Multilayer Adsorption Using Lattice Theory*, J. Colloid and Interface Sci., 189, 101-108, 1997.

Aranovich, G.L., Donohue, M.D., *Surface Compression in Adsorption Systems*, Colloid and Surfaces A., 187-188, 95-108, 2001.

Benard, P., Chahine, R., *Modeling of High Pressure Adsorption Isotherms above the Critical Temperature on Microporous Adsorbents: Application to Methane,* Langmuir, 13(4), 808-813, 1997.

Benard, P., Chahine, R., *Modeling of Adsorption Storage of Hydrogen on Activated Carbons,* International Journal of Hydrogen Energy, 26(8), 849-855, 2001.

Beutekamp, S., Harting, P., *Experimental Determination and Analysis of High Pressure Adsorption Data of Pure Gases and Gas Mixture*, Adsorption, 8, 255-269, 2002.

Brunauer, S., Deming, L.S., Deming, E., Teller, E., J., *On A Theory of the van der Waals Adsorption of Gases*, Am.Chem.Soc. 62, 1723-1732, 1940.

de Boer, J. H., "The Dynamical Character of Adsorption," 2nd Ed., Oxford at The Clarendon Press, London, 1968.

Fitzgerald, J.E., Sudibandriyo, M., Pan. Z., Robinson, Jr., R.L., Gasem, K.A.M., *Modeling the Adsorption of Pure Gases on Coals with the SLD Model*, Carbon, 41, 2203-2216, 2003.

Frére, M.G., De Weireld, G.F., *High Pressure and High-Temperature Excess Adsorption Isotherms of N_2, CH_4, and C_3H_8 on Activated Carbon*, J. Chem. Eng. Data, 47, 823-829, 2002.

Friend, D.G., Ingham, H., Ely, J.F., *Thermophysical Properties of Ethane*, J. Phys. Chem. Ref. Data, 20(2), 275-347, 1991.

Gasem, K.A.M., Robinson, Jr., R.L., Fitzgerald, J.E., Pan, Z., Sudibandriyo, M., *Sequestering Carbon Dioxide in Coalbeds*, Final Report, 1999-2003, Prepared for the U.S. Department of Energy, 2003.

Goodman, A.L., Busch, A., Duffy, G.J., Fitzgerald, J.E., Gasem, K.A.M., Gensterblum, Y., Krooss, B.M., Levy, J., Ozdemir, E., Pan, Z., Robinson, Jr., R.L., Schroeder, K., Sudibandriyo, M., White, C.M., *An Inter-laboratory Comparison of CO_2 Isotherms Measured on Argonne Premium Coal Samples*, Energy & Fuels, 18, 1175-1182, 2004.

Gunter W.D., Gentzis T., Rottenfusser B.A., Richardson, R.J.H., *Deep Coalbed Methane in Alberta*, *Canada*, Energy Conversion Management, 38, S217 to S222, 1997.

Hall, F.E., Jr., "Adsorption of Pure and Multicomponent Gases on Wet Fruitland Coal," M.S. Thesis, Oklahoma State University, Stillwater, Oklahoma, 1993.

Hall, F., Zhou, C., Gasem, K.A.M., Robinson, Jr., R.L., *Adsorption of Pure Methane, Nitrogen, and Carbon Dioxide and Their Binary Mixtures on Wet Fruitland Coal,* presented at the Eastern Regional Conference & Exhibition, Charleston, November 8-10, 1994.

Haydel, J.J., Kobayashi, R., *Adsorption Equilibria in the Methane-Propane-Silica Gel System at High Pressures*, I&EC Fundamentals, 6, 546-554, 1967.

Hocker, T., Aranovich, G.L., Donohue, M.D., *Monolayer Adsorption for The Subcritical Lattice Gas and Partially Miscible Binary Mixture*, J. Colloid and Interface Sci., 211, 61-80, 1999.

http://energy.cr.usgs.gov/oilgas/cbmethane/

http://www.naturalgas.org/overview/resources.asp

Humayun, R., Tomasko, D.L., *High-Resolution Adsorption Isotherms of Supercritical Carbon Dioxide on Activated Carbon*, AIChE J., 46, 2065-2075, 2000.

Krim, J., Watts, E.T., *Roughness and Porosity Characterization of Solid Films Through Adsorption Isotherms Recorded with a Quartz Crystal Microbalanc*e in "Fundamentals of Adsorption", Mersmann, A.B., Scholl, S.E., Eds., Engineering Foundation, New York, 1991.

Krooss, B.M., van Bergen, F., Gensterblum, Y., Siemons, N., Pagnier, H.J.M., David, P., *High pressure Methane and Carbon Dioxide Adsorption on Dry and Moisture-equilibrated Pennsylvanian Coals,* International Journal of Coal Geology, 51, 69-92, 2002.

Mavor M., Pratt T., DeBruyn R. *Study Quantifies Powder River Coal Seam Properties*, Oil and Gas Journal, April 26, 35-50,1999.

Mavor, M., Pratt T., Nelson C.R., *Quantitative Evaluation of Coal Seam Gas Content Estimate Accuracy*, SPE Paper 29577, 1995.

Nelsen, F.M., Eggertsen, F.T., *Determination of Surface Area: Adsorption Measurements by a Continuous Flow Method*, Anal. Chem., 30, 1387, 1958.

Ono, S., Kondo, S., *Molecular Theory of Surface Tension in Liquids*, in "Encyclopedia of Physics (S. Flugge, Ed.), Vol. X.," Springer-Verlag, Gottingen, 1960.

Pan, Z., "Modeling of Gas Adsorption Using Two-Dimensional Equation of State," PhD Dissertation, Oklahoma State University, Stillwater, Oklahoma, 2003.

Pieters, W. J. M., Gates, W. E., U.S. Patent 4, 489, 593, 1984.

Reich, R., Ziegler, W. T., Rogers, K.A., *Adsorption of Methane, Ethane, and Ethylene Gases and Their Binary and Ternary Mixtures and Carbon Dioxide on Activated Carbon at 212-301 K and Pressures to 35 Atmospheres*, Ind. Eng.Chem. Process Des. Dev., 19, 336, 1980.

Reid, R.C., Prausnitz, J.M., Poling, B.E., "The Properties of Gases & Liquids, Fourth Ed.," McGraw-Hill Inc., New York, (1987).

Salem, M.M.K., Braeuer, P., Szombathely M., Heuchel, M., Harting, P., Quitzsch, K., *Thermodynamics of High Pressure Adsorption of Argon, Nitrogen, and Methane on Microporous Adsorbents,* Langmuir, 14, 3376-3389, 1998.

Span, R.,Wagner, W., *A New Equation of State for Carbon Dioxide Covering the Fluid Region from the Triple Point Temperature to 1100 K at Pressures up to 800 MPa*, J. Phys. Chem. Ref. Data, 25 1509-1590 (1996).

Stevens S.H., Spector, D., Riemer, P., *Enhanced Coalbed Methane Recovery Using CO_2 Injection: Worldwide Resource and CO_2 Sequestration Potential*, 1998 SPE International Conference in China, Beijing, China, November 1998.

Stevens S., Spector D., Reimer P., *Enhanced Coalbed Methane Recovery Using CO_2 Injection: Worldwide Resource and CO_2 Sequestration Potential*, Proceedings, Sixth International Oil and Gas Conference and Exhibition in China, Vol. 1, November, 1998.

Sudibandriyo, M., Pan, Z., Fitzgerald, J.E., Robinson, Jr., R.L., Gasem, K.A.M., *Adsorption of Methane, Nitrogen, Carbon Dioxide and their Binary Mixtures on Dry Activated Carbon at 318.2 K and Pressures to 13.6 MPa*, Langmuir, 19(13), 2003.

Sudibandriyo, M., "A Generalized Ono-Kondo Lattice Model for High Pressure Adsorption on Carbon Adsorbents," PhD Dissertation, Oklahoma State University, Stillwater, Oklahoma, 2003.

van der Vaart, R., Huiskes, C., Bosch, H., Reith, T., *Single and Mixed Gas Adsorption Equilibria of Carbon Dioxide/Methane on Activated Carbon*, Adsorption, 6, 311-323, 2000.

Vermesse, J., Vidal, D., Malbrunot, P., *Gas Adsorption on Zeolites at High Pressure*, Langmuir, 12, 4190-4196, 1996.

Yang, R.T., "Gas Separation by Adsorption Processes," Butterworths, Boston, 1987.

Zhou, C., "Modeling and Prediction of Pure and Multicomponent Gas Adsorption," PhD Dissertation, Oklahoma State University, Stillwater, Oklahoma, 1994.

APPENDIX A

TEMPERATURE AND PRESSURE CALIBRATIONS

A1. Temperature Calibration

The temperature of the equilibrium cell section was measured using an RTD digital thermometer, model 2180A, manufactured by Fluke. The platinum probe was inserted inside a hole in an aluminum block, which was attached to the surface of the equilibrium cell. The pump section temperature was measured using a thermocouple mounted to the inside of the Ruska injection pump. In addition, the pump section temperature was also monitored by three other thermocouples attached on the surface and surrounding of the injection pump.

Calibrations were performed routinely during the course of the experiments. The temperature measuring devices were calibrated against a Minco platinum resistance reference thermometer model RT 88078. Table A1 presents an example of the calibration results conducted in November 2003. Figures A1 present deviations of the cell and pump section temperatures from the Minco reference thermometer.

Table A1: Temperature Calibration Results

Points No.	Cell Section Temperature (°F)	Minco Reference Temperature (°F)	Pump Section Temperature (°F)	Minco Reference Temperature (°F)
1	120	119.27	120	120.21
2	120	119.29	120	120.22
3	125	124.36	125	125.27
4	125	124.37	125	125.29
5	131	130.26	131	131.23
6	131	130.29	131	131.25

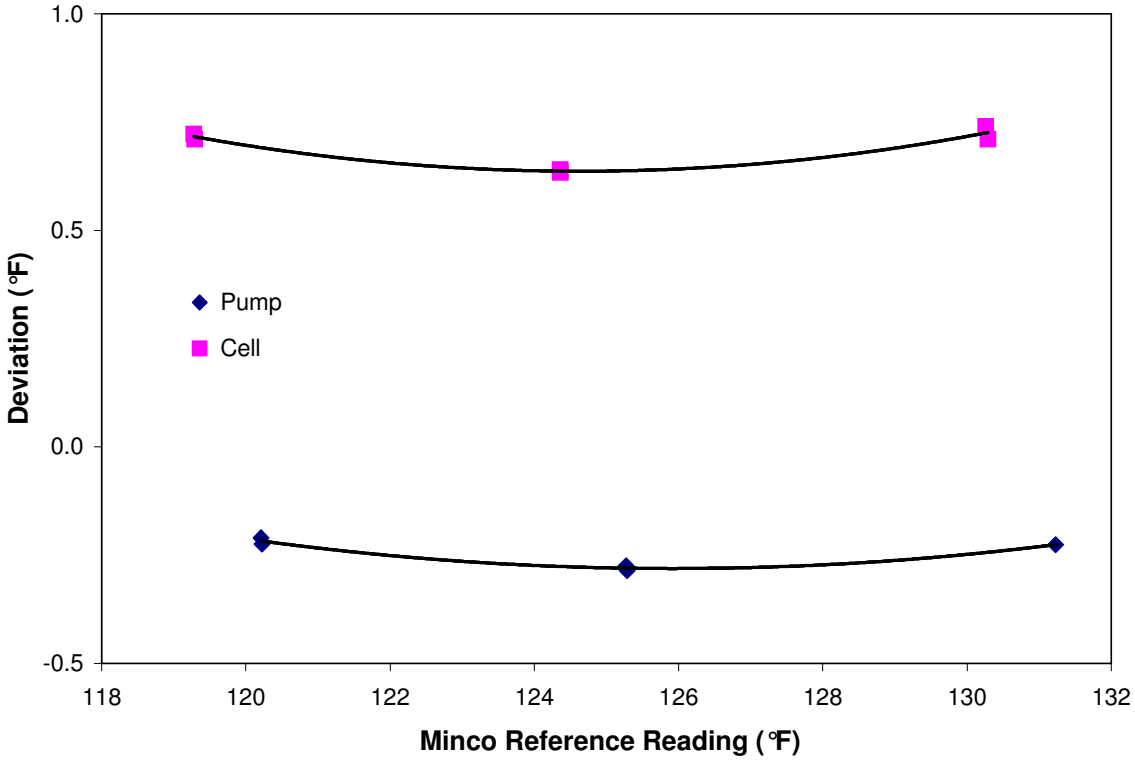

Figure A1: Pump and Cell Temperature Calibrations

A2. Pressure Calibration

The pressures measured by Super TJE transducers were calibrated against a Ruska deadweight tester with calibration traceable to the National Institute of Science and Technology. Calibrations were performed routinely during the course of the experiments. The pump and cell section pressure transducers were calibrated at pressures from zero to 1800 psia at intervals of about 100 psia. The results were used to construct pressure calibration plots similar to the one illustrated in Figure B1. Deviations between standard dead weight pressure and the transducer pressure were plotted as a function of transducer pressure. The pressure calibration data were fit to a second order polynomial in pressure using a least-squares method. Results showed root-mean-square errors (RMSE) of the fit to be 0.1 psia. The pressure calibration regression coefficients were entered into the data reduction software routines to make the appropriate pressure corrections.

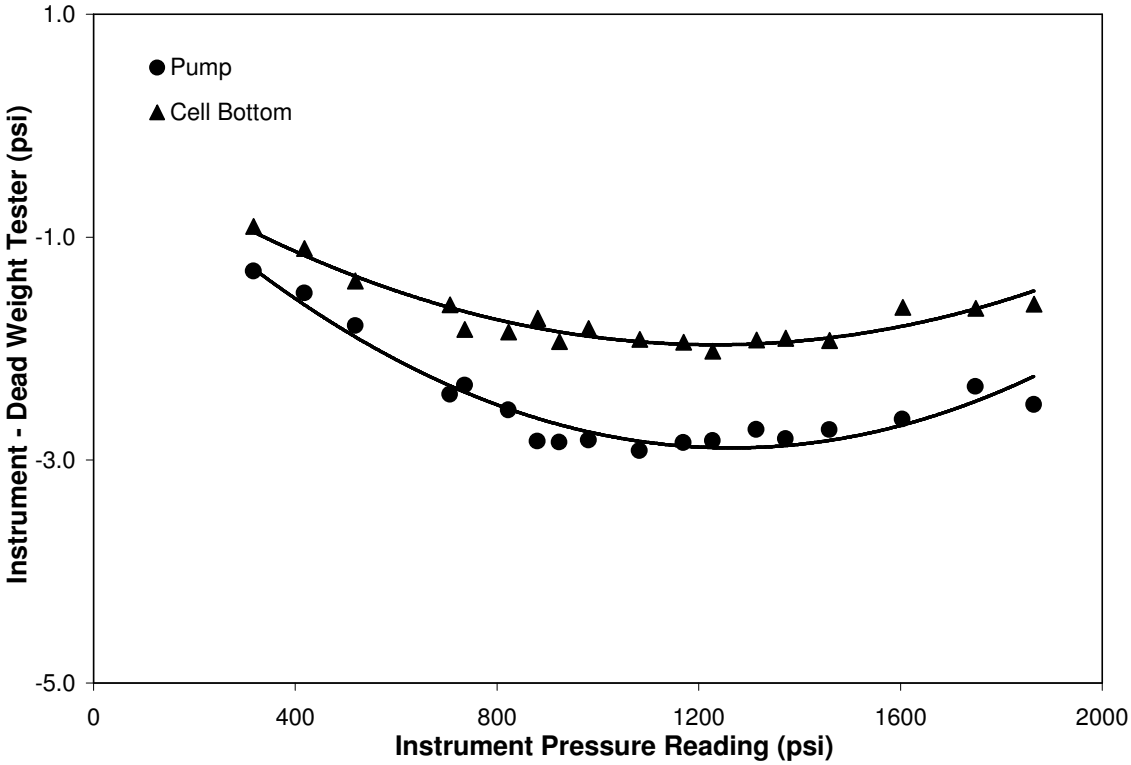

Figure A2: Pump and Cell Pressure Calibrations

APPENDIX B

ERROR ANALYSIS

B. Error Analysis

The Gibbs excess adsorption in units of mg mole/g adsorbent was calculated as follows:

$$n^{Gibbs} = \frac{1000\, n_{ads}}{L} \tag{B1}$$

where L is the amount of activated carbon loaded in the cell [g] and n_{ads} is the Gibbs excess adsorption (mmol/g coal) obtained from the experiment according to Equation 2-10.

Therefore, the uncertainty in calculating the Gibbs excess adsorption is determined by:

$$\sigma^2_{n^{Gibbs}} = \left(\frac{\partial n^{Gibbs}}{\partial n_{ads}}\right)^2 \sigma^2_{n_{ads}} + \left(\frac{\partial n^{Gibbs}}{\partial L}\right)^2 \sigma^2_L \tag{B2}$$

or

$$\sigma^2_{n^{Gibbs}} = \left(\frac{1000}{L}\right)^2 \sigma^2_{n_{ads}} + \left(\frac{1000\, n_{ads}}{L^2}\right)^2 \sigma^2_L \tag{B3}$$

where σ_L was estimated to be 0.1 g, and n_{ads} was calculated as:

$$\sigma^2_{n_{ads}} = \sigma^2_{n_{inj}} + \sigma^2_{n_{unads}} + \sigma^2_{n_{sol}} \tag{B4}$$

$\sigma_{n_{inj}}$ is dependent on the uncertainty of determining the density of the gas in the pump, ρ_p and the uncertainty of the gas volume injected.

$$\sigma^2_{n_{inj}} = (V_f^2 + V_i^2)\sigma^2_{\rho_p} + 2\rho_p^2\sigma_V^2 \tag{B5}$$

where V_f and V_i are the final and initial volume in the pump.

The uncertainty of injected gas volumes, σ_v, is estimated to be equal to 0.02 cm^3, and σ_{ρ_p} is calculated as follow:

$$\rho_p = (P/ZRT)_p \tag{B6}$$

which leads to

$$\sigma_{\rho_p}^2 = \left(\frac{\partial \rho_p}{\partial T}\right)_P^2 \sigma_T^2 + \left(\frac{\partial \rho_p}{\partial P}\right)_T^2 \sigma_P^2 + \left(\frac{\partial \rho_p}{\partial Z}\right)_{T,P}^2 \sigma_Z^2 \tag{B7}$$

Therefore

$$\sigma_{\rho_P}^2 = \rho^2 \left(\left(\frac{1}{T} + \frac{(\partial Z/\partial T)_P}{Z} \right)^2 \sigma_T^2 + \left(\frac{1}{P} - \frac{(\partial Z/\partial P)_T}{Z} \right)^2 \sigma_P^2 + \left(\frac{1}{Z} \right)^2 \sigma_Z^2 \right) \tag{B8}$$

where σ_z is the accuracy of the compressibility factor model used. σ_T and σ_P are estimated to be 0.1 K and 6.9 kPa respectively.

Using a similar technique, $\sigma_{n_{unads}}$ in Equation B-4 can also be derived resulting the following expression:

$$\sigma_{unads}^2 = (\rho_{cell})^2 \sigma_{V_{void}}^2 + (V_{void})^2 \sigma_{\rho_{cell}}^2 \tag{B9}$$

The void volume is measured several times within the range of the operating pressure. Generally, each void volume measured is less than 0.3 cm^3 removed from the average void volume taken over at least five injections. So, $\sigma_{V_{void}}$ was estimated to be 0.3 cm^3.

Equation B-8 can also be used to calculate the uncertainty of the gas density in the cell, $\sigma_{\rho_{cell}}$.

For adsorption on a dry matrix, $\sigma_{n_{sol}}$ is equal to zero, and for adsorption on a wet matrix, the accuracy of the model for calculating the gas solubility in water is estimated to be 5 % of the amount of gas absorbed in water.

Combining Equations B-5 through B-9 yields the total uncertainty associated with the pure-component adsorption value. The largest error contribution to the amount

adsorbed originates from the unadsorbed gas calculation, in which the uncertainties in the adsorbed-phase density and the void volume measurements make up to approximately 80% of the error [Hall, 1993].

Error Estimates for Absolute Adsorption

Relation between Gibbs and absolute adsorption is expressed as:

$$n^{Abs} = \frac{n^{Gibbs}}{1 - \frac{\rho}{\rho_a}} \tag{B10}$$

Therefore, the uncertainty in calculating the absolute adsorption can be expressed as:

$$\sigma^2_{n^{Abs}} = \left(\frac{\rho_a}{\rho_a - \rho}\right)^2 (\sigma_{n^{Gibbs}})^2 + \left(\frac{n^{Abs}}{\rho_a - \rho}\right)^2 \sigma^2_\rho \tag{B11}$$

VITA

Arunkumar Arumugam

Candidate for the Degree of

Master of Science

Thesis: HIGH PRESSURE ADSORPTION OF PURE COALBED GASES ON DRY COALS

Major Field: Chemical Engineering

Biographical:

Personal Data: Born in Chennai, India, on July 04, 1977, son of Arumugam Kuppuswamy and Pramodhini Arumugam

Education: Graduated from AV. Meiyappan MHSS, Chennai, India, in May 1995; received Bachelor of Technology in Chemical Engineering from Sri Venkateswara College of Engineering, Chennai, India, in May 1999; Completed the requirements for the Master of Science degree with a major in Chemical Engineering at Oklahoma State University in December 2004.

Experience: Panel Engineer in TamilNadu Petroproducts Limited, Chennai, India from August 1999-October 2002; employed by Oklahoma State University, School of Chemical Engineering, as a research assistant, 2003-present.

Professional Membership: American Institute of Chemical Engineers